

# **Transfer Hydrogenation of Ketones Mediated By (Pyrazolylmethyl)pyridine Nickel(II) & Iron(II) Complexes**

By

**Makhosazane Nkosingiphile Magubane**

Master of Science



**UNIVERSITY OF  
KWAZULU-NATAL**

---

**INYUVESI  
YAKWAZULU-NATALI**

School of Chemistry and Physics

Pietermaritzburg

**Transfer Hydrogenation of Ketones Mediated By (Pyrazolylmethyl)pyridine  
Nickel(II) & Iron(II) Complexes**

by

**Makhosazane Nkosingiphile Magubane**

210522440

Submitted in fulfilment of the academic requirements for the degree of

**Master of Science**

in

**Chemistry**

School of Chemistry & Physics

College of Agriculture, Engineering and Science

University of KwaZulu-Natal

Pietermaritzburg

South Africa

**January 2016**

## DECLARATION

I hereby declare that the dissertation titled ‘Transfer hydrogenation of ketones mediated by (pyrazolylmethyl)pyridine nickel(II) & iron(II) complexes’ is my original work that was carried out in the Discipline of Chemistry, School of Chemistry & Physics of the College of Agriculture, Engineering and Science, University of KwaZulu-Natal, Pietermaritzburg Campus, South Africa.

The contents of this work have not been submitted for the award of any degree or examination in any other university, and all sources of information in the form of references and other sources used have been duly acknowledged.

\_\_\_\_\_ Date: \_\_\_\_\_

Makhosazane N. Magubane (210522440)

I hereby confirmed that this dissertation has been submitted for examination with my approval as a university supervisor

\_\_\_\_\_ Date: \_\_\_\_\_

Dr. Stephen O. Ojwach (Supervisor)

## **DEDICATIONS**

**To**

My angel (Iminathi Andiswa), My mother (Khanyisile Prizer)

My family

&

Friends

## ABSTRACT

Transfer hydrogenation of ketones is one of the most used processes for the reduction of ketones to alcohols using ruthenium complexes, due to its high selectivity. However, ruthenium is very expensive, its complexes are difficult to synthesize and unstable. Therefore the development of nickel(II) and iron(II) catalysts for the transfer hydrogenation of ketones has the potential to offer some advantages over the ruthenium(II) catalysts. Reactions of 2-(pyrazolylmethyl)pyridine (**L1**), 2,6-bis(pyrazolylmethyl)pyridine (**L2**) and 2,6-bis(3,5-dimethylpyrazolyl)pyridine (**L3**) with nickel(II) and iron(II) halides produced the corresponding complexes  $[\text{Ni}(\mathbf{L1})\text{Br}_2]$  (**1**),  $[\text{Ni}(\mathbf{L1})\text{Cl}_2]$  (**2**),  $[\text{Fe}(\mathbf{L1})\text{Cl}_2]$  (**3**),  $[\text{Ni}(\mathbf{L2})\text{Br}_2]$  (**4**),  $[\text{Ni}(\mathbf{L2})\text{Cl}_2]$  (**5**),  $[\text{Fe}(\mathbf{L2})\text{Cl}_2]$  (**6**),  $[\text{Ni}(\mathbf{L3})\text{Br}_2]$  (**7**),  $[\text{Ni}(\mathbf{L3})\text{Cl}_2]$  (**8**),  $[\text{Fe}(\mathbf{L3})\text{Br}_2]$  (**9**) in good yields. Solid state structures of **4** and **6** revealed the presence of two tridentately bound **L2** units in the metal coordination sphere to give six-coordinate cationic species, while only one tridentate **L3** unit is bound to the metals in **7** and **8**.

Since asymmetric transfer hydrogenation is a highly efficient method for the synthesis of enantiomerically enriched alcohols, attempts were made to synthesize chiral 2-[1-(3,5-dimethylpyrazol-1-yl)ethyl]pyridine nickel(II) and iron(II). However the synthesis of the ligands was not successful and thus chiral complexes could not be accessed. Complexes in asymmetric transfer hydrogenation of ketones did not materialize. Reactions of racemic mixtures of 2-[1-(3,5-dimethylpyrazol-1-yl)ethyl]pyridine (**L4**) and 2-[1-(3,5-diphenylpyrazol-1-yl)ethyl]pyridine (**L5**) with nickel(II) and iron(II) halides produced  $\text{Ni}(\mathbf{L4})\text{Br}_2$  (**10**),  $\text{Ni}(\mathbf{L4})\text{Cl}_2$  (**11**),  $\text{Fe}(\mathbf{L4})\text{Cl}_2$  (**12**) and  $\text{Ni}(\mathbf{L5})\text{Br}_2$  (**13**), in fair yields (51 – 73 %). The molecular structures revealed that complex **10** is dinuclear while complex **13** is mononuclear. Both complexes **10** and **13** were isolated formed as racemic mixtures.

All the complexes (**1-13**) formed active catalysts for the transfer hydrogenation of acetophenone in 2-propanol at 82°C. The effect of ligand structure, catalyst concentration, base variation and substrate variation was investigated using selected complexes. Both the nature of the metal atom and ligand moiety controlled the catalytic activities of the complexes. Generally iron(II) complexes were more active than their nickel(II) analogues, while complexes of **L1** were better efficient catalysts than those of **L2**. Complexes of **L3**, an unsubstituted ligand **L3** were more active than complexes of **L2**. Complexes of **L5** were more active than those of **L4** in the transfer hydrogenation of ketones suggesting that catalytic activity could be enhanced by using ligands which are bulky. By changing the catalyst amount, base and substrate, the catalytic activities of the complexes also varied.

## TABLE OF CONTENTS

TITLE PAGE.....	i
DECLARATION .....	ii
DEDICATIONS.....	iii
ABSTRACT .....	iv
LIST OF FIGURES .....	x
LIST OF SCHEMES.....	xiii
LIST OF TABLES .....	xv
ABBREVIATIONS .....	xvi
ACKNOWLEDGEMENTS.....	xvii

### CHAPTER ONE

#### Introduction and literature review

<b>1.1 Introduction</b> .....	1
1.1.1 General background.....	1
1.1.2 Role of hydrogen donors in THK.....	3
1.1.3 Role of base in THK.....	4
1.1.4 Mechanistic overview.....	4
1.1.5 Significance of transfer hydrogenation of ketones.....	7
<b>1.2 Literature review</b> .....	9
1.2.1 General remarks .....	9
1.2.2 Ruthenium(II) complexes as catalysts for the THK.....	9
1.2.2.1 P <sup>^</sup> P based ligands systems .....	9
1.2.2.2 P <sup>^</sup> N based ligand systems .....	11
1.2.2.3 N <sup>^</sup> C heterocyclic carbene based ligand systems .....	13
1.2.2.4 N <sup>^</sup> N based ligand systems.....	15

1.2.3	Iron(II) complexes as catalysts in the THK .....	18
1.2.4	Nickel(II) complexes as catalysts in the THK .....	20
1.2.5	Other transition metal complexes as catalysts in THK.....	21
<b>1.3</b>	<b>Asymmetric transfer hydrogenation</b> .....	<b>24</b>
1.3.1	Asymmetric transfer hydrogenation using ruthenium(II) complexes .....	24
1.3.2	Asymmetric transfer hydrogenation of ketones using nickel(II) and iron(II) complexes .....	28
<b>1.4</b>	<b>Problem identification</b> .....	<b>31</b>
<b>1.5</b>	<b>Rationale and justification of the study</b> .....	<b>31</b>
<b>1.6</b>	<b>Aims of the project</b> .....	<b>32</b>
<b>1.7</b>	<b>References</b> .....	<b>32</b>

## CHAPTER TWO

### Transfer hydrogenation of ketones mediated by (pyrazolylmethyl)pyridine nickel(II) & iron(II) complexes: Influence of complex structure on catalytic activity.

<b>2.1</b>	<b>Introduction</b> .....	<b>39</b>
<b>2.2</b>	<b>Experimental</b> .....	<b>41</b>
2.2.1	General methods and instrumentation .....	41
2.2.2	Synthesis of nickel(II) and iron(II) complexes .....	41
2.2.2.1	Synthesis of [ $\{2-(3,5\text{-dimethylpyrazolyl})\text{pyridine}\}\text{NiBr}_2$ ] ( <b>1</b> ) .....	41
2.2.2.2	Synthesis of [ $\{2-(3,5\text{-dimethylpyrazolyl})\text{pyridine}\}\text{NiCl}_2$ ] ( <b>2</b> ). .....	42
2.2.2.3	Synthesis of [ $\{2-(3,5\text{-dimethylpyrazolyl})\text{pyridine}\}\text{FeCl}_2$ ] ( <b>3</b> ). .....	42
2.2.2.4	Synthesis of [ $\{2,6\text{-bis}(3,5\text{-dimethylpyrazolyl})\text{pyridine}\}\text{NiBr}_2$ ] ( <b>4</b> ). .....	43
2.2.2.5	Synthesis of [ $\{2,6\text{-bis}(3,5\text{-dimethylpyrazolyl})\text{pyridine}\}\text{NiCl}_2$ ] ( <b>5</b> ). .....	43
2.2.2.6	Synthesis of [ $\{2,6\text{-bis}(3,5\text{-dimethylpyrazolyl})\text{pyridine}\}\text{FeCl}_2$ ] ( <b>6</b> ). .....	44
2.2.2.7	Synthesis of [ $\{2,6\text{-bis}(3,5\text{-dimethylpyrazolyl})\text{pyridine}\}\text{NiBr}_2$ ] ( <b>7</b> ). .....	44



2.2.2.8 Synthesis of [ $\{2,6\text{-bis}(3,5\text{-dimethylpyrazolyl})\text{pyridine}\}\text{NiCl}_2$ ] ( <b>8</b> ).....	45
2.2.2.9 Synthesis of [ $\{2,6\text{-bis}(3,5\text{-dimethylpyrazolyl})\text{pyridine}\}\text{FeCl}_2$ ] ( <b>9</b> ).....	45
2.2.3 X-ray Crystallography .....	46
2.2.4 Transfer hydrogenation of ketones reactions .....	46
<b>2.3 Results and discussion</b> .....	47
2.3.1 Syntheses and characterization .....	47
2.3.2 Molecular structures of complexes <b>4 - 8</b> .....	51
2.3.3 Transfer hydrogenation of acetophenone catalyzed by complexes <b>1-9</b> .....	60
2.3.3.1 Effect of catalyst structure on the transfer hydrogenation of acetophenone .....	61
2.3.3.2 Effect of reaction conditions on the transfer hydrogenation reactions .....	65
2.3.3.3 Variation of ketone substrates using complex <b>1 &amp; 9</b> .....	67
<b>2.4 Conclusions</b> .....	70
<b>2.5 References</b> .....	70

## CHAPTER THREE

### Orientation towards the asymmetric transfer hydrogenation using 2-(1-(Pyrazolyl)ethyl)pyridine nickel(II) and iron(II) complexes

<b>3.1 Introduction</b> .....	74
<b>3.2 Experimental</b> .....	75
3.2.1 General methods and instrumentation .....	75
3.2.2 Synthesis of ligands <b>L4</b> and <b>L5</b> .....	75
3.2.2.1 Synthesis of 2-[1-(3,5-dimethylpyrazol-1-yl)ethyl]pyridine ( <b>L4</b> ) .....	75
3.2.2.2 Synthesis of 2-[1-(3,5-diphenylpyrazol-1-yl)ethyl]pyridine ( <b>L5</b> ) .....	76
3.2.3 Synthesis of iron(II) and nickel(II) complexes .....	76
3.2.3.1 Synthesis of [ $\{2\text{-}[1\text{-}(3,5\text{-dimethylpyrazol-1-yl)ethyl]pyridine}\}\text{NiBr}_2$ ] ( <b>10</b> ).....	76
3.2.3.2 Synthesis of [ $\{2\text{-}[1\text{-}(3,5\text{-dimethylpyrazol-1-yl)ethyl]pyridine}\}\text{NiCl}_2$ ] ( <b>11</b> ).....	77
3.2.3.3 Synthesis of [ $\{2\text{-}[1\text{-}(3,5\text{-dimethylpyrazol-1-yl)ethyl]pyridine}\}\text{FeCl}_2$ ] ( <b>12</b> ).....	77
3.2.3.4 Synthesis of [ $\{2\text{-}[1\text{-}(3,5\text{-diphenylpyrazol-1-yl)ethyl]pyridine}\}\text{NiBr}_2$ ] ( <b>13</b> ).....	77

3.2.4 X-ray crystallography .....	78
<b>3.3 Results and discussion .....</b>	<b>78</b>
3.3.1 Attempted synthesis of chiral ligands .....	78
3.3.2 Synthesis of (pyrazolylmethyl)pyridine ligands <b>L4</b> and <b>L5</b> .....	80
3.3.3 Synthesis of nickel(II) and iron(II) complexes .....	82
3.3.4 Molecular structures of complexes <b>10</b> and <b>13</b> .....	84
3.3.5 Transfer hydrogenation of ketones catalyzed by complexes <b>10-13</b> .....	88
3.3.4.1 <i>Effect of catalyst structure on the transfer hydrogenation of acetophenone</i> .....	88
3.3.4.2 <i>Effect of reaction conditions on the transfer hydrogenation reactions</i> .....	91
3.3.4.3 <i>Variation of ketone substrates using complex 13</i> .....	92
<b>3.4 Conclusions .....</b>	<b>94</b>
<b>3.5 References .....</b>	<b>95</b>

## CHAPTER FOUR

### General concluding remarks and future prospects

<b>4.1 General conclusions .....</b>	<b>97</b>
<b>4.2 Future prospects .....</b>	<b>98</b>
<b>4.3 References .....</b>	<b>101</b>

## LIST OF FIGURES

<b>Figure 1.1.</b> The ruthenium(II) anionic tripodal phosphine ligand employed in the THK. <sup>41</sup> .....	10
<b>Figure 1.2.</b> The ruthenium(II) phosphine complex used in the transfer hydrogenation of acetophenone. <sup>42</sup> .....	10
<b>Figure 1.3.</b> Ruthenium(II) complex of the N <sup>^</sup> P <sup>^</sup> N type ligand used in the THK. <sup>45</sup> .....	12
<b>Figure 1.4.</b> The ruthenium(II) complex anchored on a P <sup>^</sup> N ligand system used in transfer hydrogenation of cyclohexanone. <sup>17</sup> .....	13
<b>Figure 1.5.</b> The ruthenium(II) N <sup>^</sup> C systems employed in the THK. <sup>48</sup> .....	13
<b>Figure 1.6.</b> The ruthenium(II) complexes anchored on, N <sup>^</sup> C <sup>^</sup> N and N <sup>^</sup> N <sup>^</sup> C ligands used in THK. <sup>51</sup> .....	14
<b>Figure 1.7.</b> Structures of highly active NNN ruthenium(II) catalysts in THK. <sup>54</sup> .....	16
<b>Figure 1.8.</b> Structure of a pyridine-bridged ruthenium based complex use in the transfer hydrogenation of acetophenone. <sup>57</sup> .....	17
<b>Figure 1.9.</b> The ruthenium(II) complexes bearing the (pyridyl)benzoazole ligand employed in the THK. <sup>58</sup> .....	18
<b>Figure 1.10.</b> Pyridine pincer based ligand ligated on iron(II) complex used in transfer hydrogenation of acetophenone. <sup>63</sup> .....	19
<b>Figure 1.11.</b> Structure of an NHC-iron(II) dimethyl complex used in the transfer hydrogenation of 2-acetonaphthone. <sup>65</sup> .....	19
<b>Figure 1.12.</b> Nickel(II) complexes bearing diamine ligands employed in transfer hydrogenation of acetophenone. <sup>46</sup> .....	20
<b>Figure 1.13.</b> Nickel(II) complex of a Schiff base ligand employed in transfer hydrogenation of acetophenone. <sup>66</sup> .....	21

<b>Figure 1.14.</b> The rhodium(I) complex supported by N <sup>^</sup> C <sup>^</sup> N ligand employed in transfer hydrogenation of acetophenone. <sup>67</sup> .....	22
<b>Figure 1.15.</b> The osmium(II) complexes employed in the THK. <sup>68</sup> .....	23
<b>Figure 1.16.</b> The iridium(III) complexes anchored on N <sup>^</sup> N ligand used in the transfer hydrogenation of acetophenone. <sup>71</sup> .....	23
<b>Figure 1.17.</b> The ss-configuration of ruthenium(II) chloride complexes <b>XXVIII</b> and <b>XXIX</b> from their respective ligands. <sup>76</sup> .....	25
<b>Figure 1.18.</b> General structure of Noyori's second generation BINAP ruthenium(II) catalyst. <sup>78</sup>	26
<b>Figure 1.19.</b> Chiral ruthenium(II) complex lacking the "N-H" functionality on the oxazoly-pyridyl)benzomidazole-based NNN ligand <sup>80</sup> .....	27
<b>Figure 1.20.</b> The chiral P,N containing ligands and the resulting chiral ruthenium(II) complex with (R,R) configuration. ....	28
<b>Figure 1.21.</b> The iron(II) complexes <b>1-XXXIII</b> and <b>1-XXXIV</b> from the chiral diaminodiphosphine ligands employed in ATHK. <sup>82,83</sup> .....	29
<b>Figure 1.22.</b> Nickel complex of P <sup>^</sup> N <sup>^</sup> O ligands used in ATH. <sup>89</sup> .....	30
<b>Figure 2.1.</b> ESI-MS spectrum showing m/z peak of the fragments for complex <b>4</b> .....	50
<b>Figure 2.2.</b> HR-MS spectrum complex <b>7</b> showing [M <sup>+</sup> -Br] as the base peak. ....	50
<b>Figure 2.3.</b> Molecular structure of complex <b>4a</b> drawn at 50% probability ellipsoids.....	52
<b>Figure 2.4.</b> Molecular structure of <b>6a</b> drawn with 50% probability ellipsoids and selected atom labels. ....	54
<b>Figure 2.5.</b> Molecular structure of <b>7a</b> drawn at 50% probability ellipsoids. ....	57
<b>Figure 2.6.</b> Molecular structure of <b>8.2H<sub>2</sub>O</b> drawn at 50% probability ellipsoids.....	59
<b>Figure 2.7.</b> NMR percentage conversion of acetophenone by complex <b>3</b> .....	61

<b>Figure 2.8.</b> Time dependence of catalytic transfer hydrogenation of acetophenone; by complexes <b>1-9</b> .....	62
<b>Figure 2.9.</b> Effect of ketone substrate on the THK using complex <b>9</b> , KOH, substrate, [S]/[ <b>9</b> ]=200.....	67
<b>Figure 3.1.</b> <sup>1</sup> H NMR spectrum of 2-(3,5-dimethylpyrazol-1-yl)ethyl pyridine ligand <b>L4</b> .....	81
<b>Figure 3.2.</b> ESI-MS of 2-(3,5-dimethylpyrazol-1-yl)ethyl pyridine ligand <b>L4</b> .....	82
<b>Figure 3.3.</b> The LR-MS spectrum for complex <b>10</b> .....	84
<b>Figure 3.4.</b> Molecular structure of <b>10</b> drawn at 50% probability ellipsoids. ....	85
<b>Figure 3.5.</b> Molecular structure of <b>13</b> drawn at 50% probability ellipsoids. ....	86
<b>Figure 3.6.</b> Time dependence of catalytic transfer hydrogenation of acetophenone; by complexes <b>10-13</b> .....	89
<b>Figure 3.7.</b> Effect of ketone substrate on the THK using complex <b>13</b> .....	93
<b>Figure 4.1.</b> Four system ligands used in this research project .....	97

## LIST OF SCHEMES

<b>Scheme 1.1.</b> Transfer hydrogenation of ketones catalyzed by metal complexes.....	2
<b>Scheme 1.2.</b> General asymmetric transfer hydrogenation of ketones catalyzed by chiral metal complexes.....	3
<b>Scheme 1.3.</b> An illustration of the direct transfer hydrogenation mechanism.....	5
<b>Scheme 1.4a.</b> Mechanism of THK demonstrating the inner sphere mechanism.....	5
<b>Scheme 1.4b.</b> Mechanism of THK demonstrating the outer sphere mechanism.....	6
<b>Scheme 1.5.</b> Proposed catalytic cycle for the transfer hydrogenation of the ketones by transition metals anchored on tridentate ligands.....	7
<b>Scheme 1.6.</b> The transition state for the transfer of a proton and hydride from the metal complex to the ketone substrate.....	26
<b>Scheme 1.7.</b> The transfer hydrogenation of propiophenone using nickel(II) pre-catalyst anchored on N <sup>^</sup> P <sup>^</sup> N type chiral ligands <sup>87</sup> .....	30
<b>Scheme 2.1.</b> Nickel(II) and iron(II) complexes used as catalysts in the transfer hydrogenation of ketones in this chapter.....	40
<b>Scheme 2.2.</b> Synthesis of nickel(II) and iron(II) complexes of bidentate ligand <b>L1</b> .....	47
<b>Scheme 2.3.</b> Synthesis of nickel(II) and iron(II) complexes of tridentate ligand <b>L2</b> .....	48
<b>Scheme 2.4.</b> Synthesis of nickel(II) and iron(II) complexes of <b>L3</b> .....	49
<b>Scheme 2.5.</b> Catalytic transfer hydrogenation of acetophenone.....	60
<b>Scheme 3.1.</b> Attempted synthetic route for chiral ligands using CBS as a catalyst.....	79
<b>Scheme 3.2.</b> The transition state showing the coordination of pyridine nitrogen.....	79
<b>Scheme 3.3.</b> The synthetic route for ligands <b>L4</b> and <b>L5</b> using NaBH <sub>4</sub> reducing agent.....	80
<b>Scheme 3.4.</b> Synthesis of nickel(II) and iron(II) complexes of <b>L4</b> and <b>L5</b> .....	82

<b>Scheme 3.5.</b> Catalytic transfer hydrogenation of acetophenone .....	88
<b>Scheme 4.1.</b> Proposed route for synthesis of (R)-1-(pyridyl)ethanol.....	99
<b>Scheme 4.2.</b> Synthetic routes of ligands bearing phosphine ligands, and their corresponding metal complexes. ....	100
<b>Scheme 4.3.</b> Examples of an introduction of ancillary phosphine ligands in the metal complexes .....	101

## LIST OF TABLES

<b>Table 2.1.</b> X-ray data collection and structure refinement parameters for compounds <b>4a</b> , <b>6a</b> , <b>7</b> and <b>8</b> .....	55
<b>Table 2.2.</b> The data for the transfer hydrogenation of acetophenone to 1-phenylethanol catalysed by <b>1-9</b> . <sup>a</sup> .....	63
<b>Table 2.3.</b> Dependence of TH of acetophenone on the nature of base and catalyst concentration using complex <b>1</b> .....	66
<b>Table 2.4.</b> Effect of substrate scope on the transfer hydrogenation reactions by <b>1</b> and <b>9</b> .....	69
<b>Table 3.1.</b> Data collection and structural refinement parameters of <b>10</b> and <b>13</b> .....	87
<b>Table 3.2.</b> Catalysis data for transfer hydrogenation of ketones by <b>10-13</b> .....	90
<b>Table 3.3.</b> Dependence of THK on base and catalyst concentration by complex <b>13</b> .....	92
<b>Table 3.4.</b> Effect of substrate scope on the transfer hydrogenation reactions by <b>13</b> .....	94



## ABBREVIATIONS

TH	Transfer hydrogenation
THK	Transfer hydrogenation of ketones
ATHK	Asymmetric transfer hydrogenation of ketones
L	Ligand
K	Kelvin
NMR	Nuclear magnetic resonance
MS	Mass spectroscopy
ESI-MS	Electrospray ionisation
HR-MS	High resolution mass spectroscopy
LR-MS	Low resolution mass spectroscopy
TOF	Turn over frequency
TON	Turn over number
BM	Bohr magneton
NHC	N-heterocyclic carbenes
DPEN	Diphenylethylenediamine
CBS	Corey-Bakshi-Shibata
$M_w$	Molecular weight
m/z	mass to charge ratio
ee	enantiomeric excess
py	pyridine
pz	pyrazole

## ACKNOWLEDGEMENTS

I would like to express my sincerest gratitude to God, for the gift of life and for giving me strength and continuous guidance through the difficulties and challenges faced during my studies. I would also like to express my gratitude to my supervisor, Dr. Stephen O. Ojwach whose expertise, understanding and skills added considerably to my graduate experience. I appreciate his patience, dedication and guidance throughout this project.

My gratefulness also goes to my mother, Khanyisile P. Gwala, for her support and endless encouragement that gave me courage to carry on throughout the hardships I faced. I would also like to thank both my families, Magubane family and Gwala family for the support they provided me through my entire life. I am also thankful to Sandile Zondi for his love, support, inspiration and encouragement that gave me strength and will to continue. I must also acknowledge my friends who have supported me through good times and bad times, particularly Thandubuhle Gonose, Thobeka Hlengwa and Vusi Ntema.

I am thankful to Prof. Orde Munro for the single crystal X-ray diffraction analysis of my crystals. For Mass spectroscopy and Elemental analysis I am thankful to Caryl Janse Van Rensburg. The assistance from staff and friends in the department are highly appreciated. Appreciation also goes to the catalysis group, in particular George Nyamoto, Aloice Ogweni, Mngqobi Zikode and Alam Gulfam for exchanges of knowledge, skills and resources that helped me to finish this project.

Lastly, I recognize that this research would not have been possible without the financial assistance as well as a research friendly environment. I therefore acknowledge NRF and the University of KwaZulu Natal, Pietermaritzburg campus.

# CHAPTER ONE

## Introduction and literature review

### 1.1 Introduction

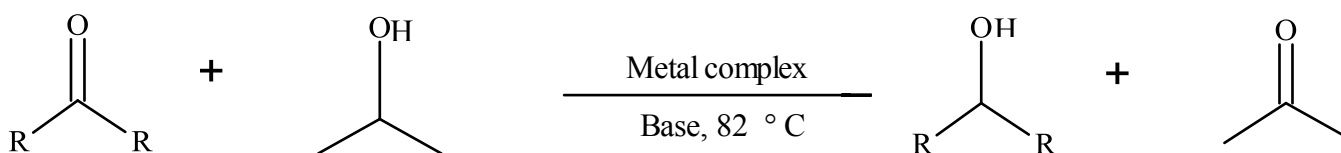
#### 1.1.1 General background

Catalytic hydrogenation of unsaturated organic compounds has been of theoretical and practical interest for many years.<sup>1-3</sup> Hydrogenation reactions is a process that is used mainly to reduce organic compounds such as alkenes,<sup>2</sup> alkynes,<sup>3</sup> ketones,<sup>4</sup> imines<sup>5</sup> and aldehydes,<sup>6</sup> with hydrogen. Transfer hydrogenation refers to a process in which a source of hydrogen donor, such as an alcohol, is employed to reduce a compound.<sup>7</sup> Transfer hydrogenation (TH) of ketones is one of the processes that have been extensively studied for the reduction of ketones to secondary alcohols due to its high selectivity.<sup>8,9</sup> In addition, asymmetric transfer hydrogenation (ATH) is used for the production of enantiomerically enriched products, on both the laboratory and industrial scales.<sup>10</sup>

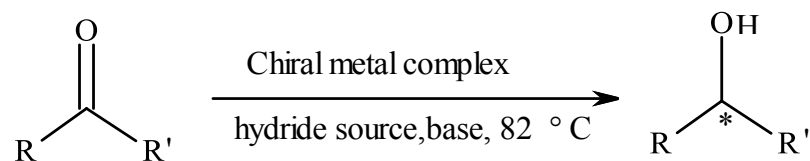
The carbonyl functional groups like aldehydes and ketones can undergo hydrogenation *via* other methods that makes use of molecular hydrogen (H<sub>2</sub>),<sup>11</sup> reducing agents such as lithium tetrahydridoaluminate(III),<sup>12</sup> sodium tetrahydridoborate(III),<sup>13</sup> organolithium,<sup>14</sup> and Grignard reagents.<sup>15</sup> Organolithium and grignard reagents make use of an alkali metal (lithium) and an alkaline earth metal (magnesium) as agents, respectively. The first efficient high pressure hydrogenation of ketone using molecular hydrogen (H<sub>2</sub>) was reported by Casey and Guan<sup>16</sup> using 3 atmospheres of H<sub>2</sub> at 25 °C.

Over and above these methods, transfer hydrogenation of ketones is preferred due to it being highly selective and achieving high activities.<sup>8</sup> Transfer hydrogenation of ketones employing hydrogen donor solvent was first discovered by Meerwein and co-workers in the mid 1920's, and is commonly referred to as the MPV (Meerwein-Ponndorf-Verley) reduction reaction.<sup>17</sup> Later in 1967, Meerwein reported on an Ir-DMSO-complex, which catalyses the transfer hydrogenation reactions.<sup>17a</sup> Soon after, an efficient ruthenium(II) complex [Ru(PPh<sub>3</sub>)Cl<sub>2</sub>] was reported for the transfer hydrogenation reactions.<sup>17b</sup>

Transfer hydrogenation of ketones is usually catalyzed by homogeneous solutions of transition-metal complexes in the presence of a base and a source of hydrogen (Scheme 1.1). On the other hand, the synthesis of enantiomerically enriched alcohols from ketones through ATHK is catalyzed by chiral s transition-metal complexes (Scheme 1.2). Some of the mostly used catalysts are derived from Co, Ru, Rh, Re, Ir, Ni, Fe and Ir metal complexes. To date, the most studied metal complexes that have been found to form the best catalyst system for the THK are those derived from ruthenium.<sup>11,18,19</sup>



**Scheme 1.1.** Transfer hydrogenation of ketones catalyzed by metal complexes.



**Scheme 1.2.** General asymmetric transfer hydrogenation of ketones catalyzed by chiral metal complexes.

### 1.1.2 Role of hydrogen donors in THK

The source of hydrogen differs in transfer hydrogenation reactions, depending on the type of the organic substrate. Organic compounds such as 2-propanol, glycerol, triethylamine/formic acid and ethanol are the most used hydrogen donors for the transfer hydrogenation reactions of ketones.<sup>20</sup> Other transfer hydrogenation reactions use aminoboranes<sup>21</sup> as a source of one or two hydrogen atoms. Another convenient hydrogen source that have been employed in the transfer hydrogenation of ketones reaction is triethylamine/formic acid, as it results in an irreversible reaction. However, there are few catalysts that are compatible with high pressure and high temperature usually required for its reactions.<sup>22</sup>

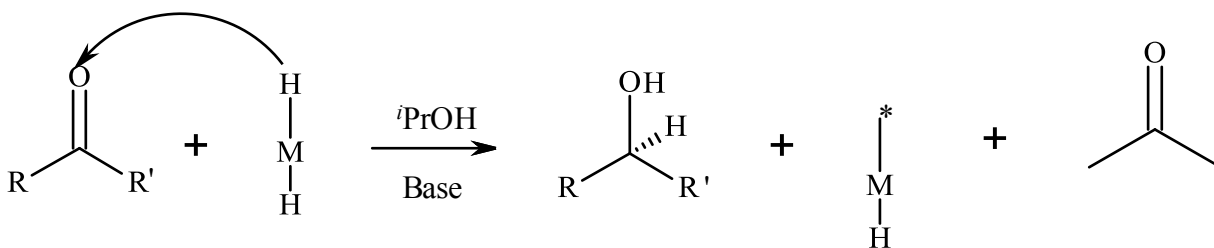
Generally 2-propanol is the most used solvent as the source of hydrogen although it results in a reversible reaction, producing acetone as a by-product.<sup>23</sup> This is however compensated by the use of large amount of donor solvent to shift the equilibrium to the alcohol product. The acetone bi-product is readily removed,<sup>24</sup> which also shifts the equilibrium to the products. In addition 2-propanol is stable, easy to handle, environmentally friendly, less toxic, dissolves most organic compounds and has a moderate boiling point of 82 °C, moderate enough to drive the majority of transfer hydrogenation.<sup>25</sup>

### 1.1.3 Role of base in THK

The use of a base is very important in the transfer hydrogenation of ketones reactions. It initiates the process of transfer hydrogenation of ketones. In most cases, the role of the base is to promote the removal of the weak ligand from a precatalyst complex<sup>26</sup> (e.g. Cl as HCl). This also allows the catalyst to remain in the most active neutral form.<sup>27</sup> Inorganic bases like KOH, NaOH, NaHCO<sub>3</sub>, Na<sub>2</sub>CO<sub>3</sub>, <sup>t</sup>BuOK or CH<sub>3</sub>COONa have been employed in the transfer hydrogenation of ketones.<sup>16</sup> Organic bases such as triethylamine, pyridine, and pyrrolidine have also been used in the transfer hydrogenation of ketones reactions.<sup>28</sup> It has been observed that the use of weaker bases like NaHCO<sub>3</sub>, Na<sub>2</sub>CO<sub>3</sub> or CH<sub>3</sub>COONa or organic bases like triethylamine, pyridine, pyrrolidine reduces the catalytic activity, while the use of strong inorganic bases like KOH, NaOH and <sup>t</sup>BuOK enhances the catalytic activity.<sup>29</sup> On the other hand, some transfer hydrogenation reactions can occur successfully in base free conditions.<sup>30</sup>

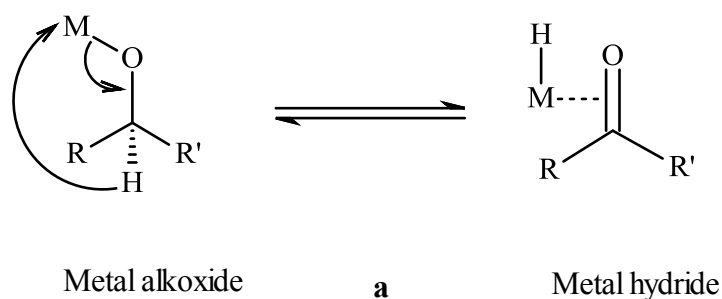
### 1.1.4 Mechanistic overview

Transfer hydrogenation of ketones using hydrogen donor molecules is believed to proceed *via* two different mechanisms; direct transfer of hydrogen to the substrate or *via* the formation of the metal hydride intermediate prior to the substrate reduction.<sup>31</sup> Scheme 1.3 demonstrates the direct transfer hydrogenation from the hydrogen donor to the substrate.

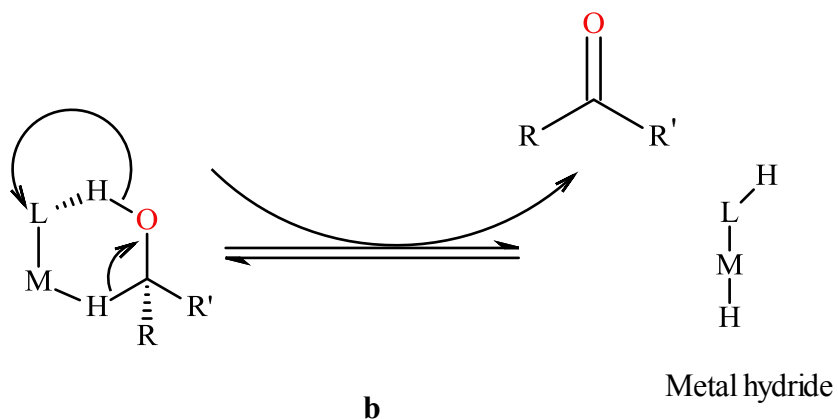


**Scheme 1.3.** An illustration of the direct transfer hydrogenation mechanism

Most transition metal complexes follow the metal hydride route.<sup>32</sup> The formation of the metal hydride intermediate is thought to occur *via* both as an inner-sphere and an outer-sphere mechanism. The former mechanism proceeds *via* the formation of a metal alkoxide intermediate which undergoes  $\beta$ -hydride elimination to generate the metal hydride (Scheme 1.4a).<sup>33</sup> On the other hand, the outer sphere mechanism results in the formation of a 6-membered transition state, in which the hydride donor and the ketone substrate do not coordinate to the metal centre but hydrogen is transferred in a stepwise manner (Scheme 1.4b).<sup>33</sup>



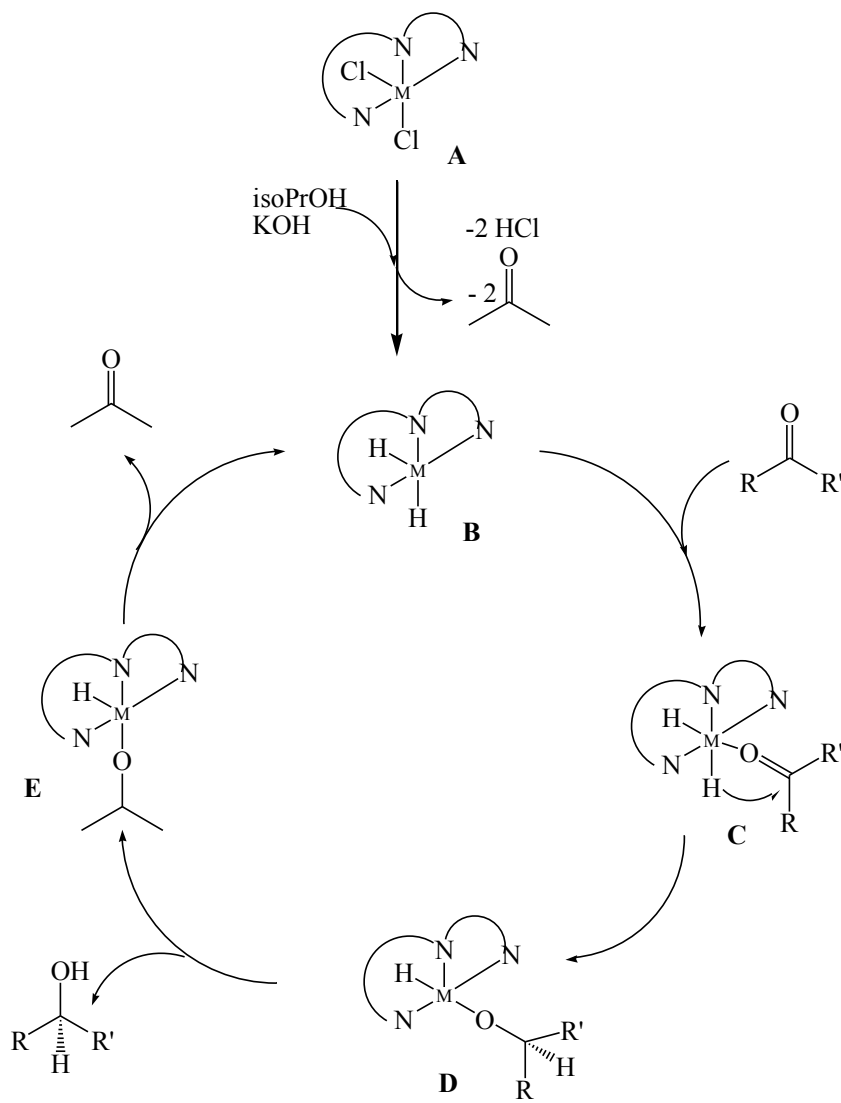
**Scheme 1.4a.** Mechanism of THK demonstrating the inner sphere mechanism.



**Scheme 1.4b.** Mechanism of THK demonstrating the outer sphere mechanism.

The mechanism of transfer hydrogenation of ketones by early transition metals is generally believed to occur *via* the inner sphere mechanism (Scheme 1.5). The process is initiated directly at the metal complex **A** by the abstraction of a chloride ligand followed by the formation of metal alkoxide subsequently leading to the formation of a metal hydride intermediates **B**. Coordination of ketone substrate on **B** gives **C** which is followed by transfer of a hydride to the coordinated ketone to form the metal-alkoxide **D**. Protonation of the coordinated ketone by the hydrogen donor (alcohol) affords the desired product and regeneration of the active catalyst **B** to complete the catalytic cycle.





**Scheme 1.5.** Proposed catalytic cycle for the transfer hydrogenation of the ketones by transition metals anchored on tridentate ligands.

### 1.1.5 Significance of transfer hydrogenation of ketones

Many raw materials used for the production of fine chemicals and pharmaceutical industries are derived from various organic compounds such as ketones, amines and olefins.<sup>9</sup> These raw materials are produced in large quantities through various catalytic processes.<sup>34-36</sup> As the demand

for these raw materials increases, so does the need for effective catalytic systems with abilities to quantitatively and selectively produce these raw materials.

Introduction of alcohols via transfer hydrogenation of ketones is a preferred synthetic route since it is safe, inexpensive, highly active and selective.<sup>35,36</sup> This reaction is particularly convenient for larger-scale synthesis, as it avoids the use of pressurized hydrogen and other hazardous reducing agents.

Asymmetric hydrogenation is by far the most industrially relevant enantioselective transformation, due to its inherent atom economy and operational simplicity, as well as the high level of stereocontrol that allows it to achieve secondary alcohol products that are required by diverse industries.<sup>8,34</sup> Products from asymmetric transfer hydrogenation that are in great demand are the active pharmaceutical ingredients (APIs) which are used for the manufacture of drugs in the pharmaceutical industries.<sup>37</sup> An example is (R)-sotalol, which is used to treat a life-threatening heart rhythm problem called ventricular arrhythmia.<sup>37</sup> Other examples include (R)-tembamide and (R)-aegeline which are the receptor agonist mostly applicable in the treatment of cardiovascular diseases.<sup>38</sup> Another important product from transfer hydrogenation of ketones is (R)-citraonella which is an intermediate in the industrial synthesis of menthol, which is a toner as well as a perfume ingredient.<sup>39</sup> Thus, products from THK and ATHK research process have practical applications in various industries.

## **1.2 Literature review**

### **1.2.1 General remarks**

There is considerable effort to develop late transition metal catalysts for the transfer hydrogenation of ketones reactions.<sup>36</sup> However, this remains a challenging research area, generally with respect to the catalyst's activity, selectivity and stability. The balance between these three catalyst properties therefore motivates the development of suitable transition metal catalysts for the transfer hydrogenation of ketones. This section reviews the development of transition metal complexes based on various donor ligands as catalysts for the transfer hydrogenation of ketones.

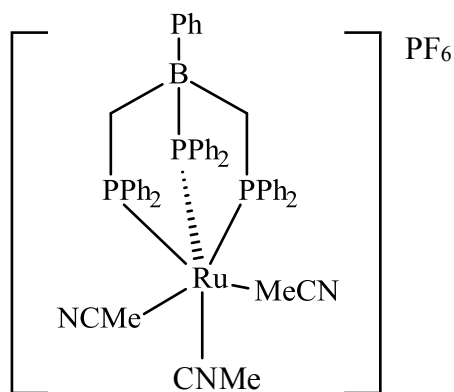
### **1.2.2 Ruthenium(II) complexes as catalysts for the THK**

Ruthenium(II) complexes are chemically diverse, which arise from different ligand types that can be coordinated to the ruthenium(II) metal. The variation of the ligand type is essential in providing the right electronic properties of the complex that can maximise the catalytic activities of the complexes.<sup>40</sup> Several ruthenium(II) complexes supported on diverse ligand systems have been reported as effective catalysts in the transfer hydrogenation of ketones.<sup>41,19</sup>

#### **1.2.2.1 P<sup>3</sup> based ligands systems**

The design of the transfer hydrogenation of ketones catalysts have witnessed the use of ruthenium(II) anchored on P<sup>3</sup> ligand systems. Ruthenium(II) complexes containing a facially coordinated anionic tripodal phosphine ligand (Figure 1.1) have been applied as catalysts in the transfer hydrogenation of ketones.<sup>42</sup> Complex **1-I** is an active catalyst in the transfer hydrogenation of acetophenone, giving a conversion of 87 % with a turn over frequency (TOF)

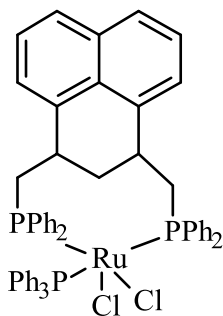
of 30 000 h.<sup>-1</sup> The shortfall of complex **1-I** is the lability of the acetonitrile ligands, which readily changes the catalytic activity of the complex. However, PhBP<sub>3</sub> ligand appears to control the extent of substitution and therefore gives stable catalysts.<sup>42</sup>



**1-I**

**Figure 1.1.** The ruthenium(II) anionic tripodal phosphine ligand employed in the THK.<sup>42</sup>

Recently, Fu *et al.*<sup>43</sup> reported new ruthenium(II) phosphine complexes as catalysts in the transfer hydrogenation of ketones (Figure 1.2). Complex **1-II** gives catalytic activities of up to 85 % for acetophenone after 2 h with a TOF of 425 h.<sup>-1</sup>

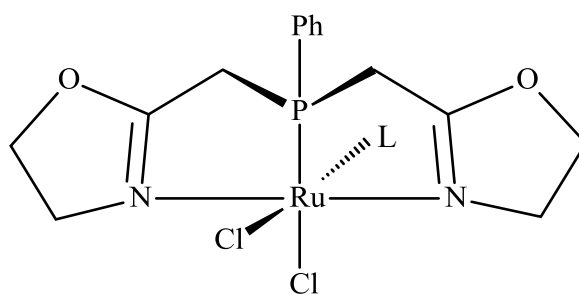


**1-II**

**Figure 1.2.** The ruthenium(II) phosphine complex used in the transfer hydrogenation of acetophenone.<sup>43</sup>

### 1.2.2.2 P<sup>^</sup>N based ligand systems

Another well-known ligand system used to prepare ruthenium(II) complexes as catalysts is based on the P<sup>^</sup>N bidentates. For example, Baratta *et. al.*<sup>44</sup> reported 1-(pyridine-2-yl)phosphinomethanamine based ruthenium(II) complexes as active catalysts for the transfer hydrogenation of acetophenone giving mean percentage conversion of 97 % with a mean TOF of  $3.0 \times 10^5 \text{ h}^{-1}$ . Recently, Ramachandran *et. al.*<sup>45</sup> reported different types of P<sup>^</sup>N coordinated ruthenium(II) complexes as effective catalysts for the transfer hydrogenation of ketones. For instance, complex **1-III** a ruthenium(II) complex anchored on a N<sup>^</sup>P<sup>^</sup>N ligand (Figure 1.3) displays improved catalytic activities compared to the systems reported by Baratta *et.al.*<sup>46</sup> In addition, Zhang and co-workers have also reported ruthenium(II) catalysts anchored on N<sup>^</sup>P<sup>^</sup>N donor ligands.<sup>47</sup> One of their complexes give a catalytic activity of 72 % in the TH for acetophenone when the spectator ligand is DMSO. Catalytic activity improves to 97 % when PPh<sub>3</sub> is an auxillary ligand on the complex. Dissociation of the labile ligand is required during the catalytic cycle.<sup>48</sup> Since PPh<sub>3</sub> dissociates faster than DMSO due to its bulky groups, the complex in which it features has a better activity.

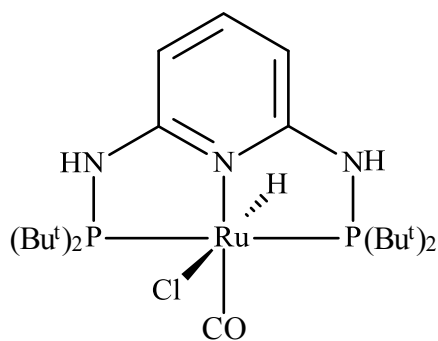


1. L = DMSO
2. L = PPh<sub>3</sub>

**1-III**

**Figure 1.3.** Ruthenium(II) complexes of the N<sup>^</sup>P<sup>^</sup>N type ligands used in the THK.<sup>46</sup>

In another study, the ruthenium(II) complex bearing *N,N'*-bis(di-*tert*-butylphosphino)-2,6-diaminopyridine (PN<sup>3</sup>P) ligand was employed as a catalyst in the transfer hydrogenation of ketones.<sup>30</sup> The complex **1-IV** shown in Figure 1.4 catalyzes the TH of cyclohexanone to cyclohexanol, giving 100 % conversion in 16 h. The activity and selectivity of this catalyst varies with different substrates. In the transfer hydrogenation of acetophenone, only the desired products the products 1-phenylethanol was produced (69 %) along with styrene (14 %), indicating reduction in yield.

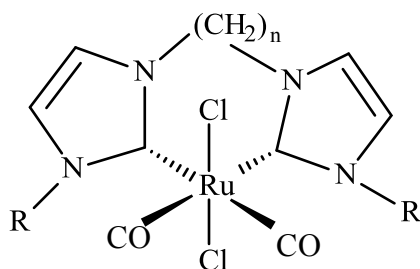


**1-IV**

**Figure 1.4.** The ruthenium(II) complex anchored on a P<sup>N</sup> ligand system used for transfer hydrogenation of cyclohexanone.<sup>17</sup>

### 1.2.2.3 N<sup>C</sup> heterocyclic carbene based ligand systems

A series of ruthenium(II) complexes anchored on bis-N-heterocyclic carbenes (NHC) have been reported by Cheng. *et. al.* as catalysts for the transfer hydrogenation of ketones.<sup>49</sup> Complexes **1-V** to **1-VIII** shown in Figure 1.5 are efficient catalysts in the transfer hydrogenation of ketones. For instance, complex **1-V** ( $n=1$  and R = <sup>n</sup>Bu), gives TOF of 260 h<sup>-1</sup> for the transfer hydrogenation of acetophenone within 2 h.



- $n=1$  ; R = <sup>n</sup>Bu **1-V**  
 $n=2$  ; R = <sup>n</sup>Bu **1-VI**  
 $n=3$  ; R = <sup>n</sup>Bu **1-VII**  
 $n=4$  ; R = <sup>n</sup>Bu **1-VIII**

**Figure 1.5.** The ruthenium(II) N<sup>C</sup> systems employed in the THK.<sup>49</sup>

On the other hand, complex **1-VII** ( $n=3$ ) is the most active and catalyzes the transfer hydrogenation of cyclohexanone to cyclohexanol giving 99 % conversion with a TOF of  $675 \text{ h}^{-1}$ . This catalytic activity is greater than those of the closely related ruthenium(II) carbonyl chloride containing pyridine functionalized-bis-N-heterocyclic carbenes.<sup>50</sup> The difference in catalytic activities of these complexes is considered to be due to the length of the  $-CH_2$  linker.<sup>42</sup> From this observation, an increase in  $n$  decreases the catalytic activity of the complexes.

In another study, ruthenium(II) complexes with  $N^{\wedge}C^{\wedge}N$  and  $N^{\wedge}N^{\wedge}C$  pincer ligands were reported as catalysts in the transfer hydrogenation of ketones (Figure 1.6).<sup>51</sup> The  $N^{\wedge}C^{\wedge}N$  ruthenium(II) complex **1-IX** reported by Nishayama and coworkers<sup>52</sup> gives a conversion of 70 % with the TOF of  $36 \text{ h}^{-1}$  for acetophenone. The related ruthenium(II)  $N^{\wedge}N^{\wedge}C$  systems (**1-X**) reported by Barratta and co-workers<sup>53</sup> display a higher conversion of 98 % and  $TOF_{50}$  (turn over frequency at 50 %) of  $1.1 \times 10^6 \text{ h}^{-1}$ .

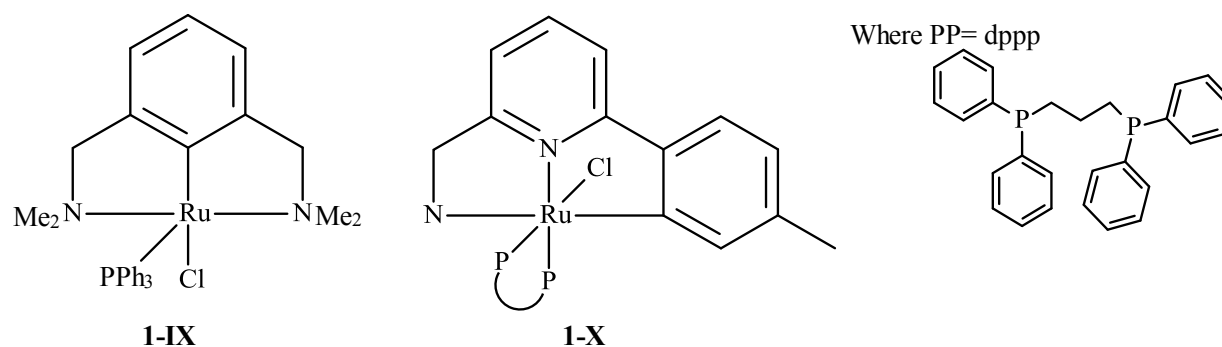


**Figure 1.6.** The ruthenium(II) complexes anchored on,  $N^{\wedge}C^{\wedge}N$  and  $N^{\wedge}N^{\wedge}C$  ligands used in THK.<sup>52</sup>



#### 1.2.2.4 N<sup>N</sup> based ligand systems

In recent years, there has been an increased interest in developing new ruthenium(II) catalysts based on nitrogen donor ligands. It has been revealed that nitrogen ligands give metal catalysts that are highly stable at elevated temperatures and highly active.<sup>19</sup> Noyori and co-workers<sup>54</sup> discovered highly active and selective ruthenium(II) catalysts containing diamine/diphosphine ligands (**1-XI**) for the transfer hydrogenation of ketones (Figure 1.7). In complexes **1-XI** and **1-XIV** (Figure 1.7) the high activities displayed is attributed to the presence of the “N-H” functionality group in the ligand backbone. Among the reported catalysts is the highly active ruthenium(II) complex **1-XI** that contains the 2-(benzoimidazole-2-yl)-6-(pyrazol-1-yl)pyridine ligand (Figure 1.7). Conversions of acetophenone substrate by complex **1-XI** is as high as 99 % with a final TOF value of up to  $7.2 \times 10^5 \text{ h}^{-1}$ .<sup>55</sup> This complex is coordinatively unsaturated, which is key for effective coordination of the substrate to the active site.<sup>55</sup>

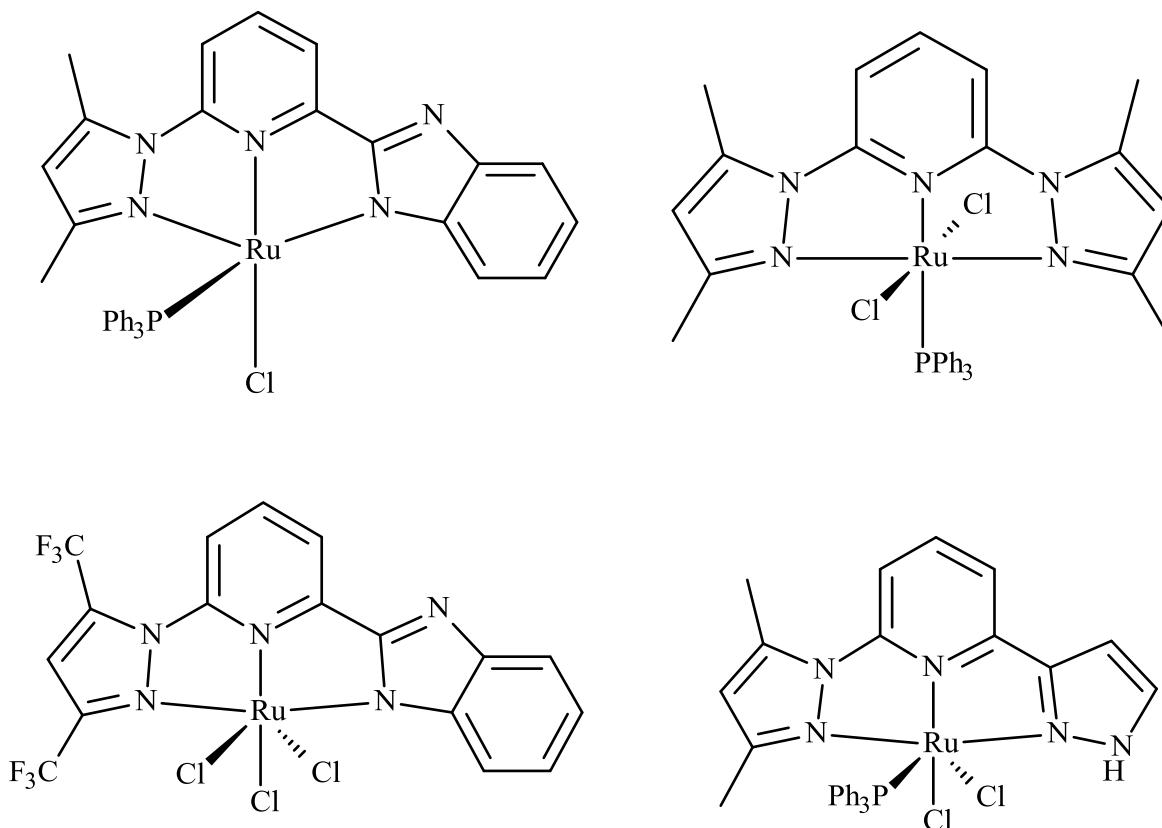


**Figure 1.7.** Structures of highly active NNN ruthenium(II) catalysts in THK.<sup>54</sup>

Another nitrogen-donor ruthenium(II) complex which has been investigated in the transfer of hydrogenation of ketones is 2,6-bis(3,5-dimethylpyrazol-1-yl)pyridineruthenium(II) complex **1-XII** reported by Spivak *et al.*<sup>56</sup> Complex **1-XII** (Figure 1.7) contains a planar tridentate ligand and adopts an octahedral geometry. The complex displays good catalytic activities giving percentage conversions of 96 % and turnover frequencies of 5 760 h<sup>-1</sup> for the hydrogenation of acetophenone and other related ketones.<sup>56</sup> In another similar report, the (pyrazolyl)pyridyl based N<sup>^</sup>N<sup>^</sup>N ligands (Figure 1.7) were used to synthesize highly active catalysts for the transfer hydrogenation of ketones.<sup>19</sup> For instance, complex **1-XIII** displays high TOF of up to 5 940 h<sup>-1</sup>. The substitution of the Cl co-ligand with PPh<sub>3</sub> ligand in **1-XIII** leads to an increase in the

catalytic activity. The higher catalytic activity observed for **1-XI** compared to **1-XIII** is attributed to the PPh<sub>3</sub> bulky ligand in **1-XI**, which promotes the reactivity of the metal centre by enhancing dissociation of the ligand.<sup>54</sup>

In another system, the ruthenium(II) complex of 2,6-bis(5-thioxo-4,5-dihydro-1,2,4-triazole-3-yl)pyridine<sup>57</sup> (**1-XV**) (Figure 1.8), have been studied towards the catalytic transfer hydrogenation of acetophenone. Complex **1-XV** contains a pyridine-bridged tridentate nitrogen donor based ligand, and catalyzes the transfer hydrogenation of acetophenone giving conversion of 94 % and TOF of 2 600 h<sup>-1</sup>. Variation of the ligand involves the use of different functional groups on the triazole ring which affects the catalytic activities of the respective complexes. For example, the introduction of the hindering and bulky phenyl group on the triazole ring decreases the catalytic activity of the complex, while incorporation of a smaller methyl group increases the catalytic activity due to steric hinderance.<sup>57</sup>

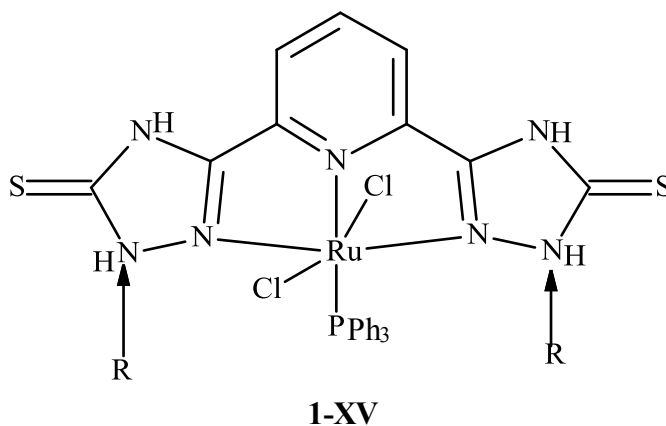


**Figure 1.8.** Structure of a pyridine-bridged ruthenium based complex use in the transfer hydrogenation of acetophenone.<sup>57</sup>

More recently, Ogwenó and co-workers reported ruthenium(III) and ruthenium(II) complexes anchored on bidentate (pyridyl)benzoazole ligands as active catalyst in the transfer hydrogenation of ketones (Figure 1.9).<sup>58</sup> High catalytic activities were observed for all the complexes ranging from 77 % - 95 % within 4 h. Ruthenium(II) complexes bearing PPh<sub>3</sub> ligands are more active than the analogous ruthenium(III) complexes. The most active complex **1-XVI**, where X=NH, displays conversion of up to 95 % and TOF of 24 h<sup>-1</sup> compared to the analogous complexes where X=S (**1-XVII**) and X=O (**1-XVIII**).<sup>58</sup>

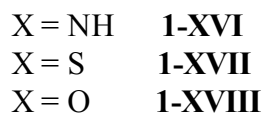
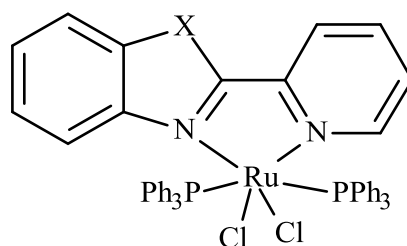
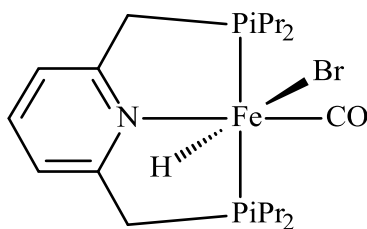


**Figure 1.9.** The ruthenium(II) complexes bearing the (pyridyl)benzoazole ligand employed in the THK.<sup>58</sup>

### 1.2.3 Iron(II) complexes as catalysts in the THK

Recent developments to overcome the shortcomings of the ruthenium catalyst involve the use of nickel(II) and iron(II) complexes. The development of iron(II)<sup>59</sup> and nickel(II)<sup>60</sup> catalysts for the transfer hydrogenation has the potential to offer some advantages over the ruthenium(II) catalysts. These include their ease of synthesis and stability compared to ruthenium(II) compounds.<sup>61-62</sup>

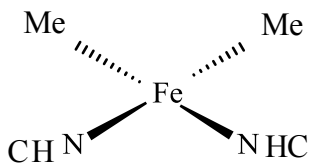
Milstein and his group<sup>63</sup> reported the pyridine pincer based iron(II) complex in the transfer hydrogenation of ketones under mild conditions (Figure 1.10). This iron(II) complex (**1-XIX**) is active in the conversion of acetophenone, giving 94% of 1-phenylethanol in 22 h with TON of 1880 and TOF of 85 h.<sup>-1</sup>



**1-XIX**

**Figure 1.10.** Pyridine-bridged pincer iron(II) complex used in transfer hydrogenation of acetophenone.<sup>63</sup>

NHC iron(II) complexes have demonstrated effectiveness in the transfer hydrogenation of ketones.<sup>64</sup> For example, the iron(II) complex anchored on NHC<sup>65</sup> (**1-XX**) shown in Figure 1.11 displays moderate activity in the transfer hydrogenation of 2-acetonaphthone to afford percentage conversion of 48 % within 6 h.



**1-XX**

**Figure 1.11.** Structure of an NHC-iron(II) complex used in the transfer hydrogenation of 2-acetonaphthone.<sup>65</sup>

### 1.2.4 Nickel(II) complexes as catalysts in the THK

There are few reports on the applications of nickel(II) complexes as catalysts in the transfer hydrogenation of ketones.<sup>47,66</sup> Zhang *et al.*<sup>47</sup> reported nickel(II) complexes supported by diamine ligands (Figure 1.12) as catalysts in the hydrogenation of acetophenone. The highest percentage conversion of acetophenone when using complex **1-XXI** is 4.3 % in isopropanol and KOH as a base. Under the same conditions, complex **1-XXII** is almost inactive giving only the conversion of 0.5 %. The main advantage of these nickel(II) complexes is that they represent are cheaper to produce and stable transfer hydrogenation catalyst.<sup>62</sup>

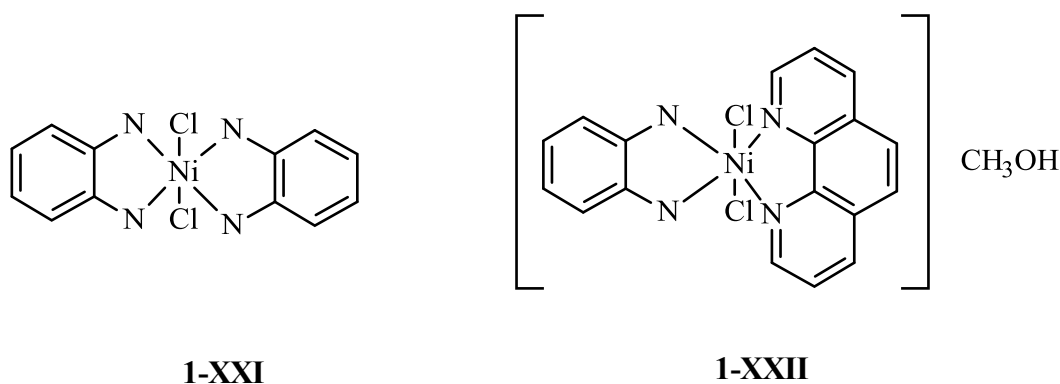
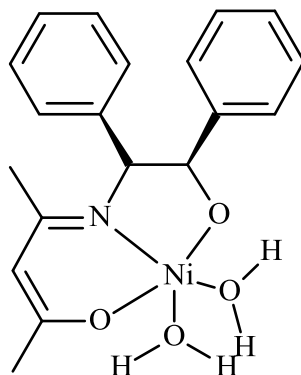


**Figure 1.12.** Nickel(II) complexes bearing diamine ligands employed in transfer hydrogenation of acetophenone.<sup>47</sup>

In a similar study, the nickel(II) complex supported by Schiff base ligand *N*-[(1*R*,2*S*)-2-hydroxy-1,2-diphenyl]-acetylacetonimine (**1-XXIII**) was prepared and applied in the transfer hydrogenation of acetophenone (Figure 1.13). The catalytic activity of this complex is dependent on temperature and the type of base used, giving conversions of 4 % and 9 % at 100 °C and 140

°C respectively.<sup>66</sup> The low catalytic activity of complex **1-XXIII** may be attributed to the strong bond formed between the nickel(II) metal and oxygen from the water ligands.

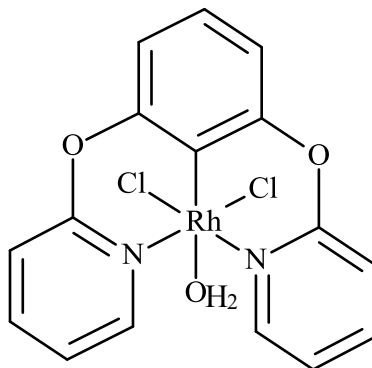


**1-XXIII**

**Figure 1.13.** Nickel(II) complex of a Schiff base ligand employed in transfer hydrogenation of acetophenone.<sup>66</sup>

### 1.2.5 Other transition metal complexes as catalysts in THK

While homogeneous ruthenium complexes are the most applied catalysts for the transfer hydrogenation and asymmetric transfer hydrogenation of ketones, other transition metal complexes such as iridium, rhodium and osmium have been employed as catalysts for these reactions. For example, the rhodium(I) complex containing the bis(2-pyridyloxy)phenyl ligand, **1-XXIV**, (Figure 1.14), reported by Raja *et. al.*<sup>67</sup> gives active and stable catalyst in the transfer hydrogenation of acetophenone with TON of 198 and conversions of 99 % within 24 h. The stability of the complex is believed to originate from the presence of the two six-membered metallacycles.



**1-XXIV**

**Figure 1.14.** The rhodium(I) complex supported by N<sup>C</sup>N ligand employed in transfer hydrogenation of acetophenone.<sup>67</sup>

A remarkably active pincer osmium(II) complex (**1-XXV**) was reported by Baratta and co-workers<sup>68</sup>, displaying high catalytic activity in the transfer hydrogenation of ketones. The complex shown in Figure 1.15 displays high conversions of 96 % corresponding to TOF of  $1.8 \times 10^5 \text{ h}^{-1}$ . In a parallel study, the osmium(II) complex bearing NNN ligand (**1-XXVI**) displays high catalytic activity with the TOF of  $1.7 \times 10^4 \text{ h}^{-1}$  in the transfer hydrogenation of acetophenone.<sup>69</sup> The observed higher activity was ascribed to the stronger thermal stability of the osmium(II) species relative to ruthenium(II) species.<sup>70</sup>



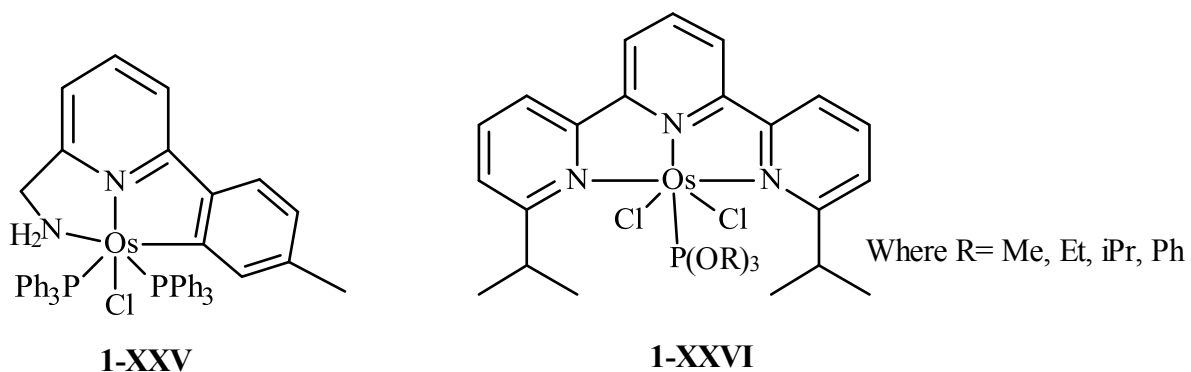


**Figure 1.15.** The osmium(II) complexes employed in the THK.<sup>68</sup>

In another system, an iridium(III) complex of the type **1-XXVII** (Figure 1.16) was used in the transfer hydrogenation of acetophenone<sup>71</sup> and achieved a conversion of 72 % with a TOF of 4990 h<sup>-1</sup> within 14 h.

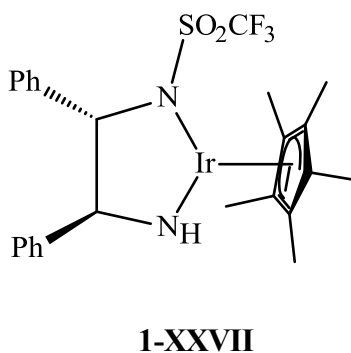


**Figure 1.16.** The iridium(III) complexes anchored on N<sup>N</sup> ligand used in the transfer hydrogenation of acetophenone.<sup>71</sup>

### 1.3 Asymmetric transfer hydrogenation

Asymmetric transfer hydrogenations of ketones have drawn attention due to the use of optically active secondary alcohol intermediates in the synthesis of biologically active compounds such as agrochemicals, medicines, flavoring agents and perfumes.<sup>72,73</sup> The asymmetric transfer hydrogenation has become an alternative to the asymmetric hydrogenation due to simplicity, the availability of hydrogen donors and an atomic efficiency of 100 %.<sup>74</sup> The design and development of efficient catalysts is paramount to the achievement of environmentally benign synthetic processes. The efficiency of chiral catalysts is estimated by the activity and enantioselectivity achieved by the complex. The activity and selectivity can be modified by fine-tuning the steric bulk; chirality and electronic properties of the ligands coordinated to, on the metal complex. This section reviews the development of transition metal compounds based on various chiral ligands as catalysts in the asymmetric transfer hydrogenation of ketones.

#### 1.3.1 Asymmetric transfer hydrogenation using ruthenium(II) complexes

In the 1990's, Noyori and Ikayira introduced chiral catalysts suitable for the asymmetric transfer hydrogenation of ketones.<sup>75-66</sup> The C<sub>2</sub>-symmetric diphosphine/diamine based ruthenium(II) complex **1-XXVIII** (Figure 1.17) is an excellent activity in the asymmetric transfer hydrogenation of acetophenone, producing optically enriched (R)-1-phenylethanol in 93 % yield with 97 % enantiomeric excess (*ee*).<sup>76</sup> The complexes **1-XXVIII** and **1-XXIX** both contains phosphine and nitrogen donor ligands that stabilize the complexes, and give the chirality of the complexes (Figure 1.17). The catalyst achieves high enantiomeric excess (>97 %) in the asymmetric reduction of aromatic ketones and its actually compares well with the related catalyst of ruthenium(II).<sup>75,76</sup>

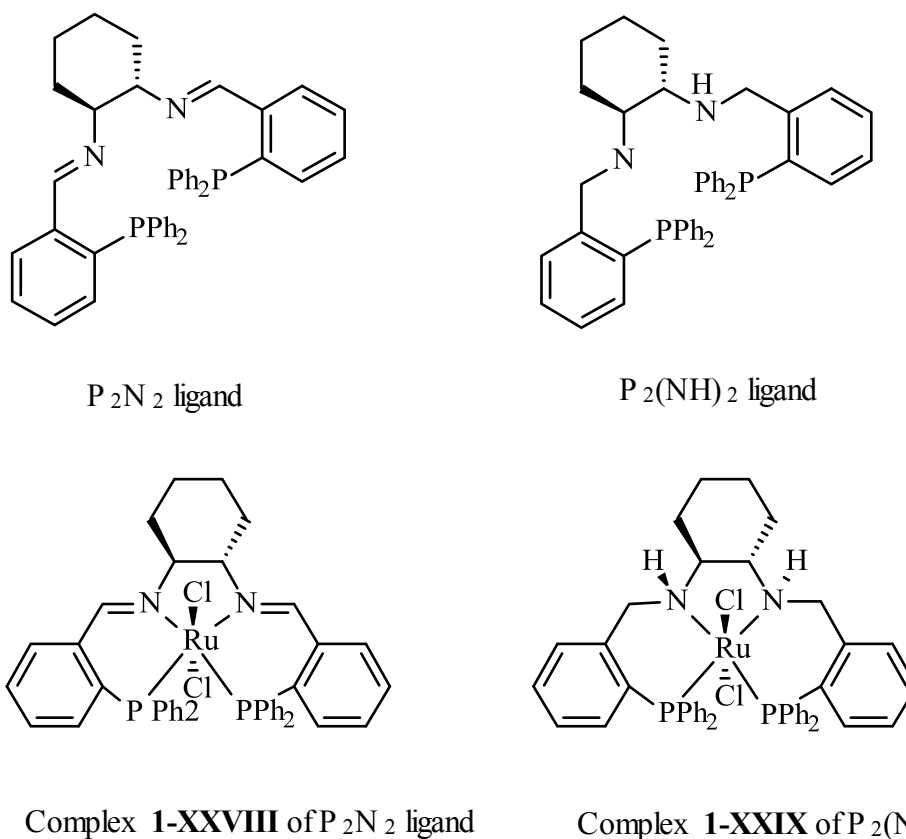


**Figure 1.17.** The SS-configuration of ruthenium(II) chloride complexes **XXVIII** and **XXIX** from their respective ligands.<sup>76</sup>

Among the best catalysts for the asymmetric transfer hydrogenation of ketones discovered, are the chiral BINAP catalysts reported by Noyori and co-workers.<sup>77</sup> The chiral diphosphine/1,2-diamine-ruthenium(II) complexes **1-XXX** shown in Figure 1.18 is selective and efficient chiral catalysts for the asymmetric transfer hydrogenation of acetophenone affording 99 % conversion and 99 % *ee*.<sup>78</sup>

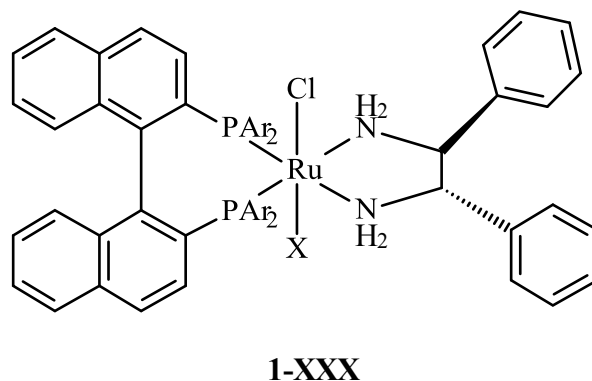
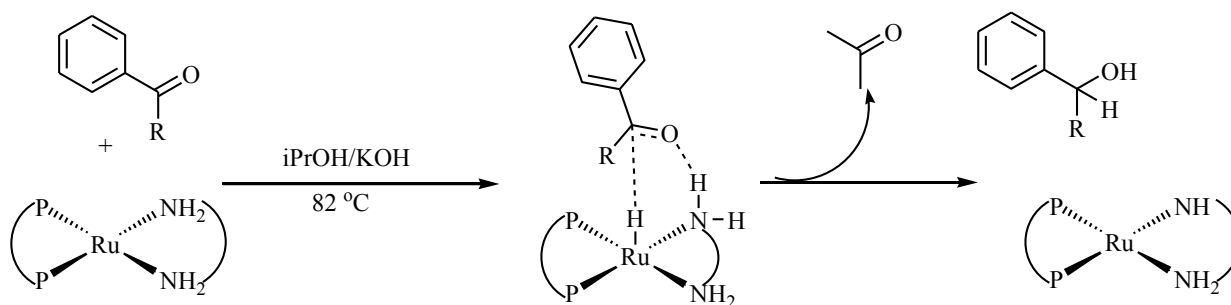


**Figure 1.18.** General structure of Noyori's second generation BINAP ruthenium(II) catalyst.<sup>78</sup>

The ruthenium(II) catalysts **1-XXIX** and **1-XXX** shown in Figures 1.17 and 1.18 respectively display similar structural features containing the chiral amino-phosphine ligands, which are reported to be responsible for their catalytic activities. This is due to the nature of transition state for dihydrogen transfer to the ketone<sup>79</sup> (Scheme 1.6), by the "N-H" moiety which is necessary for an efficient transfer of hydrogen from the ligand.<sup>76</sup> Consistent with this explanation, the related complex **1-XXVIII** without the "N-H" functionality is less active and also non-selective.



**Scheme 1.6.** The transition state for the transfer of a proton and hydride from the metal complex to the ketone substrate.

On the other hand, the ruthenium(II) complex **1-XXXI** in Figure 1.19 containing the (oxazolyl-pyridyl)benzimidazole-based NNN ligand does not feature “N-H” functionality but exhibits a high catalytic activity in the asymmetric transfer hydrogenation of different ketones.<sup>80</sup> This catalyst gives 96 % conversion of acetophenone with 79 % *ee*, and achieves a final TOF of up to 14 400 h.<sup>-1</sup> The high catalytic activity of the catalyst may be attributed to its high stability.

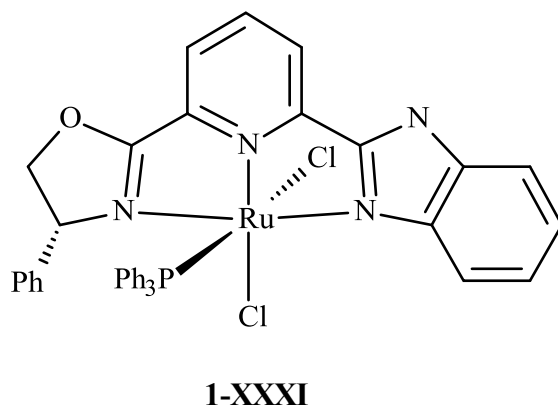


**Figure 1.19.** Chiral ruthenium(II) complex lacking the “N-H” functionality on the (oxazolyl-pyridyl)benzimidazole-based NNN ligand.<sup>80</sup>

The development of new chiral catalysts for the asymmetric transfer hydrogenation is still receiving significant attention. Recently, ruthenium(II) complexes supported by the chiral P<sup>^</sup>N bidentate ligands (**1-XXXII**) have been applied in the asymmetric transfer hydrogenation of ketones (Figure 1.20).<sup>81</sup> The asymmetric transfer hydrogenation of propiophenone catalyzed by chiral ruthenium(II) complex **1-XXXII** under mild conditions affords the corresponding chiral R-propiophenol of up to 99 % conversion and 60 % *ee*.<sup>81</sup>

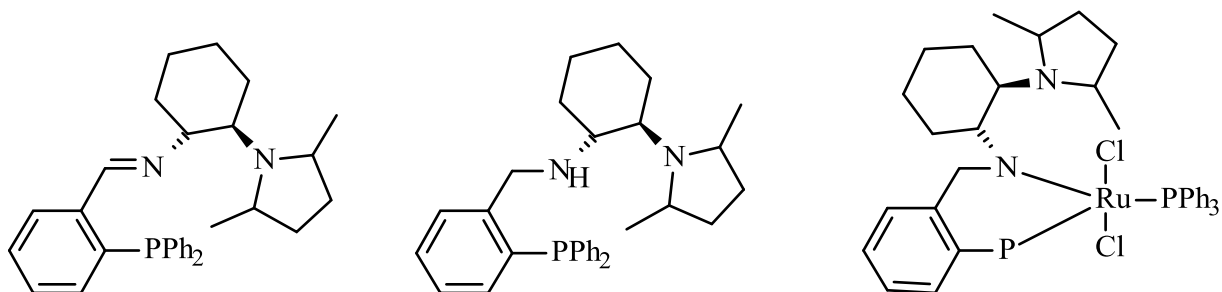


**Figure 1.20.** Two of The chiral P<sup>N</sup> ligands and a chiral ruthenium(II) complex with an (R,R) configuration.

### 1.3.2 Asymmetric transfer hydrogenation of ketones using nickel(II) and iron(II) complexes

The asymmetric reduction of ketones by transfer of hydrogen catalysed by metal complexes receives more attention as the method prepares valuable enantioenriched products. Mikhailine and co-workers<sup>82</sup> developed the iron(II) based complex **1-XXXIII** containing an (S,S)-Ph<sub>2</sub>PCH<sub>2</sub>CH=NCHPhN=CHCH<sub>2</sub>PPh<sub>2</sub> ligand (Figure 1.21). The asymmetric transfer hydrogenation of acetophenone by this catalyst achieves TOF of 55 000 h<sup>-1</sup> and *ee* of 82 % (R). In a similar report by Lagaditis *et al.*,<sup>83</sup> the iron(II) complex **1-XXXIV** of the diiminodiphosphine ligand (Figure 1.21) displays high catalytic activity for the asymmetric transfer hydrogenations of acetophenone with the TOF of greater than 3600 h<sup>-1</sup> to give (S)-1-phenylethanol with 82 % *ee*.

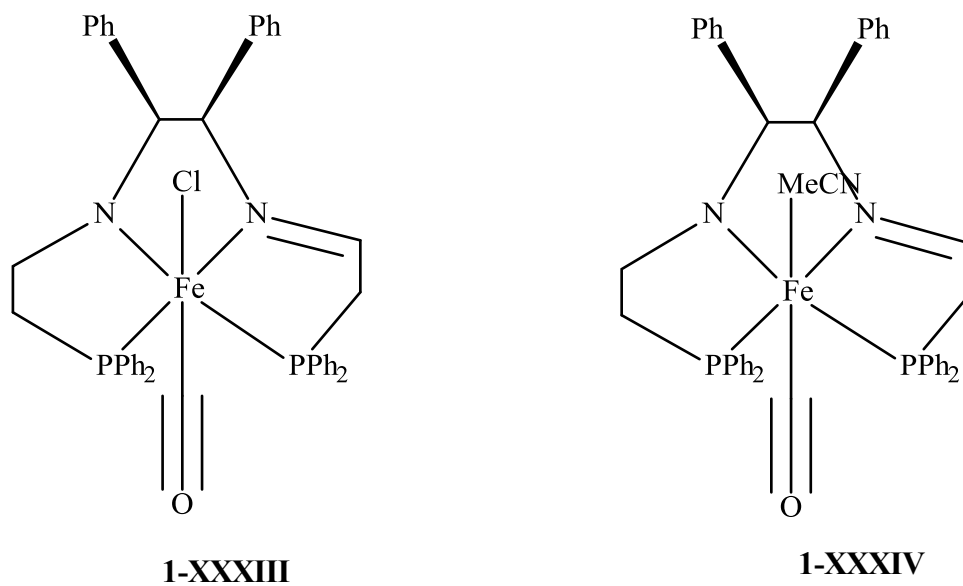


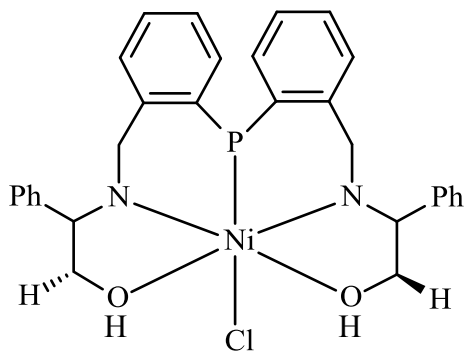
**Figure 1.21.** The iron(II) complexes **1-XXXIII** and **1-XXXIV** from the chiral diaminodiphosphine ligands employed in ATHK.<sup>82,83</sup>

Similarly, complex **1-XXXIII** (R,R) shows enantioselectivities in the reduction of acetophenone to (S)-1-phenylethanol as high as 82 % with a TOF of 3 600 h.<sup>-184</sup> It has been argued that the axial carbonyl ligand is necessary for the catalytic activity in the transfer hydrogenation of acetophenone.<sup>83</sup>

A series of iron(II) complexes bearing tetradentate ligands with two phosphine and nitrogen donor atoms are observed to be highly active in the asymmetric transfer hydrogenation of ketones,<sup>85</sup> affording TOF of 242 s<sup>-1</sup> for acetophenone. This activity exceeds those observed for similar ruthenium(II) based catalysts.<sup>86,87</sup> The *ee* of the products were as high as 98 % giving pure R or S alcohol products.<sup>85</sup>

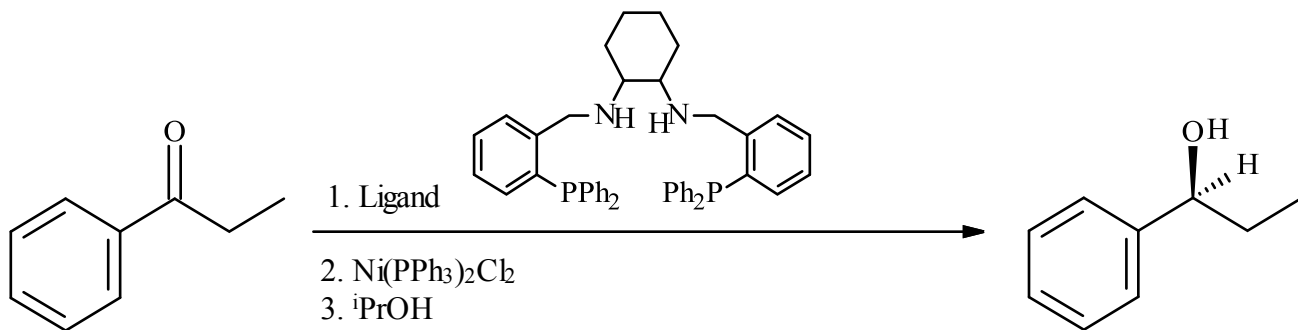
Chiral nickel(II) complexes are also emerging as potential catalysts in the asymmetric transfer hydrogenation of ketones.<sup>88-90</sup> Recently, nickel(II) complexes supported by chiral P<sup>^</sup>N<sup>^</sup>O

ligands, **1-XXXV**, (Figure 1.22) have been used as catalysts in the asymmetric transfer hydrogenation of a series of aromatic ketones using isopropanol as the source of hydrogen.<sup>89</sup> Under mild conditions, 93 % conversion of acetophenone and 84 % *ee* is obtained. However, to date there are few reports on asymmetric transfer hydrogenations of ketones using nickel(II) catalysts.<sup>88-90</sup> In a different system (Scheme 1.7), the nickel(II) complex supported by a P<sup>^</sup>N<sup>^</sup>P ligand efficiently catalyzes the asymmetric transfer hydrogenation of propiophenone and achieves 16 % conversion in 20 h with a 68 % *ee*.<sup>90</sup>



**1-XXXV**

**Figure 1.22.** Nickel complex of P<sup>^</sup>N<sup>^</sup>O ligands used in ATH.<sup>89</sup>



**Scheme 1.7.** The transfer hydrogenation of propiophenone using nickel(II) pre-catalyst anchored on N<sup>^</sup>P<sup>^</sup>N type chiral ligands.<sup>87</sup>



#### **1.4 Problem identification**

Effective catalytic systems include those which are inexpensive, highly active and selective towards the targeted product. Many catalysts based on transition metals for the transfer hydrogenation of ketones have been developed and commercially applied. Ruthenium(II) complexes are the mostly widely used catalysts in the transfer hydrogenation of ketones due to their high catalytic activity and selectivity. However, ruthenium(II) compounds are expensive, difficult to synthesize and unstable. The design and development of systems which are less expensive but more active, offering comparable catalytic activities to ruthenium(II) systems is therefore a challenge to researchers in the field of homogeneous catalysis.

#### **1.5 Rationale and justification of the study**

The application of nickel(II) and iron(II) complexes supported by (pyrazolylmethyl)pyridine ligands as catalysts in the transfer hydrogenation of ketones will lead to reduced costs of the catalysts comparable to the cost of ruthenium(II) catalysts. The choice of nickel(II) and iron(II) as central atoms is expected to improve stability and complexes/catalysts that are tolerant to impurities and easier to handle compared to the less stable ruthenium(II) compounds. In this project, it is aimed to develop active nickel(II) and iron(II) catalysts that are cheaper and stable in the transfer hydrogenation of ketones that can offer comparable catalytic activities and be used as suitable alternatives to the well-established ruthenium(II) catalysts.

## 1.6 Aims of the project

The general goal of this research project is to synthesize nickel(II) and iron(II) complexes of bis(pyrazolylmethyl)pyridine ligands and investigate their potential in the transfer hydrogenation of ketones.

The specific objectives can thus be postulated as follows:

- To synthesize nickel(II) and iron(II) complexes of (pyrazolyl)pyridine ligands
- To structurally characterize the new compounds using appropriate analytical techniques.
- To investigate the potential of the isolated complexes as catalysts in the transfer hydrogenation of ketones.
- To study the effects of reaction conditions such as temperature, catalyst concentration, nature of substrate and base on the transfer hydrogenation of ketones.

## 1.7 References

- 
1. G.V. Johannes, J. E. Cornelis., *The Handbook of Homogeneous Hydrogenation*, WILEY-VCH, 2007.
  2. S. Baghbanian, S. Meysam, F.Maryam, Vandat, S. Mohammad, *J. Mol. Catal.*, 2015, **407**, 128-136.
  3. S. Musa, A. Ghosh, L. Vaccaro, *Adv. Synth. Catal.*, 2015, **357**, 2351-2357.
  4. S. Hashiguchi, A. Fujii, J. Takehara, T. Ikariya, R. Noyori, *J. Am. Chem. Soc.* 1995, **117**, 7562-7563.

- 
5. N. Uematsu, A. Fujii, S. Hashiguchi, T. Ikariya, R. Noyori, *J. Am. Chem. Soc.* 1996, **118**, 4916-4917.
  6. A. Gyoemoere, M. Bakos, T. Foeldes, *ACS Catal.*, 2015, **5**, 5366-5372.
  7. T. Ikariya, A.J. Blacker, *Acc. Chem. Res.*, 2007, **40**, 1300-1308.
  8. A. Zanotti-Gerosa, W. Hems, M. Groarke, F. Hancock, *Platinum Met. Rev.*, 2005, **49**, 158-165.
  9. Y. Y. Li, S.L. Yu, W. Y. Shen, *Acc. Chem. Res.*, 2015, **48**, 2587-2598.
  10. R. Noyori, *Asymmetric catalysis in organic synthesis*; Wiley; New York, 1994.
  11. S. Mazza, R. Scopelliti, X.Hu, *Organometallics*, 2015, **34**, 1538-1545.
  12. D. M. Luisa; L. Antonella; G. I. Federica, *Tetrahedron Lett.*, 2015, **56**, 5341-5344.
  13. Z. Behzad; Z. Mehdi, *J. Iran. Chem. Soc.*, 2015, **12**, 1221-1226.
  14. L. Cointeaux, A. Alexakis, *Tetrahedron Asymm.*, 2005, **16**, 925-929.
  15. Y. Liu, C.S Da, S.L. Yu, *J. Org. Chem.*, 2010, **75**, 6869-6878.
  16. C. P. Casey, H. Guan, *J. Am. Chem. Soc.*, 2007, **129**, 5816-5828.
  17. a). H. Meerwein, R. Schmidt, *Justus Liebigs Ann. Chem.* 1925, **444**, 221-230. b). A. Verley, *Bull. Soc. Fr.*, 1925, **37**, 5537-5548. c). W. Ponndorf, *Angew. Chem. Int. Ed.*, 1926, **39**, 138-142.
  18. L. Delaude, A. Demanceau, A. F Noels. *Curr. Org. Chem.*, 2006, **10**, 203-215.
  19. a). W. Du, Q. Wang, L. Wang, Z. Yu. *Organometallics*, 2014, **33**, 974-982. b). W. M. Du, Q. F Wang, Z. K Yu. *Chin. J. Catal.*, 2013, **34**, 1373-1385.
  20. M. Zhao, Z. Yu, S. Yan, Y. Li, *J. Organomet. Chem.*, 2009, **694**, 3068-3075.
  21. T. D. Nixon, M. K. Whittlesey, J. M. J. Williams, *Tetrahedron Lett.*, 2011, **52**, 6652-6654.
  22. S. Gladiali, R. Taras, P. G. Andersson, I. J. Munslow, *Modern Reduction Methods*,

---

Wiley-VCH, Weinheim, 2008, p. 135.

23. S. Gladiali, E. Alberico. *Chem. Soc. Rev.*, 2006, **35**, 226-236.
24. A. J. Birch, D. H. Williamson., *Org. React.*, 1976, **24**, 1-186.
25. R. Noyori, S. Hashuguchi, *Acc. Chem. Res.*, 1997, **30**, 97-102.
26. M. Yamakawa, H. Ito, R. Noyori, *J. Am. Chem. Soc.* 2000, **122**, 1466-1478.
27. C. A. Sandoval, T. Ohkuma, K. Muniz, R. Noyori, *J. Am. Chem. Soc.*, 2003, **125**, 13490-13503.
28. A. Gyoemoere, M. Bakos, T. Foeldes, *ACS Catal.*, 2015, **5**, 5366-5372.
29. R. N. Prabhu, R. Ramesh, *J. Organomet. Chem.*, 2012, **718**, 43-51.
30. L-P. He, T. Chen, D-X. Xue, M. Eddaoudi, K-W. Huang, *J. Organomet. Chem.*, 2012, **700**, 202-206.
- 31.a) R. Noyori, M. Yamakawa, S. Hashiguchi, *J. Org. Chem.*, 2001, **66**, 7931-7945. b) M. Yamakawa, H. Ito, R. Noyori, *J. Am. Chem. Soc.*, 2000, **122**, 1466-1472.
32. R. Noyori, S. Hashiguchi, *Acc. Chem. Res.*, 1997, **30**, 97-109.
33. J. S. M. Samec, J-E. Backvall, P. G. Andersson, P. Brandt, *Chem. Soc. Rev.*, 2006, **35**, 237-250.
34. M. Bullock, *Angew. Chem. Int. Ed.* 2007, **46**, 7360-7363.
35. D. Pandiarajan, R. Ramesh. *J. Organomet. Chem.*, 2013, **723**, 26-35.
36. T. Ikariya, A. J. Blacker, *Acc. Chem. Res.*, 2007, **40**, 1300-1308.
37. J.Vaclavik, P. Sot, B. Vilhanova, J. Pechacek, M. Kuzma , P. Kacer, *Molecules*, 2013, **18**, 6804-6828
38. N. A. Cortez, G. Aguirre, M. Parra-Hake, R. Somanathan, *Tetrahedron Asymm.* 2013, **24**, 1297-1302.

- 
39. P. J. Wals, M. C. Kozlowski, *Fundamentals of asymmetric catalysis*, 1971, Ed **1**, pg 80
40. L. Wang, H-R. Pan, Q. Yang, H-Y. Fu, H. Chen, R-X. Li, *Inorg. Chem. Commun.*, 2011, **14**, 1422-1427.
41. C. Sui-Seng, F. Freutel, A. J. Lough, R. H. Morris, *Angew. Chem. Int. Ed.*, 2008, **120**, 954-957.
42. J. M. Walker, A. M. Cox, R. Wang, G. J. Spivak, *Organometallics*, 2010, **29**, 6129-6124.
43. Q. Fu, L. Zhang, T. Yi, M. Zou, X. Wang, H. Fu, R. Li, H. ua Chen, *Inorg. Chem. Commun.*, 2013, **38**, 28-32.
44. W. Baratta, P. Rigo, *Eur. J. Inorg. Chem.* 2008, 4041-4043
45. R. Ramachandran, G. Prakash, M. Nirmala, P. Viswanathamurthi, J. G. Malecki, *J. Organomet. Chem.*, 2015, **971**, 130-140.
46. P. Braunstein, M. D. Fryzuk, F. Nauda, S. J. Rettig. *J. Chem. Soc., Dalton Trans.*, 1999, **589**, 589-594.
47. Z. Chen, M. Zeng, Y. Zhang, Z. Zhang, F. Liang, *Appl. Organometal. Chem.*, 2010, **24**, 625-630
48. M. D. Fryzuk, M. J. Jonker, S. J. Rettig, *Chem. Commun.*, 1997, **4**, 377-378.
49. Y. Cheng, X-Y. Lu, H-J. Xu, Y-Z. Li, X-T. Chen, Z-L. Xue, *Inorg. Chim. Acta.*, 2010, **363**, 430-437.
50. Y. Cheng, H-J. Xu, J-F. Sun, Y-Z. Li, X-T. Chen, Z-L. Xue, *Dalton Trans.*, 2009, **35**, 7132-7144.
51. P. Dani, T. Karlen, R. A. Gossage, S. Gladiali, G. van Koten, *Angew. Chem., Int. Ed.*, 2000, **39**, 743-755.
52. J. I. Ito, H. Nishiyama, *Tetrahedron Lett.*, 2014, **55**, 3133-3146.

- 
53. W. Baratta, G. Chelucci, S. Magnolia, K. Siega, P. Rigo, *Chem. Eur. J.*, 2009, **15**, 726-733.
54. a) N. Uematsu, A. Fujji, S. Hashiguchi, T. Ikayira, R. Noyori, *J. Am. Chem. Soc.*, 1996, **118**, 4916-4930. b) N. Uematsu, A. Fujji, S. Hashiguchi, T. Ikayira, R. Noyori, *J. Am. Chem. Soc.*, 1996, **118**, 2521-2532.
55. F. Zeng, Z. Yu., *Organometallics*, 2009, **28**, 1855-1862
56. N. J Beach, G. J Spivak, *Inorg. Chim. Acta.*, 2003, **343**, 244-260.
57. C. Ahmet, D. Osman, *Chin. J. Chem.*, 2009, **27**, 972-982.
58. A. O. Ogwenio, S. O. Ojwach, M. P. Akerman, *Dalton Trans.*, 2014, **43**, 1228-1237
59. C. P. Casey, H. Guan, *J. Am. Chem. Soc.* 2007, **129**, 5816-5817.
60. G. P Boldrini, D. Savoia, E. Tagliavini, C. Trombini, A. Umani-Ronchi, *J. Org. Chem.*, 1985, **50**, 3082-3086.
61. T. Hashimoto, S. Urban, R. Hoshino, Y. Ohki, K. Tatsumi, F. Glorius, *Organometallics*, 2012, **31**, 4474-4479.
62. J. P. Collman, L. S. Hegedus, J. R. Norton, R. G. Finke, *Principles and Applications of Organotransition Metal Chemistry*, University Science Book, CA, 1987
63. R. Langer, G. Leitus, Y. Ben-David, D. Milstein. *Angew. Chem. Int. Ed.*, 2011, **123**, 2168-2172.
64. P. L. Chiu, H. M. Lee, *Organometallics*, 2005, **24**, 1692-1702.
65. T. Hashimoto, S. Urban, R. Hoshino, Y. Ohki, K. Tatsumi, F. Glorius, *Organometallics*, 2012, **31**, 4474-4479.
66. J. He, M. Zeng, H. Cheng, Z. Chen, F. Liang, *Anorg. Allg. Chem.*, 2013, **639**, 1834-1839.
67. M. U Raja, R. Ramesh, K. H. Ahn, *Tetrahedron Lett.*, 2009, **50**, 7014-7017.

- 
68. W. Baratta, M. Ballico, G. Chelucci, K. Siega, P. Rigo, *Angew. Chem. Int. Ed.*, 2008, **47**, 4362-4375.
69. F. Foubelo, C. Najera, M. Yus, *Tetrahedron Asymm.*, 2015, **26**, 769-790.
70. W. Baratta, G. Bossi, E. Putignano, P. Rigo, *Chem. Eur. J.* 2011, **17**, 3474-3481.
71. A. Matsunami, Y. Kayaki, T. Ikariya, *Chem. Eur. J.*, 2015, **21**, 13513-13517
72. R. Noyori, *Angew. Chem. Int. Ed.*, 2002, **41**, 2008-2015
73. M. B. Valenzuela, S. D. Phillips, M. B. France, M. E. Gunn, M. L. Clarke, *Chem. Eur. J.*, 2009, **15**, 1227-1232.
74. J. Mao, B. Wan, f. Wu, S. Lu, *Tetrahedron Lett.*, **2005**, **46**, 7341-7344
75. S. Hashiguchi, A. Fujii, J. Takehara, T. Ikariya, R. Noyori, *J. Am. Chem. Soc.*, 1995, **117**, 7562-7563.
76. J. Gao, T. Ikariya, R. Noyori, *Organometallics*, 1996, **15**, 1087-1089.
77. a) R. Noyori, T. Ohkuma, *Pure Appl. Chem.*, 1999, **71**, 1493-1501 b) R. Noyori, *Adv. Synth. Catal.*, 2003, **345**, 15-32.
78. C.A. Sandoval, T. Ohkuma, K. Muniz, R. Noyori, *J. Am. Chem. Soc.*, 2003, **125**, 1349-1353
79. R. Morris, *Chem. Soc. Rev.*, 2009, **38**, 2282-2291.
80. W. Ye, M. Zhao, W. Du, Q. Jiang, K. Wu, P. Wu, Z. Yu, *Chem. Eur. J.*, 2011, 4737-4741.
81. L. Zeng, F. Wu, Y. Li, Z. Dong, J. Gao, *J. Organomet. Chem.*, 2014, **762**, 34-39.
82. A. A. Mikhailine, M. I. Maishan, A. J. Lough, R. H. Morris, *J. Am. Chem. Soc.*, 2012, **134**, 12266-12270.
83. P. O. Lagaditis, A. J. Lough, R. H Morris. *Inorg. Chem.*, 2010, **49**, 1057-1066.
84. A. Mikhailine, A. J. Lough, R.H Morris, *J. Am. Chem. Soc.*, 2009, **131**, 1394-1395.

- 
85. P. E. Sues, K. Z. Demmans, R. H. Morris, *Dalton Trans.*, 2014, **43**, 7650-7667.
86. W. Zuo, A. J. Lough, Y. F. Li, R. H. Morris, *Science*, 2013, **342**, 1080-1083.
87. T. Ikariya, A. J. Blacker, *Acc. Chem. Res.*, 2007, **40**, 1300-1308.
88. T. Hashimoto, S. Urban, R. Hoshino, Y. Ohki, K. Tatsumi, F. Glorius, *Organometallics*, 2012, **31**, 4474-4479.
89. G. P. Boldrini, D. Savoia, E. Tagliavini, C. Trombini, A. Umani-Ronchi. *J. Org. Chem.*, 1985, **50**, 3082-3086.
90. Z. R. Dong, Y. Y. Li, S. L. Yu, G. S. Sun, J. X. Gao., *Chin. Chem. Lett.*, 2012, **23**, 533-536.



## CHAPTER TWO

### **Transfer hydrogenation of ketones mediated by (pyrazolylmethyl)pyridine nickel(II) & iron(II) complexes: Influence of complex structure on catalytic activity.**

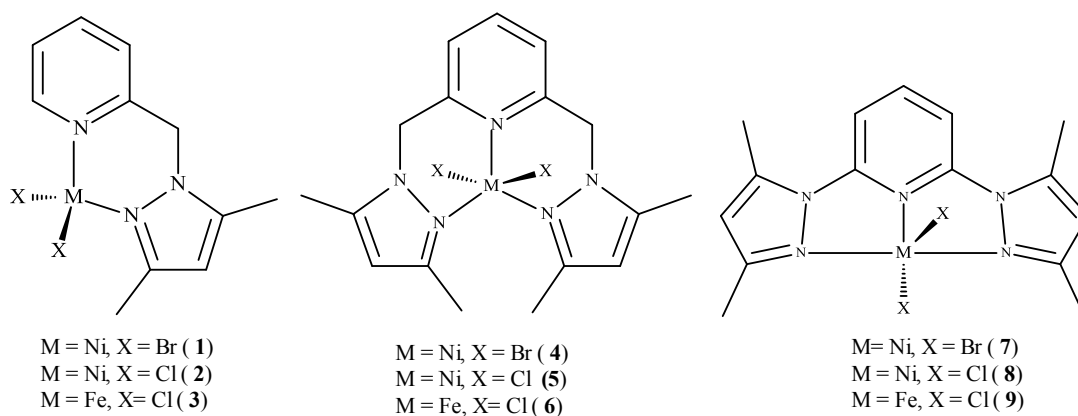
#### **2.1 Introduction**

Transfer hydrogenation of ketones is one of the most used processes for the reduction of ketones to secondary alcohols due to its high selectivity and efficiency.<sup>1</sup> Transfer hydrogenation reactions are mostly applied in industries for the synthesis of fine chemicals, pharmaceutical products, agrochemicals, fragrances and cosmetics.<sup>2-4</sup> This reaction is usually catalyzed by homogeneous transition-metal complexes in the presence of a base and an alcohol as the source of hydrogen. To date, the most commonly used and effective transition-based catalysts are derived from ruthenium compounds.<sup>5,6</sup> An example of a highly active ruthenium(II) complex contains the 2-(benzoimidazole-2-yl)-6-(pyrazol-1-yl)pyridine ligand.<sup>7</sup> Another nitrogen-donor ruthenium(II) complex that has been investigated in the transfer of hydrogenation of ketones is 2,6-bis(3,5-dimethylpyrazol-1-yl)pyridine complex reported by Spivak *et. al.*<sup>8</sup> This complex contains a potentially tridentate planar ligand and exhibits very high catalytic activities in the transfer hydrogenation of a range of ketone substrates.<sup>9</sup>

However as mentioned previously, ruthenium is very expensive and therefore not economically suitable for industrial applications. In addition, it forms complexes with poor stability.<sup>10</sup> Thus the development of alternative metal catalysts that are relatively cost effective and environmentally benign such as nickel(II)<sup>11</sup> and iron(II)<sup>12</sup> for the transfer of hydrogenation of ketones is a valuable area of research. For instance, precatalyst/precursors nickel and iron are cheaper, more abundant and stable compared to ruthenium.<sup>13</sup> Meyer *et. al.* reported iron(II) compounds of diiminodiphosphine ligands as effective catalysts in the transfer hydrogenation of ketones.<sup>14</sup> In another development, Morris and co-workers recently reported highly active

iron(II) complexes containing unsymmetrical P–N–P pincer ligands as catalysts for the asymmetric transfer hydrogenation of ketones and imines.<sup>15</sup> On the other hand, Milstein and his group<sup>16</sup> reported pyridine pincer based iron(II) complex as catalysts in the transfer hydrogenation of ketones.

Nickel(II) complexes are also emerging as potential catalysts in the transfer hydrogenation of ketones. To date, the majority of nickel(II) catalysts employed in the transfer hydrogenation are heterogeneous.<sup>17-19</sup> Recently, homogenous nickel(II) complexes have been used as catalysts for the transfer hydrogenation of ketones.<sup>11,20,21</sup> For example, Dong *et. al.* have reported the use of nickel(II) complexes supported by P<sup>^</sup>N<sup>^</sup>O ligands as catalysts in the asymmetric transfer hydrogenation of a series of ketones.<sup>22</sup> This chapter, reports the use of nickel(II) and iron(II) complexes containing (pyrazolyl)pyridine ligands (Scheme 2.1) as catalysts in the transfer hydrogenation of ketones.



**Scheme 2.1.** Nickel(II) and iron(II) complexes used as catalysts in the transfer hydrogenation of ketones in this chapter.

## 2.2 Experimental

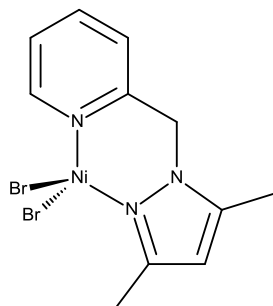
### 2.2.1 General methods and instrumentation

All reagents and solvents were obtained from Sigma-Aldrich. The starting materials NiCl<sub>2</sub>, NiBr<sub>2</sub>, FeCl<sub>2</sub>·4H<sub>2</sub>O, isopropanol, absolute ethanol and deuterated solvents were used as received without further purification. The 2-pyrazolyl(methyl)pyridine (**L1**) and 2,6-bis-(pyrazolylmethyl)pyridine (**L2**) ligands were prepared following literature procedures.<sup>23</sup> The 2,6-bis(3,5-dimethylpyrazolyl)pyridine (**L3**) ligand was prepared according to literature.<sup>24</sup> Dichloromethane was dried over P<sub>2</sub>O<sub>5</sub> and distilled prior to use. NMR spectra were recorded on a Bruker 400 MHz (<sup>1</sup>H) and a 100 MHz (<sup>13</sup>C) spectrometer. All chemical shifts were reported in δ (ppm). Elemental analyses were performed on Thermal Scientific Flash 2000 and mass spectra were recorded on LC Premier micro-mass Spectrometer. Magnetic moment measurements were performed in an Evans balance.

### 2.2.2 Synthesis of nickel(II) and iron(II) complexes

#### 2.2.2.1 Synthesis of [*2*-(3,5-dimethylpyrazolyl)pyridine]NiBr<sub>2</sub> (**1**)

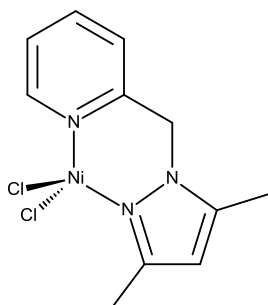
To a solution of NiBr<sub>2</sub> (0.12 g; 0.53 mmol) in CH<sub>2</sub>Cl<sub>2</sub> (10 mL) was added a solution of **L1** (0.10 g ; 0.53 mmol) in CH<sub>2</sub>Cl<sub>2</sub> (10 mL). An orange mixture was formed immediately. The mixture was stirred for 24 h at room temperature forming a solid (blue) which was filtered, air dried and weighed. Yield = 0.09 g (73 %). (ESI-MS), *m/z* (% abundance) 326 (M<sup>+</sup>-Br, 91 %), 188 (M<sup>+</sup>-NiBr<sub>2</sub>, 100 %). μ<sub>eff</sub> = 2.89 BM. Anal. Calcd. for C<sub>11</sub>H<sub>13</sub>Br<sub>2</sub>N<sub>3</sub>Ni: C, 32.56; H, 3.23; N, 10.36. Found C, 32.18, H, 4.57, N, 10.06.



Complexes **2-9** were prepared according to procedure described for complex **1** and the results are presented in the subsections that follow.

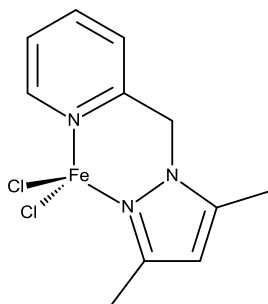
#### 2.2.2.2 Synthesis of $[\{2-(3,5\text{-dimethylpyrazolyl})\text{pyridine}\}\text{NiCl}_2]$ (**2**).

$\text{NiCl}_2$  (0.69 g; 0.53 mmol) and **L1** (0.10 g; 0.53 mmol) were used. Blue powder. Yield = 0.11 g (61 %). (ESI-MS),  $m/z$ (% abundance) 188 ( $\text{M}^+ - \text{NiCl}_2$ , 100 %).  $\mu_{\text{eff}} = 3.08$  BM. Anal. Calcd. for  $\text{C}_{11}\text{H}_{13}\text{Cl}_2\text{N}_3\text{Ni}$ : C, 41.70; H, 4.14; N, 13.26. Found C, 42.05, H, 5.48, N, 13.03.



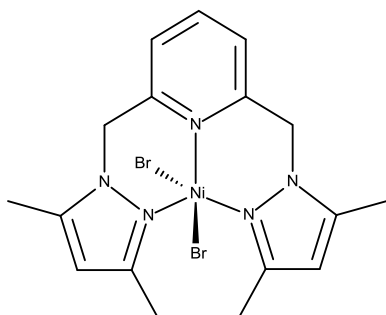
#### 2.2.2.3 Synthesis of $[\{2-(3,5\text{-dimethylpyrazolyl})\text{pyridine}\}\text{FeCl}_2]$ (**3**).

$\text{FeCl}_2$  (0.11 g; 0.53 mmol) and **L1** (0.10 g; 0.53 mmol) were used. Green powder. Yield = 0.12 g (73 %). (ESI-MS)  $m/z$ (% abundance) 188 ( $\text{M}^+ - \text{NiCl}_2$ , 100 %).  $\mu_{\text{eff}} = 5.01$  BM. Anal. Calcd. for  $\text{C}_{11}\text{H}_{13}\text{Cl}_2\text{N}_3\text{Fe}$ : C, 42.08; H, 4.17; N, 13.38. Found C, 42.16, H, 4.03, N, 13.10.



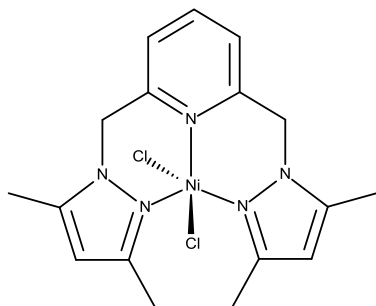
#### 2.2.2.4 Synthesis of $[\{2,6\text{-bis}(3,5\text{-dimethylpyrazolyl})\text{pyridine}\}\text{NiBr}_2]$ (4).

NiBr<sub>2</sub> (0.10 g; 0.46 mmol) and **L2** (0.14 g; 0.46 mmol) (10 mL) were used. Purple powder. Yield = 0.22 g (95 %). (ESI-MS),  $m/z$ (% abundance) 354 ( $M^+$ -Br<sub>2</sub>, 20 %), 340 ( $M^+$ -Br<sub>2</sub>-CH<sub>3</sub>, 18 %).  $\mu_{\text{eff}}$  = 3.05 BM. Anal. Calcd. for C<sub>17</sub>H<sub>21</sub>Br<sub>2</sub>N<sub>5</sub>Ni: C, 36.10; H, 3.87; N, 11.70. Found C, 35.86, H, 5.56, N, 11.99.



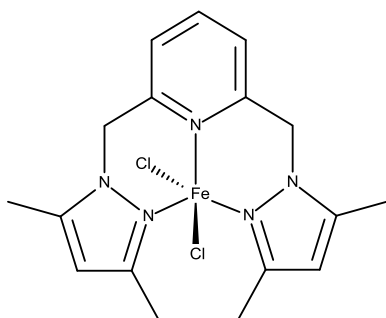
#### 2.2.2.5 Synthesis of $[\{2,6\text{-bis}(3,5\text{-dimethylpyrazolyl})\text{pyridine}\}\text{NiCl}_2]$ (5).

NiCl<sub>2</sub> (0.10 g; 0.77 mmol) and **L2** (0.23 g; 0.77 mmol) were used. Blue powder. Yield = 0.30 g (92 %). (ESI-MS),  $m/z$ (% abundance) 355 ( $M^+$ - Cl<sub>2</sub>, 3 %), 340 ( $M^+$ -Cl<sub>2</sub>-CH<sub>3</sub>, 18 %).  $\mu_{\text{eff}}$  = 3.79 BM Anal. Calcd. for C<sub>17</sub>H<sub>21</sub>Cl<sub>2</sub>N<sub>5</sub>Ni, C, 42.40; H, 4.55; N,13.73. Found C, 42.40, H, 5.65, N, 14.13.



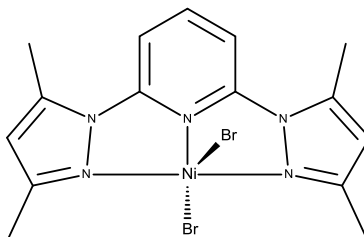
#### 2.2.2.6 Synthesis of [*2,6-bis(3,5-dimethylpyrazolyl)pyridine*]FeCl<sub>2</sub> (6).

FeCl<sub>2</sub> (0.10 g; 0.50 mmol) and **L2** (0.15 g; 0.50 mmol) were used. Yellow powder. Yield = 0.19 g (90 %). (ESI-MS), *m/z*(% abundance) 370 (M<sup>+</sup>-Cl<sub>2</sub>-CH<sub>3</sub>, 29 %), 352 (M<sup>+</sup>-Cl<sub>2</sub>, 5 %).  $\mu_{\text{eff}}$  = 4.98 BM Anal. Calcd. for C<sub>17</sub>H<sub>21</sub>Cl<sub>2</sub>N<sub>5</sub>Fe: C, 42.64; H, 4.57; N, 13.81. Found C, 42.54, H, 4.26, N, 14.31.



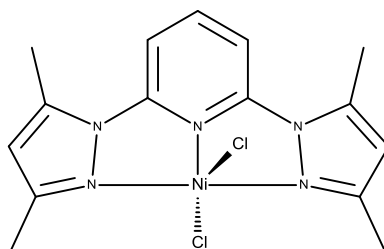
#### 2.2.2.7 Synthesis of [*2,6-bis(3,5-dimethylpyrazolyl)pyridine*]NiBr<sub>2</sub> (7).

NiBr<sub>2</sub> (0.10 g; 0.46 mmol) and **L3** (0.12 g; 0.46 mmol) were used. Green powder. Yield = 0.14 g (63 %). (ESI-MS), *m/z*(% abundance) 406. (M<sup>+</sup>-Br, 100 %), 404 (M<sup>+</sup>-Br, 73.5 %).  $\mu_{\text{eff}}$  = 2.39 BM. Anal. Calcd. for C<sub>17</sub>H<sub>21</sub>Br<sub>2</sub>N<sub>5</sub>Ni: C, 29.44; H, 4.15; N, 11.69. Found C, 29.22, H, 3.38, N, 11.36.



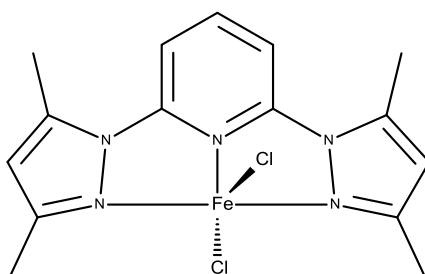
### 2.2.2.8 Synthesis of $[2,6\text{-bis}(3,5\text{-dimethylpyrazolyl})\text{pyridine}]\text{NiCl}_2$ (8).

$\text{NiCl}_2$  (0.10 g; 0.77 mmol) and **L3** (0.21 g; 0.77 mmol) were used. Light green powder. Yield = 0.14 g (47 %). (ESI-MS),  $m/z$ (% abundance) 360 ( $\text{M}^+\text{-Cl}$ , 100 %), 362 ( $\text{M}^+\text{-Cl}$ , 70.8 %), 364 ( $\text{M}^+\text{-Cl}$ , 18.6 %).  $\mu_{\text{eff}} = 2.76$  BM. Anal. Calcd. for  $\text{C}_{17}\text{H}_{21}\text{Cl}_2\text{N}_5\text{Fe}$ : C, 33.30; H, 4.77; N, 12.94. Found C, 33.86, H, 3.89, N, 13.12.



### 2.2.2.9 Synthesis of $[2,6\text{-bis}(3,5\text{-dimethylpyrazolyl})\text{pyridine}]\text{FeCl}_2$ (9).

$\text{FeCl}_2$  (0.10 g; 0.50 mmol) and **L3** (0.13 g; 0.50 mmol) were used. Orange powder. Yield = 0.05 g (68 %) (ESI-MS),  $m/z$ (% abundance) 358 ( $\text{M}^+\text{-Cl}$ , 11 %), 296 ( $\text{M}^+\text{-Cl}_2\text{-2CH}_3$  50 %).  $\mu_{\text{eff}} = 4.52$  BM. Anal. Calcd. for  $\text{C}_{17}\text{H}_{21}\text{Cl}_2\text{N}_5\text{Fe}$ : C, 35.09; H, 3.89; N, 12.03. Found C, 34.90, H, 2.95, N, 12.28.



### 2.2.3 X-ray Crystallography

Single crystal X-ray diffraction studies for complex **4-8** were carried out and the data were recorded on a Bruker Apex Duo equipped with an Oxford Instruments Cryo jet operating at 100(2) K and an Incoatec micro source operating at 30 W power. The data were collected with Mo K $\alpha$  ( $\lambda = 0.71073 \text{ \AA}$ ) radiation at a crystal-to-detector distance of 50 mm. The following conditions were used for the data collection: omega and phi scans with exposures taken at 30 W X-ray power and  $0.50^\circ$  frame widths using APEX2.<sup>25</sup> The data were reduced with the programme SAINT<sup>26</sup> using outlier rejection, scan speed scaling, as well as standard Lorentz and polarization correction factors. A SADABS semi-empirical multi-scan absorption correction was applied to the data. Direct methods, SHELXS-97 and WinGX<sup>20</sup> were used to solve all three structures. All non-hydrogen atoms were located in the difference density map and refined anisotropically with SHELXL-97. All hydrogen atoms were included as idealized contributors in the least squares process. Their positions were calculated using a standard riding model with C-H<sub>aromatic</sub> distances of 0.93  $\text{\AA}$  and  $U_{\text{iso}} = 1.2 \text{ Ueq}$ . The imidazole N-H were located in the difference density map, and refined isotropically.

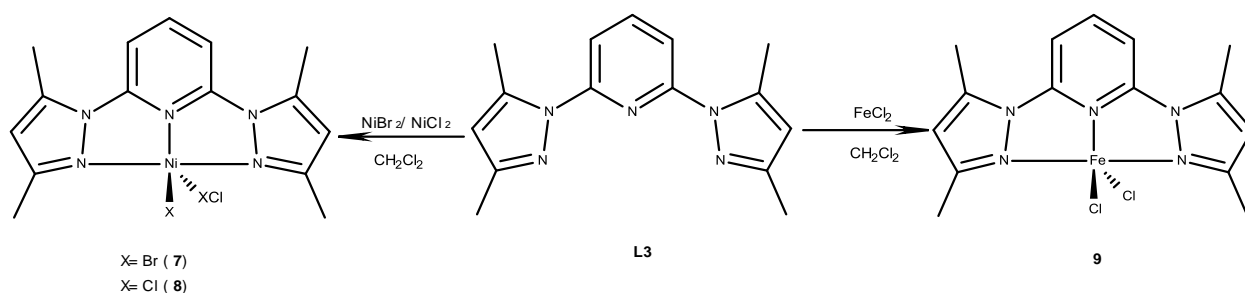
### 2.2.4 Transfer hydrogenation of ketones reactions

The catalytic transfer hydrogenation of ketone was performed in a two-necked round bottom flask under an inert atmosphere. In a typical experiment, **1-9** (0.02 mmol, 1 %), 0.4 M KOH in 2-propanol (5 mL) and acetophenone (0.23 mL, 2.0 mmol) were added and refluxed at 82  $^\circ\text{C}$  under N<sub>2</sub> atmosphere. The samples were taken at regular intervals and the course of the reaction was monitored by <sup>1</sup>H NMR spectroscopy. The percentage conversions were calculated using the <sup>1</sup>H NMR spectra by comparing the intensities of the methyl signal of acetophenone (s,  $\delta$  2.59 ppm) and methyl signal of 2-phenylethanol (d,  $\delta$  1.49 ppm) of the crude products. In all









**Scheme 2.4.** Synthesis of nickel(II) and iron(II) complexes of **L3**.

The effective magnetic moments of complexes **7** and **8** derived from **L3** were generally lower than complexes **1-3** from **L1** and **4-6** from **L2** ligands. The effective magnetic moment of complexes **7** and **8** were 2.39 BM and 2.76 BM, respectively, which is close to the theoretical value of  $2.83^{28}$  for nickel(II) complexes. For complex **9**, the effective magnetic moment was found to be 4.52 BM which is also close to the theoretical value of 4.89 BM expected for low spin iron(II) ( $d^6$ ). The observed magnetic moments were relatively lower than the calculated spin-only magnetic moments and the observed range of high spin nickel(II) and iron(II) reported in literature.<sup>28</sup> This observation signifies a better quench effect of **L3** ligand compared to **L1** and **L2** ligands.<sup>30</sup>

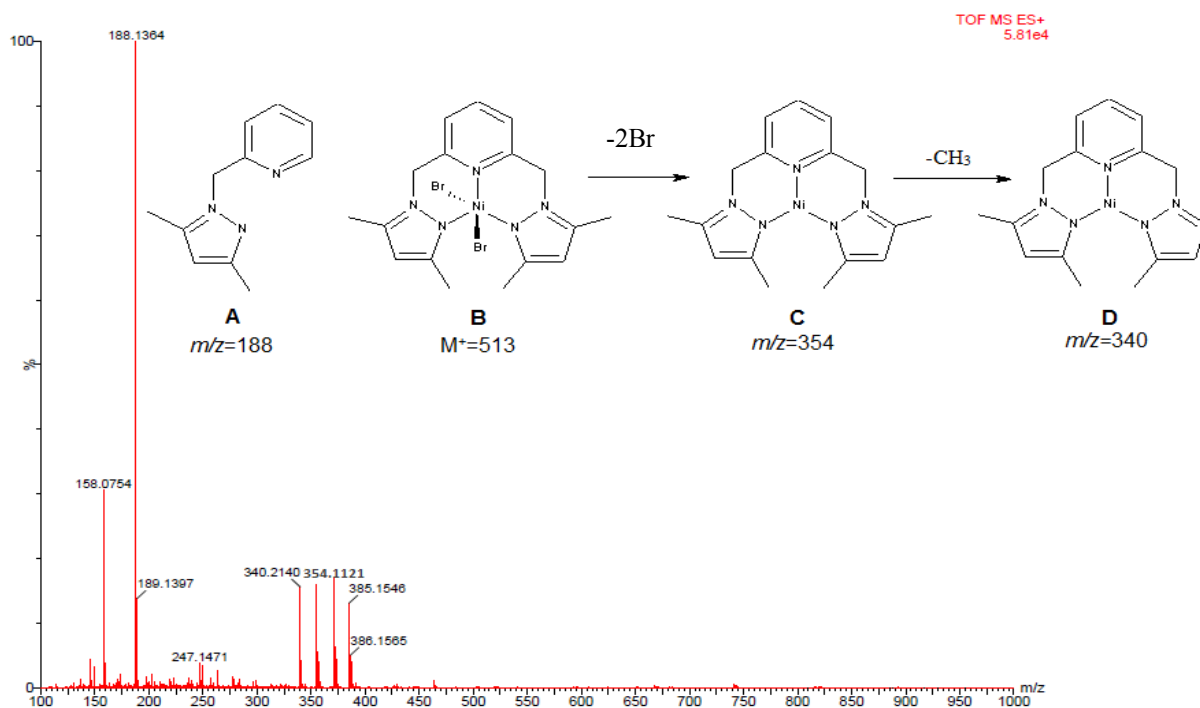


**Figure 2.1:** ESI-MS spectrum showing  $m/z$  peak of the fragments for complex 4.

Mass spectroscopy was also used to elucidate the structure of complexes 1–9 through observed fragmentation patterns. Figure 2.1 shows the mass spectrum of complex 4. Fragmentation produced from A gives B and C with  $m/z$  of 354 and 340 corresponds to  $[M^+ - 2Br]$  and  $[M^+ - (2Br, +CH_3)]$  respectively. The HR-MS for complex 7 (Figure 2.2) showed  $m/z$  at 404.004 as an isotope of the base peak at 406.002 corresponding to  $[M^+ - Br]$  fragment.

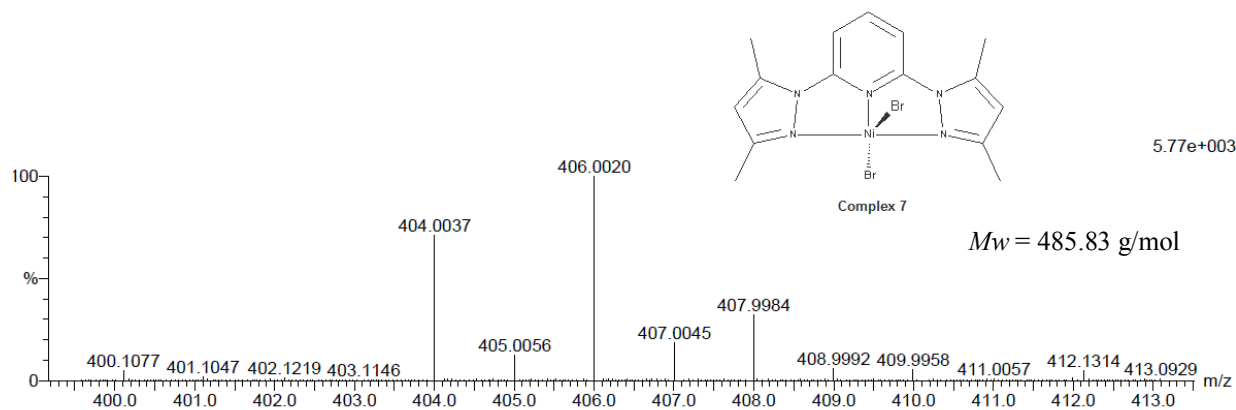


**Figure 2.2:** HR-MS spectrum complex 7 showing  $[M^+ - Br]$  as the base peak.

The elemental analyses data was performed for all the complexes (**1-9**) to confirm the purity of the compounds. The elemental analyses data were in good agreement with the proposed structures for all complexes in Schemes 2.2-2.3, with the exception of the analyses of hydrogen (H) in complexes **2**, **4**, **5**, **7**, **8**, **9** which deviated by more than 0.5. This could be due to contamination from foreign substances like dust.

### 2.3.2 Molecular structures of complexes **4 - 8**

Single crystals suitable for X-ray analyses of complexes **4** and **6** were obtained by slow diffusion of hexane into dichloromethane solutions at -4 °C while crystals of **7** and **8** were obtained by slow evaporation of their methanolic solution at room temperature. Molecular structures and selected bond parameters for compounds **4**, **6a**, **7** and **8** are shown in Figures 2.3-2.6 while Table 2.1 contains data collection, structural refinement parameters of **4**, **6a**, **7** and **8**. Complexes **4** and **6** contain two tridentate units of **L2** ligand coordinated to the metal center. This is common for the nickel(II) and iron(II) complexes anchored on tridentate ligands to forming octahedral structures.<sup>27</sup> The difference between the proposed structures and the solid state structure can also be attributed to the process of crystallization, resulting in the formation of the metal cations as observed in the molecular structures of complexes **4** and **6** in chlorinated solvents.<sup>31</sup> The geometry around the nickel(II) metal center in complexes **4** and **6** is distorted octahedral since the bond angles for N(1)-Ni(1)-N(3) of 87.06° and N(6)-Ni(1)-N(8) of 86.46° deviate from 90°. Similarly, the angles for N(1)-Ni(1)-N(5) of 173.53° is less than 180° typical of octahedral structures. The Ni-N<sub>pz</sub>(1) bond length of 2.1300(10) Å and Ni-N<sub>pz</sub>(5) bond length of 2.1162(10) Å are statistically similar confirming the symmetrical nature of **L2**. The average Ni-N<sub>pz</sub> bond distances are longer than those reported in literature for the similar complexes.<sup>32</sup>

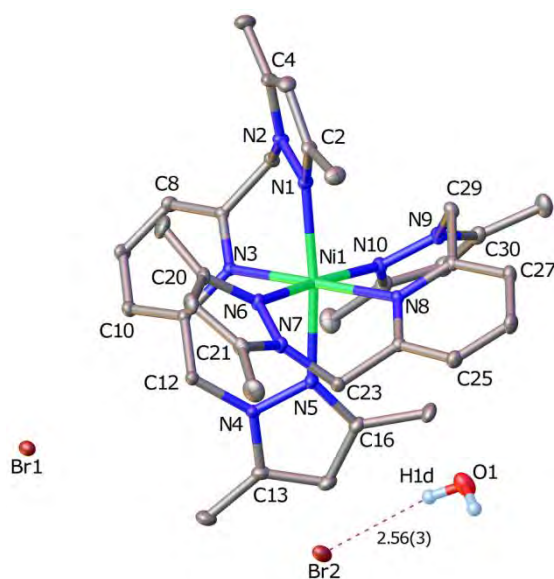


**Figure 2.3.** Molecular structure of complex **4a** drawn at 50 % probability ellipsoids.

Bond lengths (Å): Ni-N<sub>pz</sub>(1), 2.1300(10); Ni-N<sub>pz</sub>(5), 2.1162(10); Ni-N<sub>py</sub>(3), 2.1284(10); Ni-N<sub>py</sub>(8), 2.1350(10); Ni-N<sub>pz</sub>(6), 2.1129(10); Ni-N<sub>pz</sub>(10), 2.1364(11). Bond angles (°): N(1)-Ni(1)-N(3), 87.06(4); N(5)-Ni(1)-N(3), 86.51(4); N(6)-Ni(1)-N(8), 86.46(4); N(8)-Ni(1)-N(10), 86.85(4); N(1)-Ni(1)-N(6), 173.53(4); N(6)-Ni(1)-N(10), 173.24(4); N(3)-Ni(1)-N(8), 179.47(4).

The molecular structure of **6a** is similar to that of the nickel(II) derivative **4**; the two tridentate ligands adopt the same staggered conformation about the distorted octahedral metal centre. However, the distortion from a regular octahedral coordination geometry is more pronounced in **6a**, as evidenced by the rather acute mean N<sub>pz</sub>-Fe-N<sub>py</sub> bond angle of 84.7(8)° in the complex (where pz=pyrazole and py=pyridine). The mean Fe-N<sub>pz</sub> and Fe-N<sub>py</sub> bond distances measure 2.210(12) and 2.264(12) Å, respectively, and are in the ranges (2.131–2.245, Fe-N<sub>pz</sub>; 2.191–2.251, Fe-N<sub>py</sub>) observed for each bond class from the known X-ray structures of the cation present in six different salts (Figure 2.4b). The Fe-N<sub>pz</sub> bond to the metal ion is slightly shorter than the Fe-N<sub>py</sub> bond, in contrast to the bonding about the nickel(II) ion of **4a**, and likely reflects the fact that the ionic radius of high-spin iron(II) at 92 pm is 11 % larger than that of

nickel(II) (83 pm) such that the intrinsic geometric differences of the two N-donor atom types is somewhat amplified for the iron(II) chelate. It is noteworthy in this regard that the C–N<sub>py</sub>–C bond angle (ca. 117°) is significantly wider than the N–N<sub>pz</sub>–C bond angle (ca. 105°) and would account for a substantial part of the observed elongation of the Fe–N<sub>py</sub> bond relative to the Fe–N<sub>pz</sub> bond. Figure 2.4b shows a least-squares superposition of the six known X-ray structures of [Fe(L<sub>2</sub>)<sub>2</sub>]<sup>2+</sup> in the literature with that of **6a**. The wave-like conformation of the tridentate ligand is essentially constant for all of the crystallographically characterized salts. The two chelating ligands are relatively inflexible with minor conformational perturbations in the pyrazole ring orientations caused by minor rotations about the Fe–N<sub>pz</sub> bonds and crystal packing interactions involving the methyl substituents on the rings. Interestingly, the chelate ring arrangements and spiral-like ligand conformations of **6a** yield a chiral molecular structure for the cation.

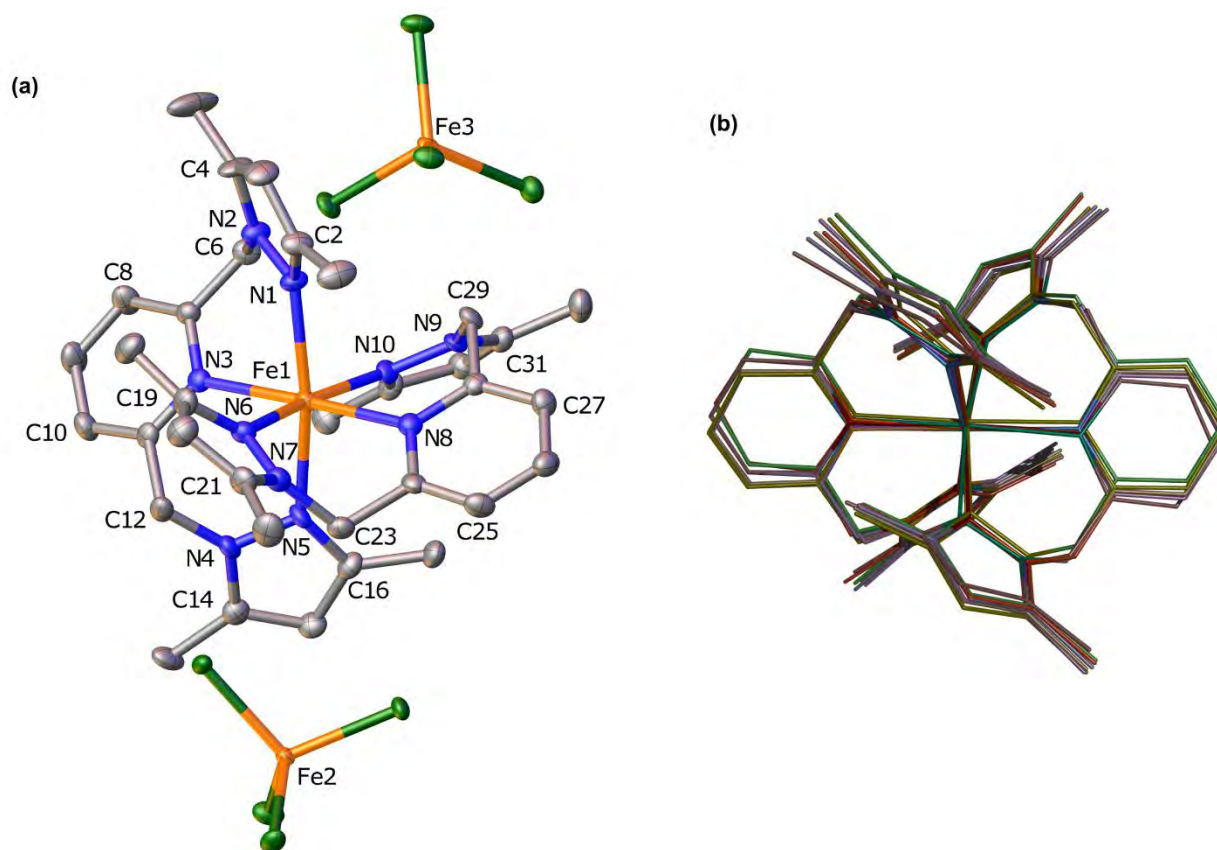


Figure 2.4: (a) Molecular structure of **6a** drawn with 50 % probability ellipsoids and selected atom labels. (b) Overlay of the X-ray structure of the **6a** with other six X-ray structures of the same cation from different salts in the literature (CSD reference codes: NIJMAU, NIJLOH, NIJLIB, ETONOR, ETONIL, and ETONEH).

Two solvent molecules ( $\text{CH}_2\text{Cl}_2$ ) and H atoms are omitted for clarity; only the major components of the two disordered  $[\text{FeCl}_4]^-$  counter-ions are shown. Bond lengths ( $\text{\AA}$ ): Fe–N1, 2.211(8); Fe–N5, 2.208(8); Fe–N3, 2.273(7); Fe–N8, 2.255(8); Fe–N6, 2.226(8); Fe–N10, 2.198(8). Bond angles ( $^\circ$ ): N1–Fe1–N3, 84.9(3); N5–Fe1–N3, 84.3(3); N6–Fe1–N8, 83.8(3); N8–Fe1–N10 85.6(3); N1–Fe1–N6, 87.9(3); N6–Fe1–N10, 169.3(3); N1–Fe1–N5, 169.2(3); N3–Fe1–N8, 178.0(3). The similarity indices range from 0.94–0.98 for all non-H atoms. (Atomic coordinates were transformed by inversion where necessary to give the same enantiomorph for least-squares fitting.)



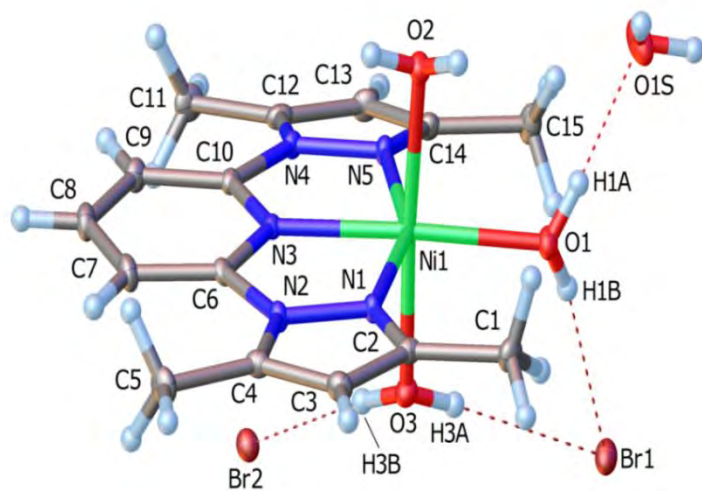
**Table 2.1.** X-ray data collection and structure refinement parameters for compounds **4a**, **6a**, **7** and **8**.

	<b>4a•H<sub>2</sub>O</b>	<b>6a•2CH<sub>2</sub>Cl<sub>2</sub></b>	<b>7•4H<sub>2</sub>O</b>	<b>8•2H<sub>2</sub>O</b>
Empirical formula	C <sub>34</sub> H <sub>44</sub> N <sub>10</sub> ONiBr <sub>2</sub>	C <sub>36</sub> H <sub>46</sub> N <sub>10</sub> Cl <sub>12</sub> Fe <sub>3</sub>	C <sub>15</sub> H <sub>25</sub> N <sub>5</sub> O <sub>4</sub> NiBr <sub>2</sub>	C <sub>15</sub> H <sub>21</sub> N <sub>5</sub> Cl <sub>2</sub> NiO <sub>2</sub>
Formula weight	827.32	1211.78	557.93	432.98
Temperature/K	100.15	100(2)	100(2)	100(2)
Crystal system	monoclinic	triclinic	monoclinic	monoclinic
Space group	<i>C2/c</i>	<i>P</i> -1	<i>Cc</i>	<i>P2<sub>1</sub>/n</i>
<i>a</i> /Å	15.2365(8)	13.7303(12)	10.4314(8)	8.2878(5)
<i>b</i> /Å	12.1008(6)	14.9885(13)	11.0104(8)	21.2490(13)
<i>c</i> /Å	38.373(2)	15.6987(13)	18.8608(13)	10.6189(6)
$\alpha$ /°	90	89.620(4)	90	90
$\beta$ /°	90.113(2)	64.621(4)	103.777(2)	107.728(2)
$\gamma$ /°	90	63.481(4)	90	90
Volume/Å <sup>3</sup>	7074.9(6)	2542.7(4)	2103.9(3)	1781.26(18)
<i>Z</i>	8	2	4	4
$\rho_{\text{calc}}$ mg/mm <sup>3</sup>	1.553	1.583	1.761	1.615
$\mu$ /mm <sup>-1</sup>	2.851	1.514	4.750	1.409
F(000)	3392.0	1228.0	1120.0	896.0
Crystal size/mm <sup>3</sup>	0.4 × 0.35 × 0.25	0.25 × 0.2 × 0.15	0.4 × 0.3 × 0.2	0.4 × 0.3 × 0.3
Radiation	MoK $\alpha$ ( $\lambda$ = 0.71073)	Mo K $\alpha$ ( $\lambda$ = 0.71073)	Mo K $\alpha$ ( $\lambda$ = 0.71073)	Mo K $\alpha$ ( $\lambda$ = 0.71073)
2 $\theta$ range for data collection/°	4.246 to 75.582	2.95 to 52.468	4.448 to 60.958	5.82 to 61.072
Index ranges	-26 ≤ <i>h</i> ≤ 15, -20 ≤ <i>k</i> ≤ 18, -54 ≤ <i>l</i> ≤ 65	-16 ≤ <i>h</i> ≤ 17, -18 ≤ <i>k</i> ≤ 18, -19 ≤ <i>l</i> ≤ 19	-14 ≤ <i>h</i> ≤ 7, -15 ≤ <i>k</i> ≤ 15, -23 ≤ <i>l</i> ≤ 26	-11 ≤ <i>h</i> ≤ 11, -30 ≤ <i>k</i> ≤ 29, -15 ≤ <i>l</i> ≤ 15
Reflections collected	61086	36960	12399	21261
Independent reflections	16101 [ <i>R</i> <sub>int</sub> = 0.0197, <i>R</i> <sub>σ</sub> = 0.0260]	9820 [ <i>R</i> <sub>int</sub> = 0.0284, <i>R</i> <sub>σ</sub> = 0.0250]	4201 [ <i>R</i> <sub>int</sub> = 0.0210, <i>R</i> <sub>σ</sub> = 0.0287]	5429 [ <i>R</i> <sub>int</sub> = 0.0197, <i>R</i> <sub>σ</sub> = 0.0163]
Data/restraints/parameters	16101/0/449	9820/54/650	4201/10/281	5429/0/246
Goodness-of-fit on <i>F</i> <sup>2</sup>	1.050	1.183	1.040	1.026
Final <i>R</i> indexes [ <i>I</i> ≥ 2 $\sigma$ ( <i>I</i> )]	<i>R</i> <sub>1</sub> = 0.0304, <i>wR</i> <sub>2</sub> = 0.0656	<i>R</i> <sub>1</sub> = 0.0966, <i>wR</i> <sub>2</sub> = 0.2454	<i>R</i> <sub>1</sub> = 0.0150, <i>wR</i> <sub>2</sub> = 0.0367	<i>R</i> <sub>1</sub> = 0.0212, <i>wR</i> <sub>2</sub> = 0.0551
Final <i>R</i> indexes [all data]	<i>R</i> <sub>1</sub> = 0.0416, <i>wR</i> <sub>2</sub> = 0.0683	<i>R</i> <sub>1</sub> = 0.0994, <i>wR</i> <sub>2</sub> = 0.2466	<i>R</i> <sub>1</sub> = 0.0153, <i>wR</i> <sub>2</sub> = 0.0368	<i>R</i> <sub>1</sub> = 0.0222, <i>wR</i> <sub>2</sub> = 0.0556
Largest diff. peak/hole / e Å <sup>-3</sup>	0.89/-0.57	1.20/-1.18	0.45/-0.39	0.52/-0.39
Flack parameter	-	-	0.014(5)	-

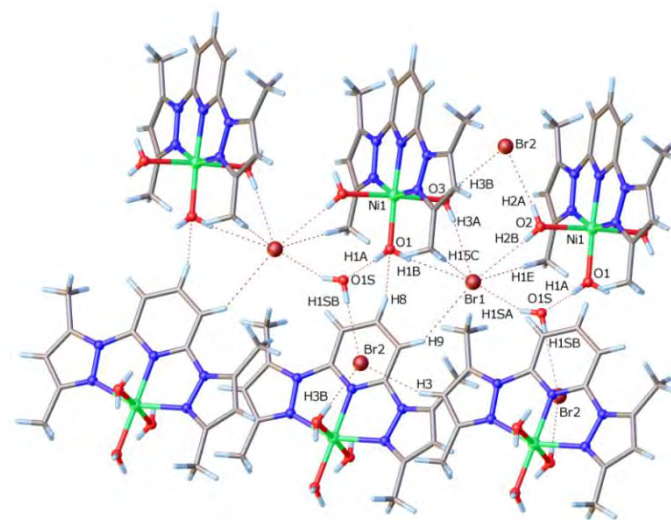
<sup>a</sup>Standard uncertainties of the least significant digits are given in parentheses.

The X-ray structures of compounds **7** and **8** are similar in several respects (Figure 2.5 and 2.6) since they both exhibit aquation of the metal ion with varying degrees of halide ion substitution, such that they are best classified as inner-sphere hydrates. The nickel(II) ion is six-coordinate in both cases and coordinated to tridentate **L3**, which deviates somewhat from planarity in both cations. The bromide salt **7•4H<sub>2</sub>O** exhibits a maximally hydrated coordination sphere with three water ligands occupying

coordination sites in the meridional plane perpendicular to the mean plane defined by **L3**. An additional solvate water molecule is hydrogen-bonded to the aqua ligand bound to Ni1 within the plane of the three N-donors of **L3**. The bromide counterions in **7•4H<sub>2</sub>O** participate in discrete hydrogen bonds with both the metal-bound and the free water molecules, leading to a complex extended structure (Figure 2.5b). In the structure of **8•2H<sub>2</sub>O**, the two water molecules are bound to the nickel(II) ion both axially and equatorially and are hydrogen-bonded to the chloride counterion. The extended structure comprises one-dimensional H-bonded chains stabilized by centrosymmetric cation and anion pairs (Figure 2.6). The cation pairs are held together by a pair of hydrogen bonds involving the water molecule of one cation and the axial chloride ligand of the partner cation, forming an 8-membered 2-donor/2-acceptor ring ( $8R_2^2$ ). The centrosymmetric anion pair linking adjacent centrosymmetric cation dimers in the chain is characterized by the anions each accepting three hydrogen bonds from the metal-bound water ligands in neighbouring cations to form an 8-membered 4-donor/2-acceptor ring ( $8R_4^2$ ) between the cation pairs in the one-dimensional chain. The Ni–O–H•••Cl<sup>−</sup> hydrogen bond distances are in the range 2.26–2.47 Å and are consistent with the range (2.10–2.46 Å) determined from 1013 X-ray structures of non-coordinated O<sub>w</sub>–H•••Cl<sup>−</sup> hydrogen bond distances in Steiner's seminal analysis of hydrogen bonding,<sup>33</sup> suggesting that the O–H donors of the aqua ligands in **8•2H<sub>2</sub>O** remain relatively unaffected by coordination to nickel(II) atoms.



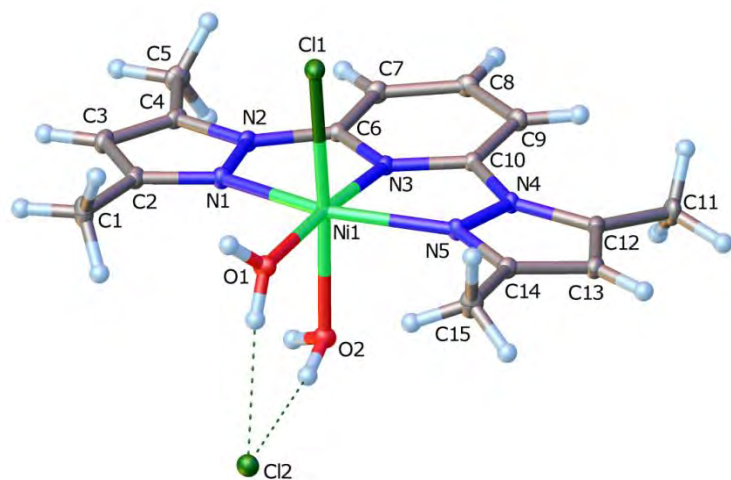
(a)



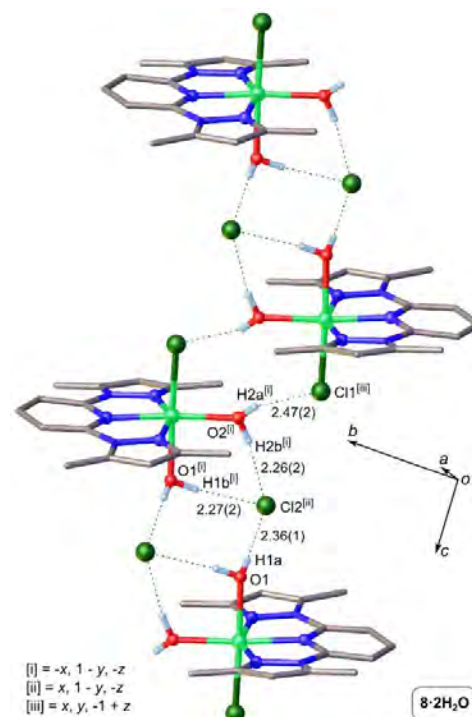
(b)

**Figure 2.5:** (a) Molecular structure of **7a** drawn at 50 % probability ellipsoids. Bond lengths (Å): Ni-N<sub>pz</sub>(1), 2.0832 (17) ; Ni-N<sub>pz</sub>(5), 2.0783 (17) ; Ni-N<sub>py</sub>(3), 2.0051 (17); Ni-O(2), 2.1134 (16); Ni-O(3), 2.0788 (16) Bond angles (°):O(1)-Ni(1)-O(3), 87.34 (6); N(1)-Ni(1)-O(3), 91.41 (7); N(3)-Ni(1)-O(2), 94.13 (7); N(1)-Ni(1)-N(3), 77.58 (7); O(2)-Ni(1)-O(3), 176.52 (6); O(1)-Ni(1)-N(3) 176.59 (7); N(1)-Ni(1)-N(5) 155.53 (6). (b) Hydrogen-bond geometry (Å, °) for **7**

The chelating bis(pyrazolyl) ligand in **7** and **8** induces an in-plane distortion of the nickel(II) coordination sphere away from ideal octahedral coordination mainly due to the fact that the nickel(II) ion fits rather poorly into the adjacent 5-membered chelate rings of the tridentate ligand. This is especially evident from the trans  $N_{pz}-Ni-N_{pz}$  angles, which deviate significantly from  $180^\circ$  and measure  $155.53(7)$  and  $154.52(4)^\circ$  for **7** and **8**, respectively. These values match the mean  $N_{pz}-Ni-N_{pz}$  angle for all crystallographically characterized nickel(II) complexes of 2,6-bis(pyrazole)pyridine currently available in the CSD<sup>22</sup>. The same observation holds for the  $N_{py}-Ni-N_{pz}$  bond angles. Inspection of the data in Table 2.1 reveals that there is surprisingly little variation in the bond angles subtended at the metal ion for this class of compounds, consistent with an essentially inflexible chelating ligand. The fact that the mean *endo*- $N_{py}-Ni-N_{pz}$  bond angle deviates significantly from  $180^\circ$  reflects the geometric constraints of the ligand framework which precludes attainment of the an “ideal” trans- $N_{py}-Ni-N_{pz}$  bond angle of  $180^\circ$  for a six-coordinate nickel(II) complex.



(a)



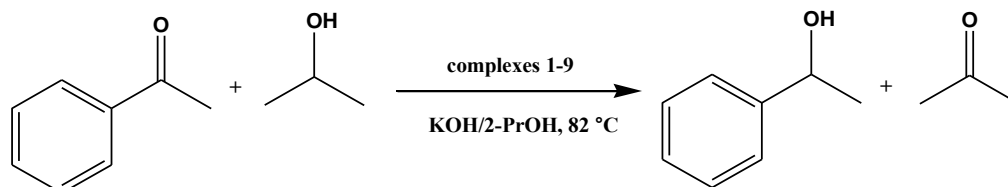
(b)

**Figure 2.6.** (a) Molecular structure of **8·2H<sub>2</sub>O** drawn at 50 % probability ellipsoids. Bond lengths (Å): Ni-N<sub>pz</sub>(1), 2.0566 (9) ; Ni-N<sub>pz</sub>(5), 2.0995 (8) ; Ni-N<sub>py</sub>(3), 2.0162 (9). Bond angles (°): O(1)-Ni(1)-O(2), 87.87 (3); N(1)-Ni(1)-O(1), 103.79 (3); Cl(1)-Ni(1)-O(1), 89.84 (2); N(5)-Ni(1)-Cl(1), 94.79 (2); O(1)-Ni(1)-N(3), 175.64 (3); O(2)-Ni(1)-Cl(1), 176.71 (2); N(1)-Ni(1)-N(5), 154.48 (3). (b) Hydrogen-bond geometry (Å, °) for **8·2H<sub>2</sub>O**.

In both **7** and **8**, the Ni–N<sub>pz</sub> bonds are inequivalent, fall in the range 2.005–2.101 Å and average 2.080(17) Å. The central Ni–N<sub>py</sub> bonds are somewhat shorter, averaging 2.011(8) Å for the two complexes. From the data in Table 2.1, it is clear that the Ni–N<sub>py</sub> bonds are normal for this class of compounds, matching the mean of 2.012(15) Å. Although the bonds between the metal ion and pyrazole nitrogen atoms in **7** and **8** are shorter than the mean [2.103(21) Å] for this class of chelates, they are equivalent within one standard deviation of the mean (1σ). Due to the rigidity of the 2,6-bis(pyrazole)pyridine nickel(II) chelate for all entries in Table 2.1, the relative invariance of the Ni–N bonds is to be expected in this class of compounds and, furthermore, appears to be insensitive to whether the pyrazole moieties are alkylated or not. Finally, it is noteworthy that the chloride salt **8**•2H<sub>2</sub>O is structurally and crystallographically isomorphous with the analogous bromide salt reported by Tastekin *et. al.*,<sup>35</sup> namely diaqua-bromo-(2,6-bis(3,5-dimethylpyrazolyl)pyridine-*N,N',N''*)-nickel(II) bromide.

### 2.3.3 Transfer hydrogenation of acetophenone catalyzed by complexes 1-9

Complexes **1-9** were investigated as potential homogeneous catalysts for the transfer hydrogenation of acetophenone as a model substrate using KOH and isopropanol as the base and hydrogen donor, respectively (Scheme 2.5).



**Scheme 2.5.** Catalytic transfer hydrogenation of acetophenone

The kinetics of transfer hydrogenation of acetophenone to the corresponding 1-phenylethanol were monitored by  $^1\text{H}$  NMR spectroscopy by comparing the intensities of the methyl signals of acetophenone (s,  $\delta$  2.59 ppm) and 1-phenylethanol (d,  $\delta$  1.49 ppm) of the crude products (Figure 2.7). As the reaction progresses, it can be observed that the peak intensity for acetophenone (s,  $\delta$  2.59 ppm) decreases while the peak for 1-phenylethanol (d,  $\delta$  1.49 ppm) appears and increases. All the complexes were found to efficiently catalyze the transfer hydrogenation of acetophenone giving conversions between 70-99 % within 48 h (Figure 2.8).

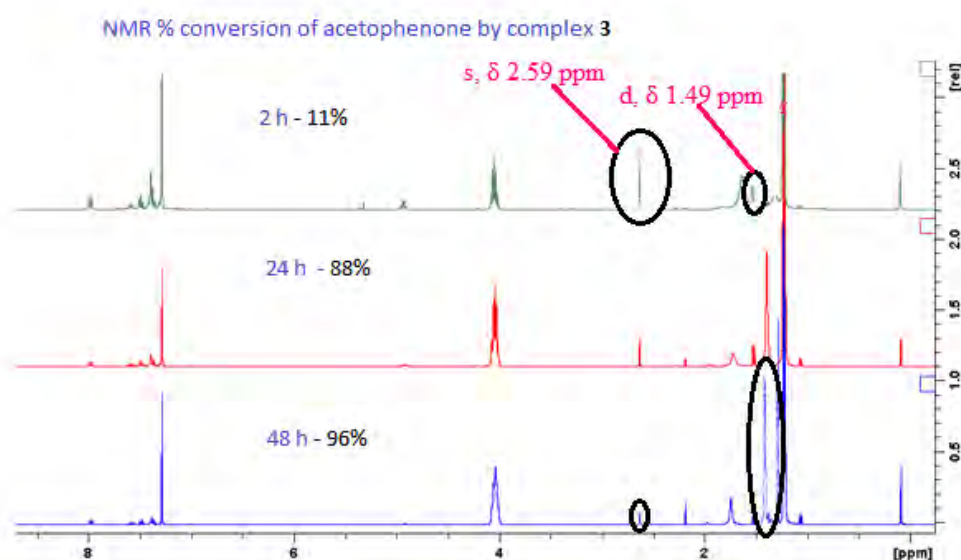


**Figure 2.7.** NMR percentage conversion of acetophenone by complex 3

### ***2.3.3.1 Effect of catalyst structure on the transfer hydrogenation of acetophenone***

Upon establishing that complexes **1-9** form active catalysts for the transfer hydrogenation of acetophenone, we subsequently investigated the effects of catalyst structure, nature of substrate and reaction conditions such as base and catalyst concentration on the transfer hydrogenation

reactions. Table 2.2 summarizes the results of the catalytic screening and kinetics data for TH of acetophenone for complexes **1-9** (Figure 2.8).

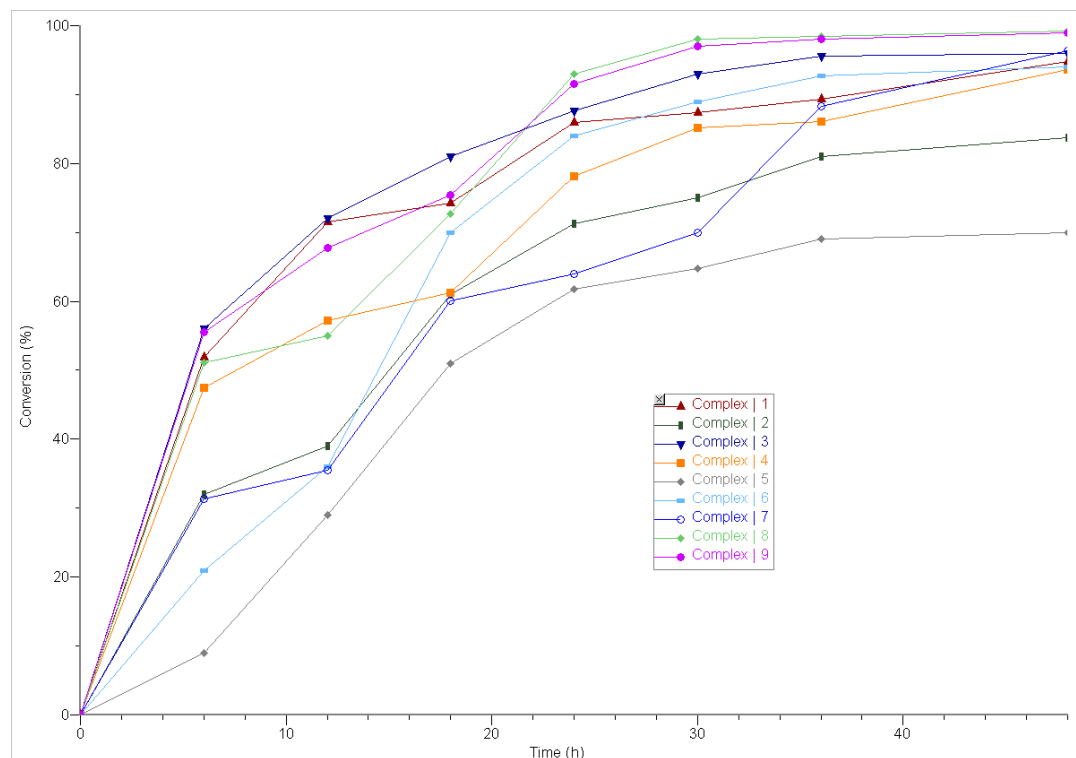


**Figure 2.8.** Time dependence of catalytic transfer hydrogenation of acetophenone by complexes **1-9**.

From Table 2.2 and Figure 2.8, it was evident that the nickel(II) and iron(II) complexes **7-9** bearing the rigid tridentate ligand **L3** exhibited higher catalytic activities than the corresponding complexes **1-3** and **4-6** bearing on **L1** and **L2** ligands. Comparatively, complexes **1-3** derived from the bidentate **L1** showed better catalytic activities than the corresponding complexes **4-6** anchored on the tridentate **L2** ligand. Thus, from these trends, it is evident that the ligand architecture influenced the catalytic activities of the respective complexes. As an illustration, while the complexes **2** (**L1**) and **5** (**L2**) afforded conversions of 85 % ( $1\,770 \times 10^{-3} \text{ h}^{-1}$ ) and 70 % ( $1\,458 \times 10^{-3} \text{ h}^{-1}$ ) respectively, complex **8** of **L3** gave conversions of 99 % ( $2\,062 \times 10^{-3} \text{ h}^{-1}$ )

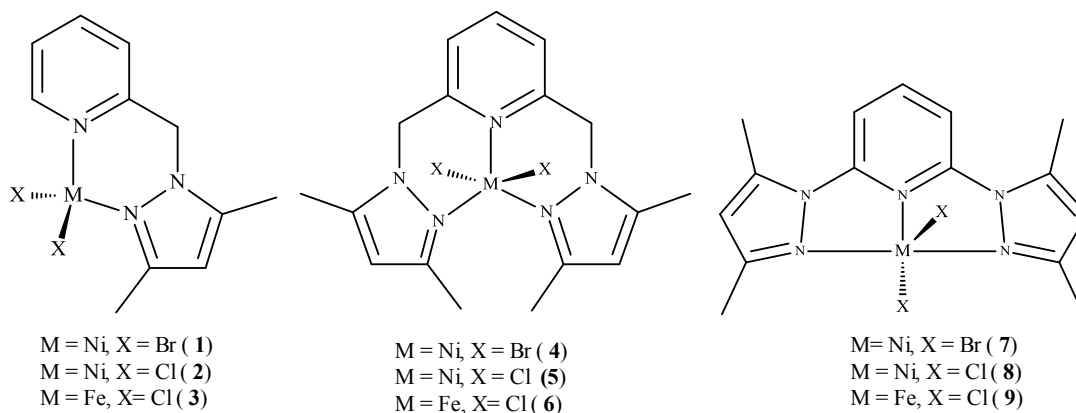


under similar experimental conditions. The lower activities of complexes **L2** could be attributed to steric hindrance around the metal atom arising from the bulkier and flexible **L2**. This has the net effect of hindering ketone substrate from coordinating to the metal center.<sup>36</sup> The planarity and the more rigid nature of complexes **7-8** allows the substrate to easily access the metal center, therefore can be associated with their catalytic activity.<sup>7</sup>

**Table 2.2.** The data for the transfer hydrogenation of acetophenone to 1-phenylethanol catalyzed by **1-9**.<sup>a</sup>

Catalyst	Conv. 48 h (%) <sup>b</sup>	TOF×10 <sup>-3</sup> (h <sup>-1</sup> )
<b>1</b>	95	1 979
<b>2</b>	85	1 770
<b>3</b>	96	2 000
<b>4</b>	94	1 958
<b>5</b>	70	1 458
<b>6</b>	94	1 958
<b>7</b>	96	2 000
<b>8</b>	99	2 062
<b>9</b>	99	2 062

<sup>a</sup>Conditions: acetophenone, 2.00 mmol; catalyst, 0.02 mmol (1.0 mol%); base, 0.40 M KOH in 2-propanol (5 mL); temperature, 82 °C. <sup>b</sup>Determined by <sup>1</sup>H NMR spectroscopy at *t* = 48 h. TOF = (mmol of substrate)/(mmol of catalyst)\*(h of time)



We also observed that the identity of the metal atom had an effect on the catalytic activities of the complexes. In general, iron(II) complexes were more active than the corresponding nickel(II) complexes. For example, conversions of 85 % ( $1\,770 \times 10^{-3} \text{ h}^{-1}$ ) and 96 % ( $2\,000 \times 10^{-3} \text{ h}^{-1}$ ) were reported for the dichloride nickel(II) and iron(II) complexes **2** and **3** (Table 2.2, entries 2 and 3). This trend is consistent with literature findings for similar complexes and could be attributed to greater positive charge of iron(II) metal compared to nickel(II) hence improved substrate coordination to the metal centre and promoted nucleophilic attack.<sup>37-39</sup> In addition, iron(II) is ‘known’ to form more stable metal hydrides (considered an intermediate in the THK), since it has more preference to oxygen than nickel(II).<sup>40</sup>

From the results, it was also clear that the nature of the halides (chloride or bromide) also controlled the catalytic activities of the complexes. For instance, while the dibromide nickel(II) complex **4** gave conversions of 94 % ( $1\,958 \times 10^{-3} \text{ h}^{-1}$ ), the corresponding dichloride complex **5** only achieved 70 % ( $1\,770 \times 10^{-3} \text{ h}^{-1}$ ) under similar conditions. In addition, the dichloride complexes **2** and **5** exhibited much longer induction periods than their corresponding bromide complexes **1** and **4** (Figure 2.8). However, an opposite trend was observed for complexes **7** and **8**. In this case, the dichloride complex **8** exhibited a faster induction period compared to the

dibromide complex **7**, giving the final percentage conversion of 99 % ( $2.062 \times 10^{-3} \text{ h}^{-1}$ ) and 96 % ( $2.000 \times 10^{-3} \text{ h}^{-1}$ ) respectively (Figure 2.9). While increased solubilities of the dibromide complexes **1** and **4** may be responsible for their higher catalytic performance, stronger hydrogen bonding observed in the bromide complex **7** (Figure 2.6b) could account for its lower activity compared to the dichloride complex **8**. The trend obtained for **7** and **8** agrees with that reported by Mikhailine *et al.* They reported greater activities of the iron(II) chloride complexes compared to their bromide analogues.<sup>41</sup>

In comparison to literature reports, the catalytic activities of complexes **1-9** in the transfer hydrogenation of acetophenone were lower than some of the most active nickel(II) and iron(II) systems. For example, while iron(II) complexes **3** and **6** display conversions of 75 %-99 % within 48 h, the iron(II) carbonyl complexes reported by Morris *et al.* show conversion of 93 % within 30 min ( $907 \times 10^{-3} \text{ h}^{-1}$ ).<sup>16</sup> However, the nickel(II) complexes also demonstrated comparable activities to some of the reported nickel(II) systems. For example, the conversion of 95 % ( $1.979 \times 10^{-3} \text{ h}^{-1}$ ) observed after 48 h for complex **1** compares favorably with conversions of 98 % within 48 h recorded in the asymmetric transfer hydrogenation of acetophenone catalyzed by nickel(II) complex of PNO ligands.<sup>17</sup>

### ***2.3.3.2 Effect of reaction conditions on the transfer hydrogenation reactions***

In order to establish the optimum reaction conditions for the transfer hydrogenation of acetophenone, we studied the effect of catalyst loading and type of base on the catalytic performance of complex **1** (Table 2.3, entry 9 and Table 3, entries 5-7). From the results, it was evident that increasing catalyst loading from 0.5 mol % to 1.0 mol % resulted in a significant increase in catalytic activity from 60 % ( $1.250 \times 10^{-3} \text{ h}^{-1}$ ) to 90 % ( $1.875 \times 10^{-3} \text{ h}^{-1}$ ), shown in

table 2.3, entries 1 vs 5. However, a further increase in catalyst concentration to 1.5 mol % resulted in a drastic drop in activity to 59 % ( $1\,229 \times 10^{-3} \text{ h}^{-1}$ ), as indicated in table 2.3, entry 6. Decrease in catalytic activity with increase in catalyst concentration has been associated with complex aggregation which might limit the number of reacting species.<sup>42</sup> Thus the optimum catalyst concentration in transfer hydrogenation of acetophenone using complex **1** was 1 mol % ( $1\,979 \times 10^{-3} \text{ h}^{-1}$ ).

**Table 2.3.** Dependence of TH of acetophenone on the nature of base and catalyst concentration using complex **1**

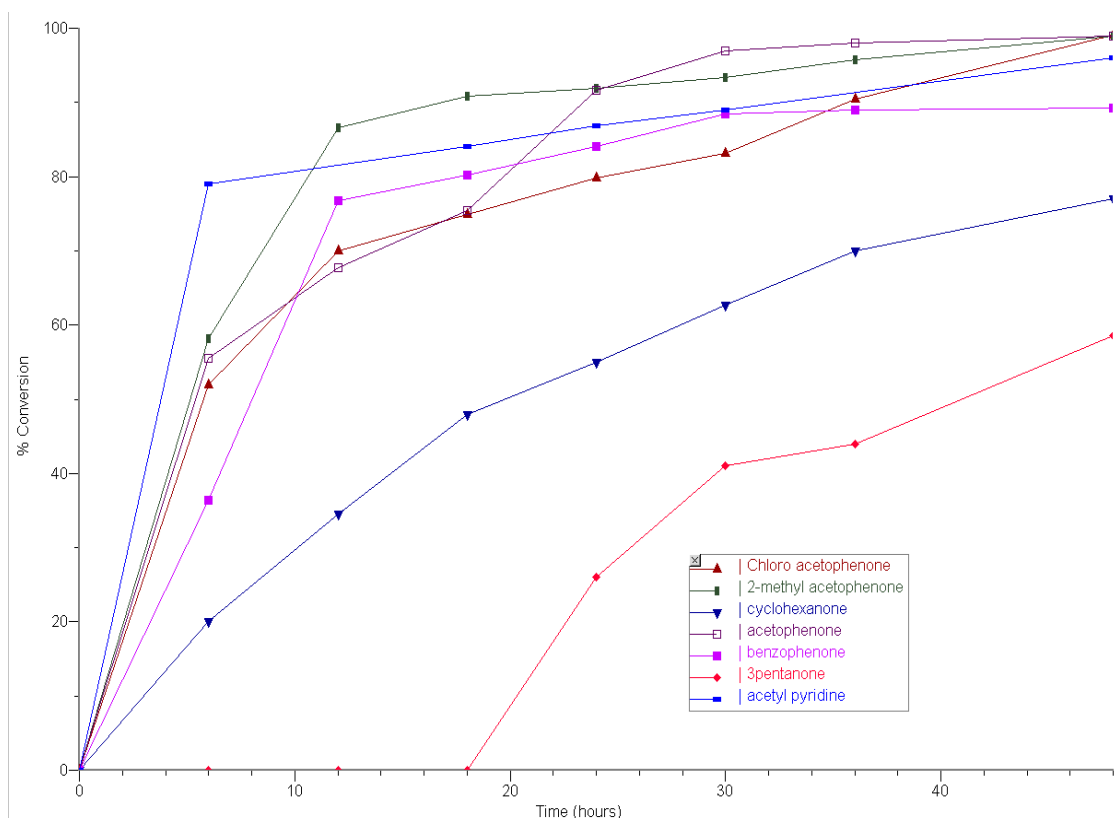
Entry	Base	Conversion (%) <sup>b</sup>	TOF x 10 <sup>-3</sup> (h <sup>-1</sup> )
1	KOH	95	1 979
2	NaOH	84	1 750
3	Na <sub>2</sub> CO <sub>3</sub>	55	1 146
4	<sup>t</sup> BuOK	97	2 021
5	KOH	60 <sup>c</sup>	1 250
6	KOH	59 <sup>d</sup>	1 229

<sup>a</sup>Conditions: ketone, 2.00 mmol; catalyst, 0.02 mmol (1 mol %); 0.40 M of base in 2-propanol (5 mL), temperature 82 °C. <sup>b</sup>Determined by <sup>1</sup>H NMR spectroscopy. <sup>c</sup>0.01 mmol catalyst (0.50 mol%); <sup>d</sup>0.03 mmol catalyst (1.50 mol%). TOF = (mmol of substrate)/(mmol of catalyst)\*(h of time)

The effect of the base was also investigated by comparing the catalytic activities of complex **1** in <sup>t</sup>BuOK, KOH, NaOH and Na<sub>2</sub>CO<sub>3</sub>. The highest catalytic activities were realized when using <sup>t</sup>BuOK, while the least activity was noted using Na<sub>2</sub>CO<sub>3</sub>. This trend is consistent with the order of stability and strengths of these bases and agrees with earlier findings in literature where stronger bases generate more active catalytic species.<sup>43</sup>

### 2.3.3.3 Variation of ketone substrates using complex **1** & **9**

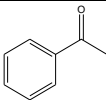
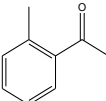
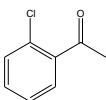
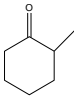
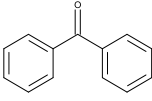
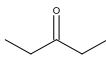
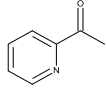
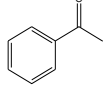
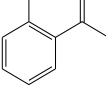
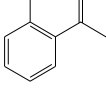
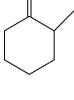
To gain more insight on the substrate scope that can be efficiently catalyzed by these catalysts, we studied the transfer hydrogenation of 2-methylacetophenone, 2-chloroacetophenone, 3-propanol, benzophenone, acetylpyridine and 2-methylcyclohexanone using catalysts **1** and **9** (Table 2.4 and Figure 2.9).



**Figure 2.9.** Effect of ketone substrate on the THK using complex **9**, KOH, substrate, [S]/[**9**]=200.

We observed that introduction of electron-donating or withdrawing groups at the ortho position of acetophenone did not significantly affect the catalytic performance of catalysts **1** and **9** (Figure 2.9). For instance, for catalyst **1**, conversions of 99 % were obtained for 2-methylacetophenone and 2-chloroacetophenone in comparison to 95 % for acetophenone (Table 2.4, entries 8-10). These findings are in contrast to those of Yu *et al.* who reported higher conversions of 95% and 99 % for the methyl and chloro *ortho*-substituted acetophenone respectively in comparison to 85 % obtained for acetophenone within 5 h.<sup>44</sup> Significantly, we observed diminished catalytic activities of 76 % and 56 % for 2-methylcyclohexanone and aliphatic 3-pentanone, respectively. This showed that aromatic ketone substrates exhibited higher reactivity compared to aliphatic analogues. Indeed, comparable higher conversion of 96 % was achieved using heterocyclic acetylpyridine substrate confirming that the aromatic ring plays a role in increasing substrate reactivity. The relatively lower reactivity observed for benzophenone 86 % could be largely assigned to ring strain occasioned by the two bulky phenyl rings.<sup>45</sup>

**Table 2.4.** Effect of substrate scope on the transfer hydrogenation reactions by **1** and **9**

Entry	catalyst	Substrate	%Conversion <sup>b</sup>	TOF x 10 <sup>-3</sup> (h <sup>-1</sup> )
1	<b>9</b>		99	2 062
2	<b>9</b>		99	2 062
3	<b>9</b>		99	2 062
4	<b>9</b>		77	1 604
5	<b>9</b>		89	1 854
6	<b>9</b>		56	1 167
7	<b>9</b>		96	2 000
8	<b>1</b>		95	1 979
9	<b>1</b>		99	2 062
10	<b>1</b>		99	2 062
11	<b>1</b>		76	1 583

<sup>a</sup>Conditions: ketone, 2 mmol; catalyst, 0.02 mmol (1 mol %); base, K<sub>2</sub>HPO<sub>4</sub> 0.4M of K<sub>2</sub>HPO<sub>4</sub> in 2-propanol (5 mL), temperature 82 °C. <sup>b</sup>Determined by <sup>1</sup>H NMR spectroscopy. TOF = (mmol of substrate)/(mmol of catalyst)\*(h of time)

## 2.4 Conclusions

Iron(II) and nickel(II) complexes anchored on bidentate (2-pyrazol-1-ylmethyl)pyridine and tridentate 2-6-bis-(pyrazol-1-ylmethyl)pyridine form active catalysts for the transfer hydrogenation of acetophenone displaying moderate catalytic activities. Solid state structures of complexes **4** and **6** revealed the presence of two tridentately bound ligand **L2** units in the metal coordination sphere to give six-coordinate cationic species, while the nickel(II) complexes derivatives **7** and **8** consists of one tridentately bound **L3** unit in addition to H<sub>2</sub>O molecules and bromide ligands. Both the identity of the ligand and the metal atom influenced the catalytic behavior of these complexes. Iron(II) complexes were generally more active than the nickel(II) complexes while complexes containing bulkier ligands showed reduced catalytic activities. More aliphatic as well as rigid ketones showed lower reactivity. Generally, the nickel(II) and iron(II) complexes displayed the least active catalytic systems compared to the literature reported ruthenium(II) catalysts. However, we observed that the architecture of the ligands also plays a role in influencing the catalytic activity of the nickel(II) and iron(II) complexes, therefore syntheses of highly modified ligands may form nickel(II) and iron(II) complexes that would be comparable with ruthenium complexes. The synthesized nickel(II) and iron(II) complexes offer promising prospects to the transfer hydrogenation reactions and to the development of more robust and cheaper alternatives to the ruthenium catalysts.

## 2.5 References

- 
1. A. Zanotti-Gerosa, W. Hems, M. Groarke, F. Hancock, *Platinum Met. Rev.*, 2005, **49**, 158-165.



- 
2. M. Bullock, *Angew. Chem. Int. Ed.*, 2007, **46** 7360-7363.
  3. D. Pandiarajan, R. Ramesh, *J. Organomet. Chem.*, 2013, **723**, 26-35.
  4. T. Ikariya, A. J. Blacker, *Acc. Chem. Res.*, 2007, **40**, 1300-1308.
  5. L. Delaude, A. Demanceau, A. F Noels, *Curr. Org. Chem.*, 2006, **10**, 203-215.
  6. C. Sui-Seng, F. Freutel, A. J. Lough, R. H. Morris, *Angew. Chem. Int. Ed.*, 2008, **120**, 954-957.
  7. F. Zeng, Z. Yu, *Organometallics*, 2009, **28**, 1855-1862.
  8. N. J. Beach, G. J Spivak, *Inorg. Chim. Acta.*, 2003, **343**, 244-252.
  9. H. Deng, Z. Yu, J. Dong, S. Wu, *Organometallics*, 2005, **24**, 4110-4112.
  10. R. M. Bullock, *Chem. Eur. J.*, 2004, **10**, 2366-2374.
  11. G. P Boldrini, D. Savoia, E. Tagliavini, C. Trombini , A. Umani-Ronchi, *J. Org. Chem.*, 1985, **50**, 3082-3086.
  12. C. P. Casey, H. Guan, *J. Am. Chem. Soc.*, 2007, **129**, 5816-5817.
  13. T. Hashimoto, S. Urban, R. Hoshino, Y. Ohki, K. Tatsumi, F. Glorius, *Organometallics*, 2012, **31**, 4474-4479.
  14. N. Meyer, A. J. Laugh A. J, R. Morris, *Chem. Eur. J.*, 2009, **15**, 5605-5610.
  15. P. O. Lagaditis, P. E. Sues, J. F. Sonnenberg, K. Y. Wan, A. J. Lough, R. H. Morris, *J. Am. Chem. Soc.*, 2014, **136**, 1367-1380.
  16. R. Langer, G. Leitius, Y. Ben-David, D. Milstein. *Angew. Chem. Int. Ed.*, 2011, **123**, 2168-2172.
  17. R. C. Mebane, K. L. Holte, B. H. Gross, *Synth. Commun.*, 2007, **37**, 2787-2791.
  18. F. Alonso, P. Riente, J. A. Sirvent, M. Yus, *Appl. Catal. A: Gen.*, 2010, **378**, 1875-1884.

- 
19. K. Shimura, K. Shimizu, *Green Chem.*, 2012, **14**, 2983-2985.
  20. Z. Chen, M. Zeng, Y. Zhang, Z. Zhang, F. Liang, *Appl. Organometal. Chem.*, 2010, **24**, 625-630.
  21. J. He, M. Zeng, H. Cheng, Z. Chen, F. Liang, *Anorg. Allg. Chem.*, 2013, **639**, 1834-1839.
  22. Z. R. Dong, Y. Y. Li, S. L. Yu, G. S. Sun, J. X. Gao., *Chin. Chem. Lett.*, 2012, **23**, 533-536.
  23. A. A Watson, D. A House, P. J Steel, *Inorg. Chim. Acta*, 1987, **130**, 167-176
  24. D. L. Jameson, K. A. Goldsby, *J. Org. Chem.* 1990, **55**, 4992-4994
  25. Bruker (2010).APEX2, SAINT and SADABS. Bruker AXS Inc, Madison, Wisconsin, USA.
  26. G. M Sheldrick, *Acta. Cryst.* 2008, **64**, 112-122.
  27. S. Mahapatra, N. Gupta, R. Mukherjee, *Dalton Trans.* 1991, 2911-2915
  28. F. A. Cotton, G. Wilkinson, C. A. Mulrillo, M. Bochman, *Advanced Inorganic Chemistry*, **6th Ed.** (1999). John Wiley, New York, pg 835.
  29. A. L. Tchougre'eff, R. Dronskowski, *Int. J. Quantum Chem.*, 2009, **109**, 2606-2621.
  30. E. F. Khmara, D. L. Chizhov, A. A. Sidorov, G. G. Aleksandrov, P. A. Slepukhin, M. A. Kiskin, K. L. Tokarev, V. I. Filyakova, G. L. Rusinov, I. V. Smolyaninov, A. S. Bogomyakov, D. V. Starichenko, Yu. N. Shvachko, A. V. Korolev, I. L. Eremenko, V. N. Charushina, *Russ. Chem. Bull Int. Ed.*, 2012, **2**, 61-68.
  31. A. L. Tchougre'eff, R. Dronskowski, *Int. J. Quantum Chem.*, 2009, **109**, 2606-2621.
  32. M. Tastekin, S. Durmus, E. Sahin, C. Arici, K. C. Emregul, O. Atakol., *Z. Kristallogr.*, 2008, **223**, 424-429.
  33. T. Steiner, *Angew. Chem.* 2002, **114**, 50-80.

- 
35. M. Taştekin, C. Arıcı, I. Svoboda, K. C. Emregul, R. Kurtaran, . Atakol, H. Fuess, Z. *Kristallogr.* 2007, **222**, 255-258.
36. A. R. Karam, E. L. Catari, F. L. Linares, G. Agrifoglio, C. L. Albano, A. D. Barrios, T. E. Lehmann, S. V. Pekerar, L. A. Albornoz, R. Atencio, T. Gonzalez, H. B. Ortega, P. Joskowics, *Appl. Catal. A. Gen.*, 2005, **280**, 165-173.
37. I. Hussaina, T. Singh , *Adv. Synth. Catal.*, 2014, **356**, 1661-1696.
38. H. J. Koo, D. Dai, J. Ren, M. H. Whangbo, *Inorg. Chem.*, 1999, **38**, 340-345.
39. J. D. Hoeschele, J. E. Turner, M. W. England, *Sci. Total Environ.*, 1991, **109/110**, 477-492.
40. J. A. Lemire, J. J. Harrison, R.J. Turner. *Nat. Rev. Microbiol.*, 2013, **11**, 371-384.
41. A. A. Mikhailine, M. I. Maishan, A. J. Lough, R. H. Morris, *J. Am. Chem. Soc.*, 2012, **134**, 12266-12280.
42. S. A. Svejda, M. Brookhart, *Organometallics*, 1999, **18**, 65-74.
43. R. N. Prabhu, R. Ramesh., *J. Organomet. Chem.*, 2012, **718**, 43-51.
44. S. L. Yu, Y. Y. Li, Z. R. Dong, J. X. Gao, *Chin. Chem. Lett.*, 2012, **23**, 395-398.
45. V. Matias, P. Maria, C. Ernesto, *Electrochim. Acta*, 2015, **164**, 125-131.

## CHAPTER THREE

### Orientation towards the asymmetric transfer hydrogenation using 2-(1-(pyrazolyl)ethyl)pyridine nickel(II) and iron(II) complexes

#### 3.1 Introduction

Asymmetric transfer hydrogenation of ketones (ATHK) is a well-established and an extensively studied method used to achieve enantiomerically enriched secondary alcohol products, on both the laboratory and industrial scale.<sup>1-8</sup> Optically active alcohol products are useful intermediates in the synthesis of pharmaceuticals and pesticides.<sup>2</sup> For example, active pharmaceutical ingredients (APIs) are used for the manufacture of drugs like (R)-sotalol, used to treat life-threatening heart rhythm problem called ventricular arrhythmia.<sup>3</sup> As a result, the reactions are mostly applied in pharmaceutical industries, agricultural industries and flavouring industries.<sup>2-6</sup> Asymmetric catalysis can be achieved by using a suitable homogeneous chiral catalyst and selecting suitable reaction parameters. Noyori and co-workers<sup>1</sup> first reported complexes  $[\text{RuCl}(\eta^6\text{-arene})(N\text{-arylsulfonyl-DPEN})]$  as catalysts in stereoselective reduction of various aromatic ketones<sup>7</sup> to produce optically active alcohol products with high enantiomeric excess (*ee*).

Since this discovery, there has been much development of chiral catalyst and their application in the asymmetric transfer hydrogenation of ketones. However, there has been challenges with achieving high enantioselectivity and predictable stereochemistry of acetylpyridine,<sup>8</sup> used in the synthesis of 2-(1-(pyrazolyl)ethyl)pyridine. In this chapter, report on the attempted synthesis of asymmetric nickel(II) and iron(II) complexes anchored on the chiral 2-(1-(pyrazolyl)ethyl)pyridine ligand using CBS as the catalyst, for asymmetric transfer hydrogenation of ketones. The failure of chiral syntheses led to the synthesis and application of nickel(II) and iron(II) complexes of 2-(1-(pyrazolyl)ethyl)pyridine. We herein report the

synthesis, characterization and transfer hydrogenation of ketones catalyzed by 2-[1-(3,5-dimethylpyrazol-1-yl)ethyl]pyridine ligand (**L4**) and 2-[1-(3,5-diphenylpyrazol-1-yl)ethyl]pyridine ligands (**L5**) of nickel(II) and iron(II) complexes.

## 3.2 Experimental

### 3.2.1 General methods and instrumentation

General methods and instrumentation are as described in Chapter 2, section 2.2.1.

### 3.2.2 Synthesis of ligands L4 and L5

#### 3.2.2.1 Syntheses of 2-[1-(3,5-dimethylpyrazol-1-yl)ethyl]pyridine (**L4**)

The ligand (**L4**) was prepared by dissolving 2-(1-chloroethyl)pyridine (2.02 g, 14.20 mmol) and 3,5-dimethylpyrazole (1.37 g, 14.20 mmol) in toluene (30 mL), 40 % aqueous NaOH (10 mL) and 40 % aqueous tetrabutylammonium bromide (5-6 drops). The reaction mixture was refluxed for 120 h. The organic layer was then separated from the aqueous layer and washed three times with deionised water. The organic layer was dried over anhydrous Na<sub>2</sub>SO<sub>4</sub> and solvent removed under vacuum. Purification was done by column chromatography in a solution of hexane and diethyl ether (3:2) to yield a chrome yellow liquid. Yield: 1.43 g (49 %). <sup>1</sup>H NMR (CDCl<sub>3</sub>) δ 2.14 (s, 3H, CH<sub>3</sub>, pz); 2.30 (s, 3H, CH<sub>3</sub>, pz); 1.96 (d, 3H, CH<sub>3</sub>, <sup>3</sup>J<sub>HH</sub> = 8); 5.46 (q, H, CH<sub>3</sub>); 5.87 (s, <sup>1</sup>H, pz); 6.82 (d, <sup>1</sup>H, py, <sup>3</sup>J<sub>HH</sub> = 7.61 Hz); 7.15 (t, <sup>1</sup>H, py, <sup>3</sup>J<sub>HH</sub> = 7.8 Hz); 7.58 (t, <sup>1</sup>H, py, <sup>3</sup>J<sub>HH</sub> = 7.8 Hz); 8.54 (d, <sup>1</sup>H, py, <sup>3</sup>J<sub>HH</sub> = 7.8 Hz). <sup>13</sup>C NMR (100 MHz, CDCl<sub>3</sub>) δ 13.71, 14.05, 20.19, 59.17, 105.64, 120.25, 122.13, 137.07, 139.49, 147.50, 148.77, 162.10. (ESI-MS) m/z(% abundance) 201 (M<sup>+</sup>, 35%).

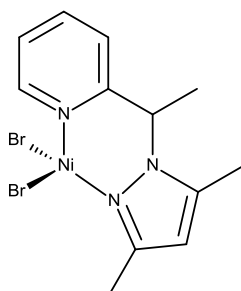
### 3.2.2.2 Synthesis of 2-[1-(3,5-diphenylpyrazol-1-yl)ethyl]pyridine (L5)

Compound **L5** ligand was prepared following the same method described for **L4** using 2-(1-chloroethyl)pyridine (2.00 g, 14.30 mmol) and 3,5-diphenylpyrazole (3.14 g, 14.30 mmol). Light red semi-solid. Yield: 1.68 (36%).  $^1\text{H}$  NMR ( $\text{CDCl}_3$ )  $\delta$  2.02 (d,  $^3\text{H}$ ,  $\text{CH}_3$ , pz); 5.67 (q, H, CH); 6.67 (s, 1H, CH, pz); 7.16 (d, 1H, py,  $^3J_{\text{HH}} = 7.61$  Hz); 7.93 (d, 1H, py,  $^3J_{\text{HH}} = 7.8$  Hz); 7.61 (t,  $^1\text{H}$ , py,  $^3J_{\text{HH}} = 7.73$  Hz), 7.36-7.45 (m, Ph).  $^{13}\text{C}$  NMR (100 MHz,  $\text{CDCl}_3$ )  $\delta$  20.04, 59.57, 103.63, 120.93, 122.19, 125.61, 125.63, 125.69, 127.61, 128.40, 128.57, 128.65, 128.69, 128.94, 129.05, 130.50, 133.74, 137.18, 145.69, 148.56, 150.80, 161.95. (ESI-MS)  $m/z$ (% abundance) 348 ( $\text{M}^+ + \text{Na}$ , 75 %).

### 3.2.3 Synthesis of iron(II) and nickel(II) complexes

#### 3.2.3.1 Synthesis of [{2-[1-(3,5-dimethylpyrazol-1-yl)ethyl]pyridine}NiBr<sub>2</sub>] (10).

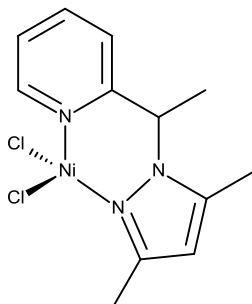
To a solution of NiBr<sub>2</sub> (0.11 g; 0.50 mmol) in CH<sub>2</sub>Cl<sub>2</sub> (10 mL) was added a solution of (**L4**) (0.10 g; 0.50 mmol) in CH<sub>2</sub>Cl<sub>2</sub> (10 mL). Upon the addition of the ligand solution, the colour changed from yellow to purple. The mixture was stirred for 24 h at room temperature. Purple crystals were obtained from the evaporation of CH<sub>2</sub>Cl<sub>2</sub>. Yield = 0.15 g (73 %). ESI-MS),  $m/z$  (% abundance) 339 ( $\text{M}^+ - \text{Br}$ , 15 %), 259 ( $\text{M}^+ - \text{Br}_2$ , 5 %), 653 [ $\text{M}^+ - (\text{NiBr}_2 + \text{ethylpyridine})$ ], 5 %).  $\mu_{\text{eff}} = 2.96$  BM



Complexes **10-15** were prepared according to procedure described for complex **10**.

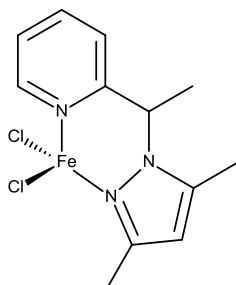
### 3.2.3.2 Synthesis of $[\{2-[1-(3,5\text{-dimethylpyrazol-1-yl)ethyl]pyridine}\}NiCl_2]$ (11).

NiCl<sub>2</sub> (0.06 g; 0.50 mmol) and **L4** (0.16 g; 0.50 mmol) were used. Orange powder. Yield = 0.12 g (65%). (ESI-MS), *m/z* (% abundance) 295 (M<sup>+</sup>-Cl, 75 %).  $\mu_{\text{eff}} = 2.95$  BM



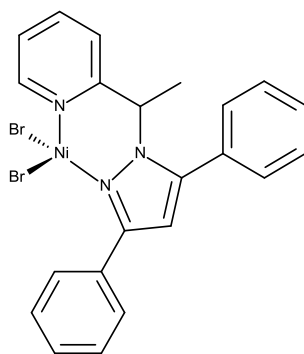
### 3.2.3.3 Synthesis of $[\{2-[1-(3,5\text{-dimethylpyrazol-1-yl)ethyl]pyridine}\}FeCl_2]$ (12).

FeCl<sub>2</sub> (0.10 g; 0.50 mmol) and **L4** (0.10 g; 0.50 mmol) were used. Dark brown powder. Yield = 0.08 g (51 %). (ESI-MS), *m/z* (% abundance) 464 (M<sup>+</sup>-Cl, 75 %).  $\mu_{\text{eff}} = 5.00$  BM



### 3.2.3.4 Synthesis of $[\{2-[1-(3,5\text{-diphenylpyrazol-1-yl)ethyl]pyridine}\}NiBr_2]$ (13).

NiBr<sub>2</sub> (0.10 g; 0.46 mmol) and (**L5**) (0.15 g; 0.46 mmol) were used. Purple powder. Yield = 0.17 g (67 %). (ESI-MS), *m/z* (% abundance) 464 (M<sup>+</sup>-Br, 11 %), 384 (M<sup>+</sup>-Br<sub>2</sub>, 5 %), 325 (M<sup>+</sup>-NiBr<sub>2</sub>, 10 %), 311 (M<sup>+</sup>-NiBr<sub>2</sub>-CH<sub>3</sub>, 18 %)  $\mu_{\text{eff}} = 3.62$  BM



### 3.2.4 X-ray crystallography

The X-ray crystallography for complexes **10** and **13** is as described in Chapter 2, section 2.2.3

### 3.2.5 Transfer hydrogenation reaction

The catalytic transfer hydrogenation of ketones was performed in a two-necked round bottom flask under an inert atmosphere. Similar to what was described in Chapter 2, see section 2.2.4. In this experiment, **10-13** (0.02 mmol, 1 %), 0.4 M KOH in 2-propanol (5 mL) and acetophenone (0.23 mL, 2.0 mmol) were added and refluxed at 82 °C under N<sub>2</sub> atmosphere. Samples aliquots were taken at regular intervals and the course of the reaction was monitored by <sup>1</sup>H NMR spectroscopy.

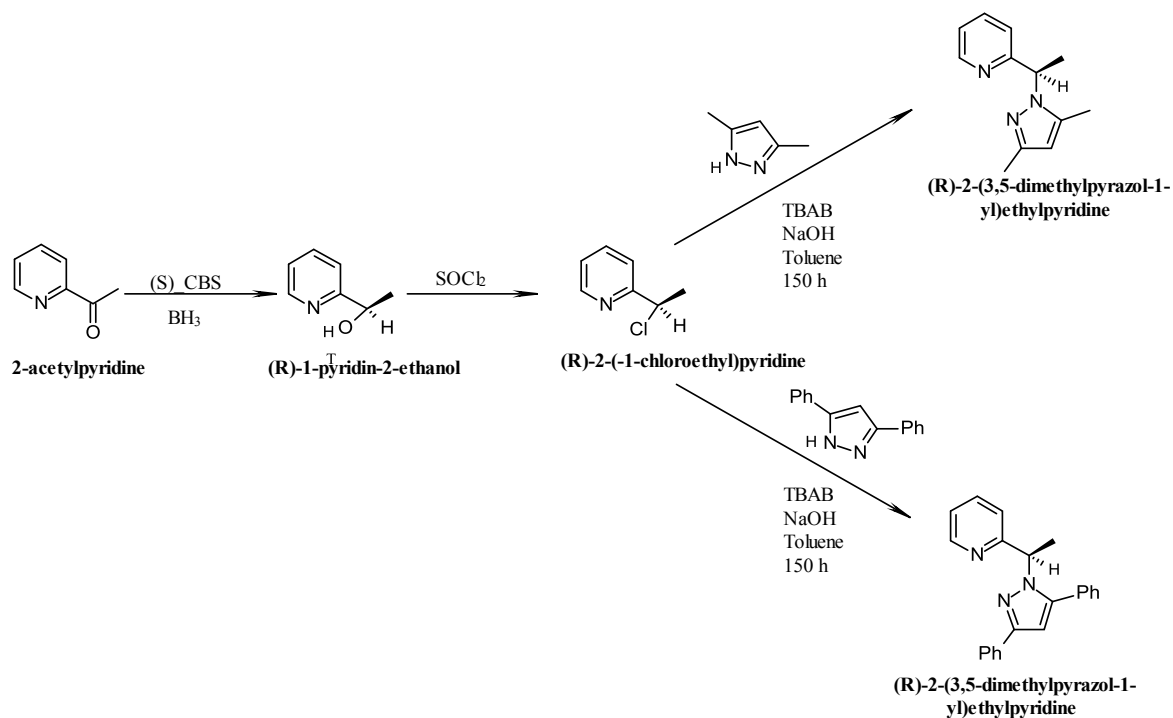
## 3.3 Results and discussion

### 3.3.1 Attempted synthesis of chiral ligands

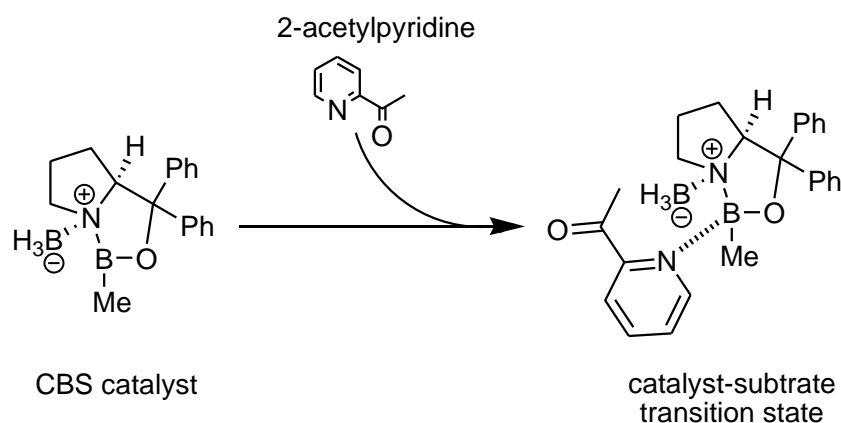
The initial objective of this section was to synthesize chiral (pyrazolylmethyl)pyridine ligands and their respective nickel(II) and iron(II) complexes as potential catalysts for the asymmetric transfer hydrogenation of ketones. Thus, attempts were made to synthesize chiral (pyrazolylmethyl)pyridine ligands *via* stereoselective reduction of 2-acetylpyridine using Corey-Bakshi-Shibata catalyst (CBS) catalyst (Scheme 3.1). Unfortunately, this reaction was



not successful possibly due to the stabilization of the CBS-borane catalyst by the pyridine nitrogen atom instead of the carbonyl oxygen, thereby reducing the enantioselectivity of the reaction<sup>9</sup> (Scheme 3.2). Thus, racemic mixtures of the ligands were obtained, which could not be quantitatively separated by column chromatography.



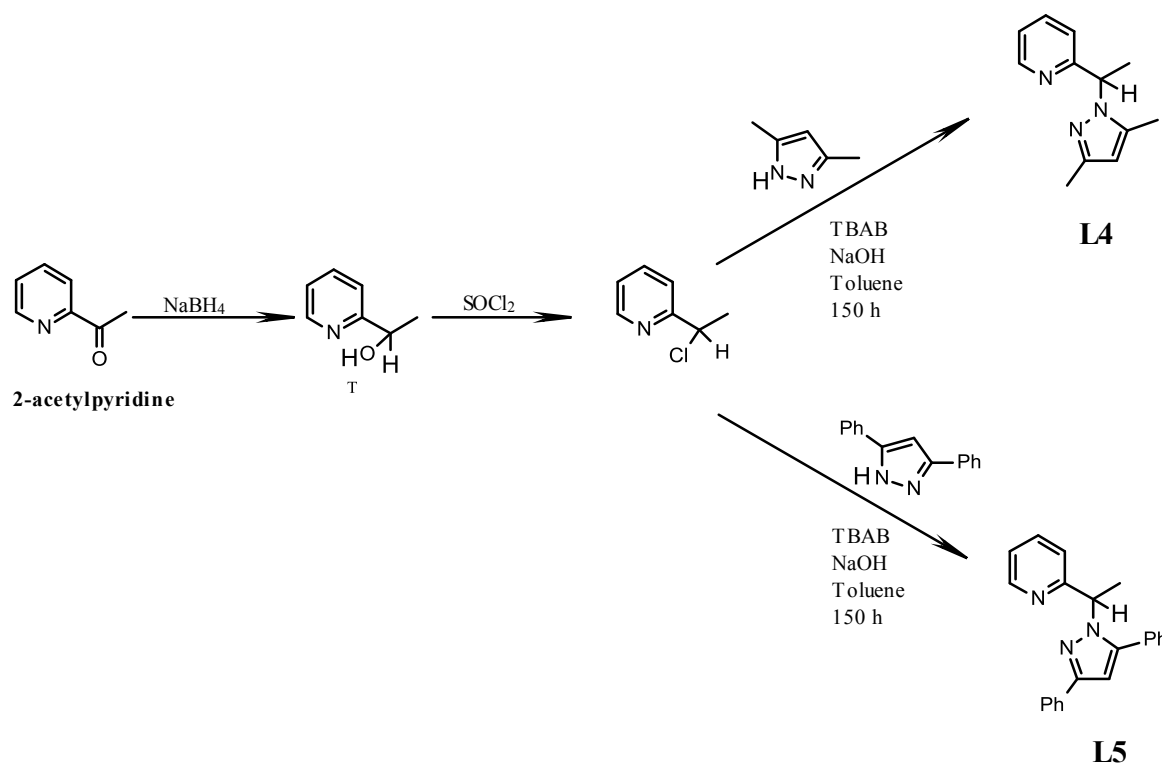
**Scheme 3.1.** Attempted synthetic route for chiral ligands using CBS as a catalyst



**Scheme 3.2.** The transition state showing the coordination of pyridine nitrogen.

### 3.3.2 Synthesis of (pyrazolylmethyl)pyridine ligands **L4** and **L5**

Following the failure to isolate pure enantiomers of pyrazolyl ligands using CBS catalyst, we adopted the conventional method of reduction of ketones using  $\text{NaBH}_4$  as the catalyst. The reduction of 2-acetylpyridine with  $\text{NaBH}_4$  produced the corresponding alcohol intermediate, and subsequent treatment of the pyridine-2-ethanol with a slight excess of thionyl chloride gave the corresponding 2-(1-chloroethyl)pyridine compound (Scheme 3.3). Reactions of 2-(1-chloroethyl)pyridine with stoichiometric amount of 3,5-dimethylpyrazole and 3,5-diphenylpyrazole produced the ligands **L4** and **L5**, respectively (Scheme 3.3). Purification of the compounds by column chromatography using a hexane:diethyl ether (3:2) solvent system afforded **L4** and **L5** as analytically pure compounds in low yields (36-49 %). Both ligands, **L4** and **L5**, showed good solubility in most polar solvents such as, dichloromethane, diethyl ether, chloroform.



**Scheme 3.3.** The synthetic route for ligands **L4** and **L5** using  $\text{NaBH}_4$  reducing agent.

The compounds synthesised were characterized by  $^1\text{H}$  NMR,  $^{13}\text{C}$  NMR and mass spectroscopy. The 2-[1-(3,5-dimethylpyrazol-1-yl)ethyl]pyridine ligand (**L4**) showed two characteristic up-field singlet peaks at about 2.02 ppm and 2.39 ppm for the two pyrazolyl methyl groups. A quartet peak at about 5.5 ppm was assigned to the proton at position one, and the doublet observed at 6.8 ppm was assigned to methyl group of the methylene linker. A singlet peak at about 5.9 ppm was observed and assigned to the 4-H of the pyrazole (Figure 3.1).

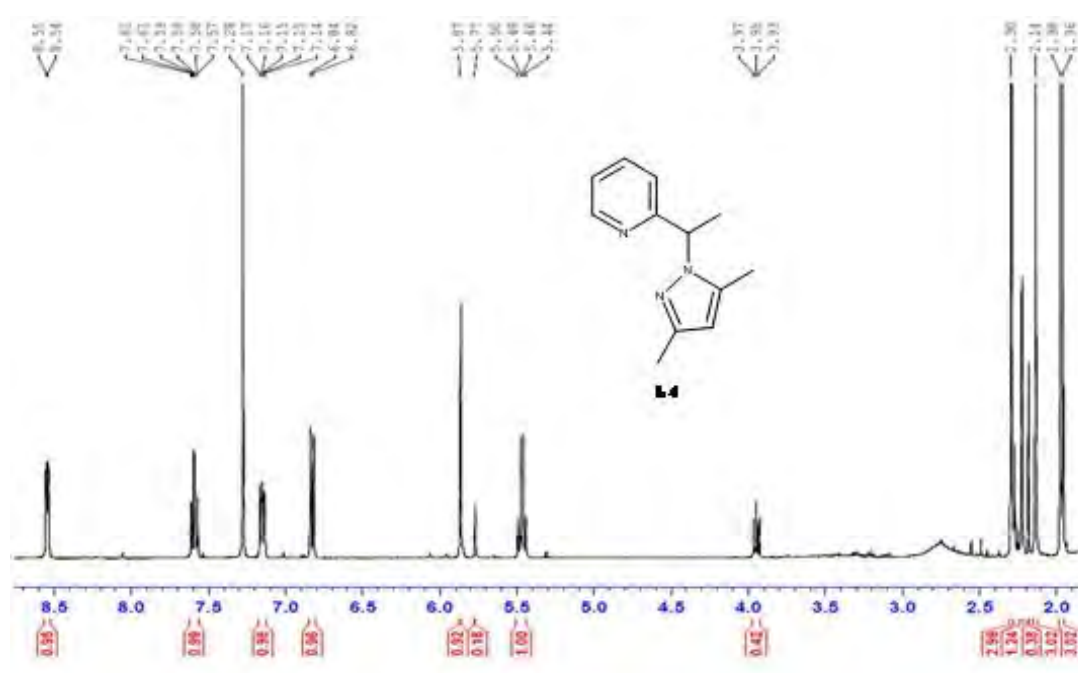


**Figure 3.1.** The  $^1\text{H}$  NMR spectrum of 2-[1-(3,5-dimethylpyrazol-1-yl)ethyl]pyridine pyridine ligand **L4**

Electron spray mass spectrometry was used to characterise ligands **L4** to **L5**. Ligand **L4** showed molecular ion  $[\text{M}^+]$  at  $m/z$  201.08, corresponding to the molecular mass of the compound. Another peak observed at  $m/z$  of 186.17 is assigned the fragment  $[\text{M}^+ - \text{CH}_3]$  due to the loss of methyl fragment (Figure 3.2).

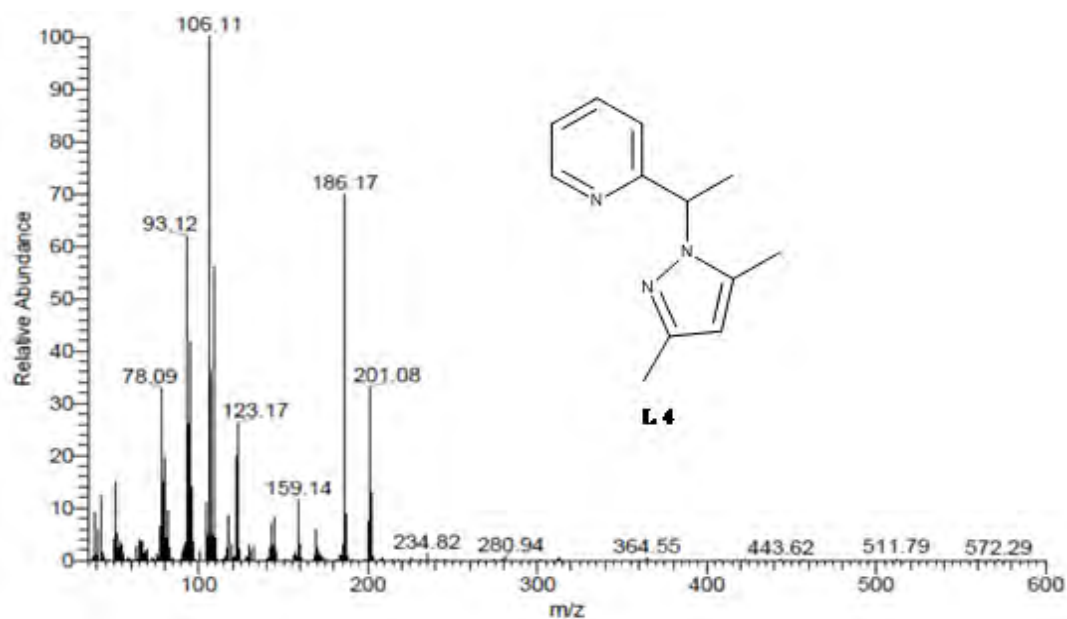
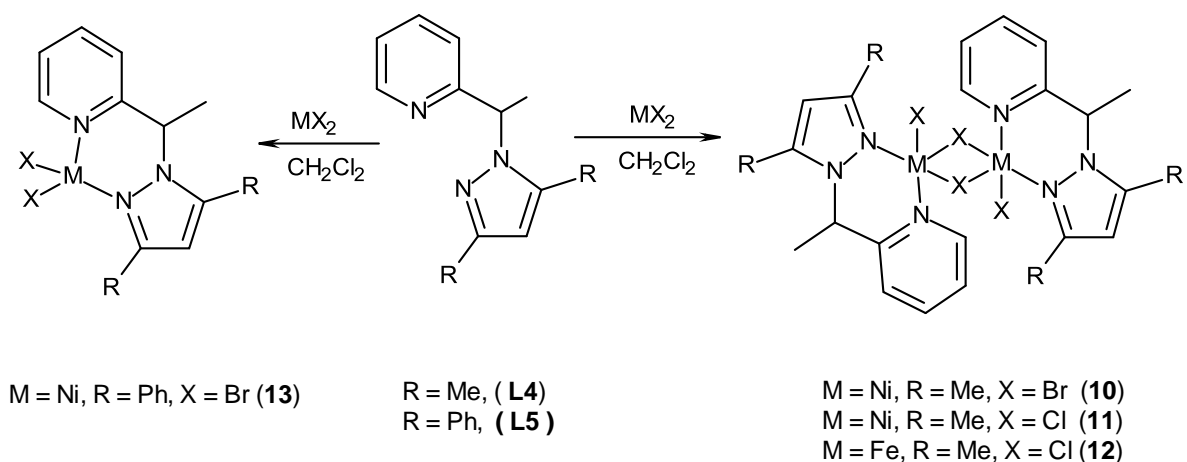


**Figure 3.2.** ESI-MS of 2-(3,5-dimethylpyrazol-1-yl)ethylpyridine ligand **L4**

### 3.3.3 Synthesis of nickel(II) and iron(II) complexes

Treatment of ligand **L4** with the metal salts of  $\text{NiBr}_2$ ,  $\text{NiCl}_2$  or  $\text{FeCl}_2 \cdot 4\text{H}_2\text{O}$  afforded the respective dinuclear nickel(II) and iron(II) complexes, while treatment of **L5** with  $\text{NiBr}_2$  afforded mononuclear nickel(II) complex (Scheme 3.4). The formation of the complexes was immediately indicated by the change of color upon addition of the ligand solutions. The complexes were isolated in fair to moderate yields ranging from (51-73 %).



**Scheme 3.4.** Synthesis of nickel(II) and iron(II) complexes of **L4** and **L5**

While the nickel(II) complexes containing less bulky ligand **L4** exhibited dimeric solid state structures, the complexes bearing bulky phenyl ligand **L5** were found to be monomeric and adopt a tetrahedral geometry.<sup>10</sup> Similar structural dependence on steric factors has been reported by Ojwach *et al.* for the (pyrazol-1-ylmethyl)pyridine nickel(II) complexes.<sup>10</sup>

However, the characterization of the compounds using elemental analyses data could not be done due to instrumental downtime. However, a combination of magnetic moment measurements, mass spectroscopy and single crystal X-ray analyses were performed to confirm the identity of complexes **10-13**. The effective magnetic moments obtained for nickel(II) complexes **10**, **11**, and **13** were in the range of 2.95-3.62 BM which is within the observed range 2.9 - 4.2 BM for nickel(II) complexes.<sup>11</sup> The magnetic moments of the iron(II) complex **12** was found as 5.00 BM which is also within the normal range of 4.90-5.11 BM reported in literature.<sup>28</sup> The observed effective magnetic moments for complexes **10-13** were relatively higher than the calculated spin-only magnetic moments of nickel(II) and iron(II) complexes. This observation can be attributed to the spin-orbital coupling effect. There was no significant difference on effective magnetic moments observed for the nickel(II) bromide and nickel(II) chloride complexes **10** and **11**, respectively. However, complex **12**, bearing dimethyl ligand substituents **L4**, exhibited higher effective magnetic moment than complexes **10** and **11**, bearing the diphenyl ligand substituents **L5**. This could be due to differences in ligand-field splitting parameters of **L4** and **L5**.<sup>12</sup>

Mass spectroscopy was also used to elucidate the structure of complexes **10-13** through the observed fragmentation patterns. For example, the spectrum of complex **10** shows fragment **A** with  $m/z$  of 653 [ $M^+-(Br+pz)$ ] corresponding to bimetallic species (Figure 3.3). Further fragmentation gave  $m/z$  of 339 [ $M^+-Br$ ] corresponding with mononuclear species (**B**). Similar fragmentation patterns were observed for other complexes.

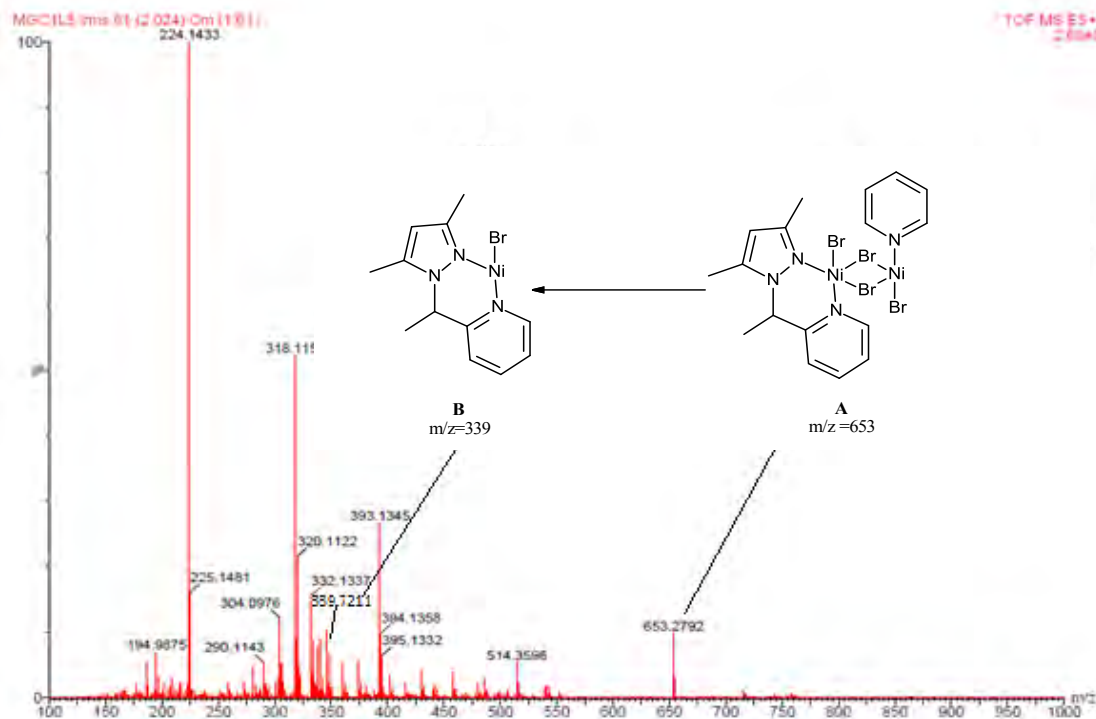


**Figure 3.3.** The LR-MS spectrum for complex **10**

### 3.3.4 Molecular structures of complexes **10** and **13**

Single crystals suitable for X-ray analyses of complexes **10** and **13** were obtained by slow evaporation of their dichloromethane solutions at room temperature. Molecular structures and selected bond parameters for compounds **10** and **13** are shown in Figures 3.5 and 3.6 respectively, while Table 3.1 contains data collection and structural refinement parameters of complexes **10** and **13**. The X-ray analyses of **10** and **13** confirmed the structures to have different geometries around the nickel(II) metal centre. The solid state structure of **10** (Figure 3.4) is a centrosymmetric dimer and is a five coordinate nickel(II) compound that contains one ligand unit, one terminal bromine in each nickel(II) centre and two bridging bromide ligands. The average Ni-N<sub>pz</sub> bondlength is 2.0472 Å is significantly longer than the reported bond distance of 2.0050 (13) Å for a similar 2-(pyrazol-1-ylmethyl)pyridine complexes.<sup>10</sup> The bond lengths of Ni-N<sub>py</sub> of 2.0587(13) Å, Ni-Br<sub>(terminal)</sub> of 2.4329(3) Å and Ni-Br<sub>(bridging)</sub>

2.5483 (3) Å are all statistically similar to the bond lengths reported for similar 2-(pyrazol-1-ylmethyl)pyridine complexes by Ojwach *et. al.*<sup>10</sup> The coordination environment about the nickel(II) atoms is a distorted trigonal bipyramidal in which the equatorial plane consist of the terminal Br atom, the basal plane including the nitrogen of the pyrazolyl ring, and one of the bridging Br atoms

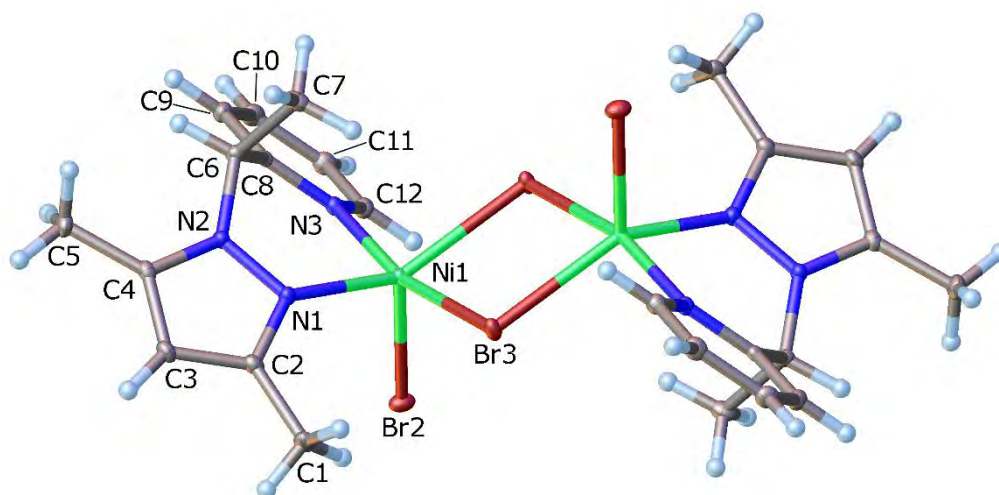


**Figure 3.4.** Molecular structure of **10** drawn at 50 % probability ellipsoids. Bond lengths (Å): Ni-N<sub>pz</sub>(1), 2.0472 (13); Ni-N<sub>py</sub>(3), 2.0587 (13); Ni(1)-Br(2), 2.4329 (3); Ni(1)-Br(3), 2.5483 (3); N(1)-N(2), 1.3709 (17). Bond angles (°): N(1)-Ni(1)-N(3), 89.55 (5); N(1)-Ni(1)-Br(3), 94.32 (4); N(3)-Ni(1)-Br(2), 92.29 (4); N(1)-Ni(1)-Br(2), 100.87 (4); N(3)-Ni(1)-Br(3), 166.15 (4)

While complex **10** is binuclear with bridging bromide, complex **13** is mononuclear with terminal bromides. The molecular structures of **10** & **13** contain racemic mixtures of both R and S configurations. It has been reported that bulky substituents adjacent to the nitrogen donor atoms render planarity of Ni(L-L)<sub>2</sub> molecule sterically impossible.<sup>13-15</sup> Complex **10** with the less bulky ligand (**L4**) therefore favors the bimetallic nickel(II) structure while complex **13** bearing the bulkier ligand (**L5**) favors the monometallic structures.

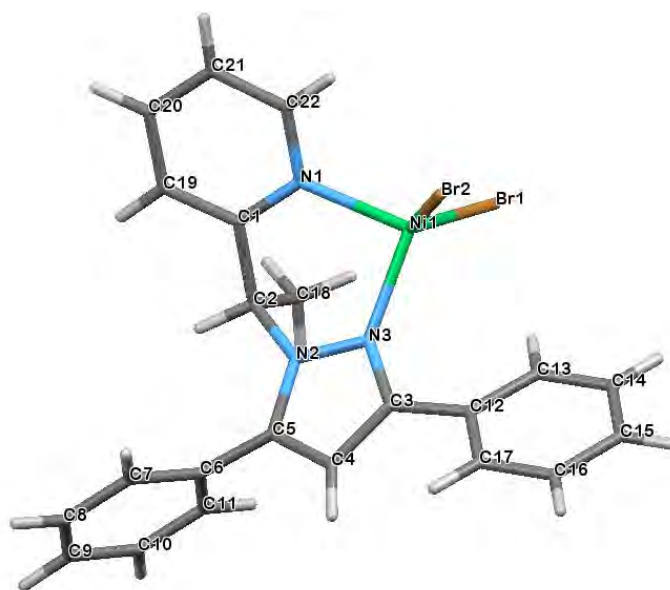


**Figure 3.5.** Molecular structure of **13** drawn at 50 % probability ellipsoids. Bond lengths (Å): Ni-N<sub>pz</sub>(1), 2.006(3); Ni-N<sub>py</sub>(3), 1.984(2); Ni(1)-Br(1), 2.3679(5); Ni(1)-Br(2), 2.3601(4); N(2)-N(3), 1.364(3). Bond angles (°): N(1)-Ni(1)-N(3), 92.54(10); N(1)-Ni(1)-Br(2), 104.57(7); N(3)-Ni(1)-Br(2), 108.89(7); N(1)-Ni(1)-Br(1), 110.98(7); N(3)-Ni(1)-Br(1), 110.77(7)

The molecular structure of **13** (Figure 3.5) contains the central nickel(II) metal that binds one bidentate ligand (**L5**) and two bromine atoms. The bond angles about the central atom in **13** vary between 92.54(10)° to 110.98(7)°. The Ni-Br<sub>(terminal)</sub> bond distances of 2.4329 in **10** are slightly longer than the corresponding distance of 2.3679 in **13**. The longer bond distances in **10** could be due to the electrostatic repulsion caused by the crowding around the metal centre which causes elongation. The nickel(II) atom adopts a distorted tetrahedral geometry around the metal center.

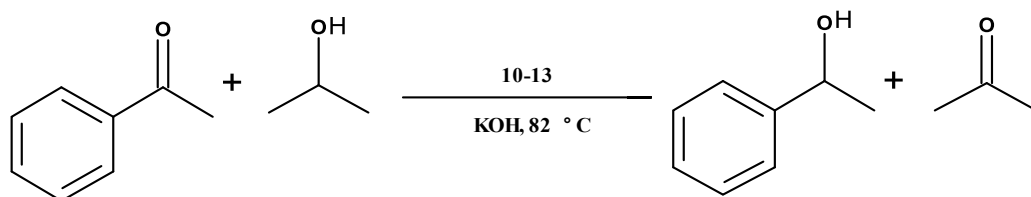


**Table 3.1.** Data collection and structural refinement parameters of **10** and **13**.

	<b>10</b>	<b>13</b>
Empirical formula	C <sub>24</sub> H <sub>30</sub> Br <sub>4</sub> N <sub>6</sub> Ni <sub>2</sub>	C <sub>22</sub> H <sub>19</sub> Br <sub>2</sub> N <sub>3</sub> Ni
Formula weight	839.60	543.93
Temperature(K)	100	100
Wavelength (Å)	0.71073	0.71073
Crystal system	Triclinic	Triclinic
Space group	<i>P</i> <sup>-1</sup>	Pca21
<i>a</i> (Å)	8.1757 (5)	16.5457(8)
<i>b</i> (Å)	8.8004 (6)	10.4476(5)
<i>c</i> (Å)	11.0344 (7)	12.0610(6)
$\alpha$ (°)	82.055 (3)	90
$\beta$ (°)	84.393 (3)	90
$\gamma$ (°)	64.290 (2)	90
Volume(A <sup>3</sup> )	707.82 (8)	2084.90(18)
Z	1	4
D <sub>calcd</sub> (mg/m <sup>3</sup> )	1.969	1.733
Absorption coefficient (mm <sup>-1</sup> )	7.001	4.776
F(000)	412.0	1080
Theta range for data collection (°)	3.13 – 28.33	1.95 to 26.04
Reflections collected / unique	25874	10162
Completeness to theta	0.983	0.991
Goodness-of-fit on F <sup>2</sup>	1.103	0.979
R indices (all data)	R <sub>1</sub> = 0.0168 wR <sub>2</sub> = 0.0436	R <sub>1</sub> = 0.0201 wR <sub>2</sub> = 0.0411
Largest diff. peak and hole (e Å <sup>-3</sup> )	0.74 and -0.47	0.56 and -0.27

### 3.3.5 Transfer hydrogenation of ketones catalyzed by complexes 10-13.

In order to evaluate the nickel(II) and iron(II) complexes for their ability to catalyze the transfer hydrogenation of ketones, complexes **10-13** were investigated using KOH as the base and isopropanol as the hydrogen donor (Scheme 3.5). All the complexes formed active catalysts in the transfer hydrogenation of acetophenone giving conversions between 58-84 % in 48 h (Figure 3.6).



**Scheme 3.5.** Catalytic transfer hydrogenation of acetophenone

#### 3.3.4.1 Effect of catalyst structure on the transfer hydrogenation of acetophenone

Upon establishing that complexes **10-13** form active catalysts for the transfer hydrogenation of acetophenone, we subsequently investigated the effects of catalyst structure, nature of substrate and reaction conditions such as base and catalyst concentration on the transfer hydrogenation reactions. Table 3.2 summarizes the results of the catalytic screening data for the TH of acetophenone for complexes **10-13**.

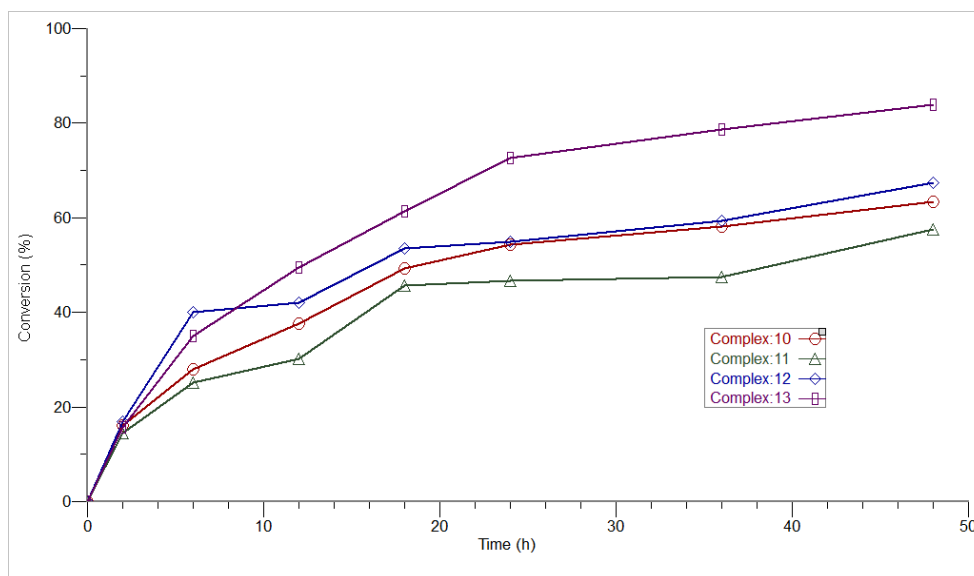


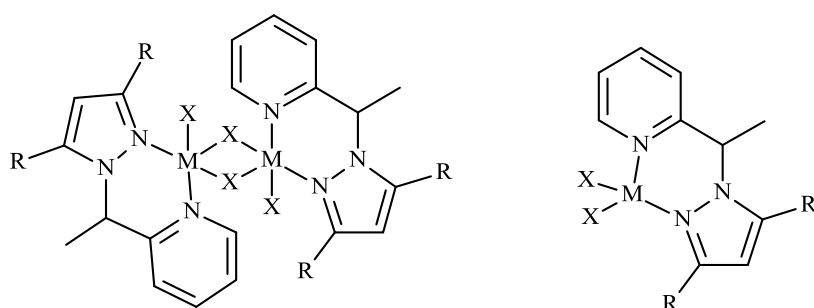
**Figure 3.6.** Time dependence of catalytic transfer hydrogenation of acetophenone; by complexes **10-13**.

The catalytic activity of the complexes was found to be in the order **13** > **12** > **10** > **11**. This nature of the substituent on the pyrazolyl ring appeared to have a significant influence on the catalytic behaviour of the complexes. The mononuclear complex **13** of 2-[1-(3,5-diphenylpyrazol-1-yl)ethyl]pyridine ligand **L5** gave the highest conversion of 84 % corresponding to the TOF of  $1\,750 \times 10^{-3} \text{ h}^{-1}$  (Table 3.2 entry 4) compared to the other complexes **10-12** of 2-[1-(3,5-methylpyrazol-1-yl)ethyl]pyridine **L4**. This trend could be attributed to the steric crowding caused by the two ligands in the dinuclear metal complexes **10-12** as opposed to one ligand in the mononuclear metal complex **13**. This steric crowding around the metal centre has the net effect of hindering coordination of the ketone substrate.<sup>16</sup>

**Table 3.2.** Catalysis data for transfer hydrogenation of ketones by **10-13**

Entry	Catalyst	Conversion [%] <sup>b</sup>	TOF x 10 <sup>-3</sup> (h <sup>-1</sup> )
1	10	63	1 319
2	11	58	1 198
3	12	67	1 404
4	13	84	1 750

<sup>a</sup>Conditions: acetophenone, 2.0 mmol; catalyst; 0.02 mmol (1.0 mol%); base, 0.4 M KOH in 2-propanol (5 ml); time, 48 h, temperature, 82 °C.<sup>b</sup>Determined by <sup>1</sup>H NMR spectroscopy. TOF= (mmol of substrate)/(mmol of catalyst)\*(h of time)



M = Ni, R = Me, X = Br (**10**)  
M = Ni, R = Me, X = Cl (**11**)  
M = Fe, R = Me, X = Cl (**12**)

M = Ni, R = Ph, X = Br (**13**)

We also observed that the identity of the metal atom had an effect on the catalytic activities of the complexes. Comparing complexes **10-12** of ligand **L4**, the iron(II) complex **12** (FeCl<sub>2</sub>**L4**) gave higher conversions of 67 % (1 404 x 10<sup>-3</sup> h<sup>-1</sup>) compared to **10** (NiBr<sub>2</sub>**L4**) with the conversion of 63 % (1 319 x 10<sup>-3</sup> h<sup>-1</sup>) and **11** (NiCl<sub>2</sub>**L4**) with the conversion of 58 % (1 198 x 10<sup>-3</sup> h<sup>-1</sup>). This is due to the general high reactivity of iron(II) complexes compared to the nickel(II) ions,<sup>17</sup> usually associated with high electropositivity of iron(II).<sup>18</sup> Similarly, the iron(II) metal centre is more reactive in the hydride transfer since it has more preference to oxygen compared to nickel(II). This originates from the Hard-Soft Acid Base (HSAB) theory since iron(II) is a hard acid compared to nickel(II).<sup>19</sup>

The nature of the halides was also found to control the catalytic activities of the complexes. In general, the chloride complexes were observed to be less active compared to the bromide analogues (Table 3.2 entries 1 vs 2). The difference was observed in their induction period where Cl complexes showed longer induction periods compared to the Br analogues. This observation contradicts with that of Mikhailine *et al.* who observed that the iron(II) complexes bearing Cl were more active compared to the bromide analogues.<sup>20</sup>

#### ***3.3.4.2 Effect of reaction conditions on the transfer hydrogenation reactions***

In order to establish the optimum reaction conditions for the transfer hydrogenation of acetophenone, studies were done to understand the effect of catalyst loading and type of base on the catalytic performance of complex **10** (Table 3.3). From the results, it could be observed that increasing catalyst loading from 0.5 mol % to 1.0 mol % resulted in a significant increase in catalytic activity from 42 % ( $875 \times 10^{-3} \text{ h}^{-1}$ ) to 84 % ( $1750 \times 10^{-3} \text{ h}^{-1}$ ) (Table 3.3, entries 1 vs 5). However, a further increase in catalyst concentration to 1.5 mol % resulted in a small drop in activity 81 % ( $1688 \times 10^{-3} \text{ h}^{-1}$ ) Table 3.3, entry 6. This observation is usually associated with complex aggregation which might limit the number of reacting species.<sup>21</sup> Thus, the optimum catalyst concentration in transfer hydrogenation of acetophenone using complex **13** was 1 mol %.

**Table 3.3.** Dependence of THK on base and catalyst concentration by complex **13**

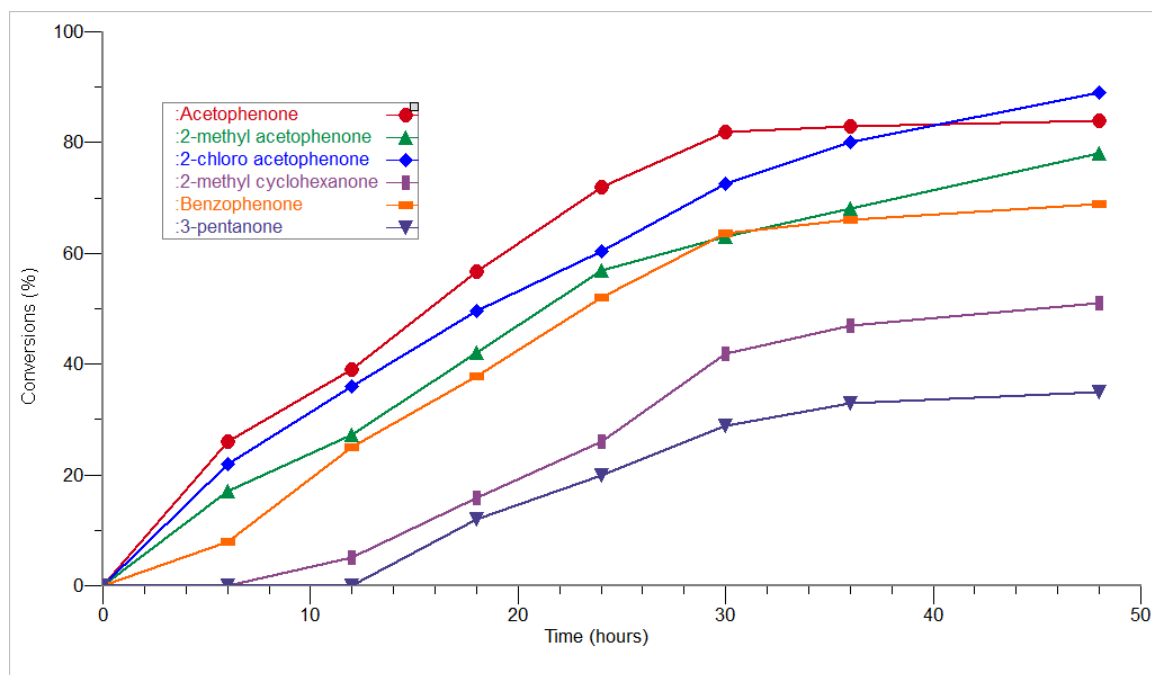
Entry	Base	Conversion (%) <sup>b</sup>	TOF x 10 <sup>-3</sup> (h <sup>-1</sup> )
1	KOH	84	1 750
2	NaOH	80	1 667
3	Na <sub>2</sub> CO <sub>3</sub>	24	500
4	<sup>t</sup> BuOK	98	2 042
5	KOH	42 <sup>c</sup>	875
6	KOH	81 <sup>d</sup>	1 688

<sup>a</sup>Conditions ketone, 2.00 mmol catalyst. 0.02 mmol (1 mol) 0.40 M of base in 2-propanol (5 m), temperature 82 C. <sup>b</sup>Determined by <sup>1</sup>H NMR spectroscopy <sup>c</sup>0.01 mmol catalyst (0.50 mol%); <sup>d</sup>0.03 mmol catalyst (1.50 mol%). TOF= (mmol of substrate)/(mmol of catalyst)\*(h of time)

The effect of the base was also investigated by comparing the activities in <sup>t</sup>BuOK, KOH, NaOH and Na<sub>2</sub>CO<sub>3</sub>. The most active conditions were realized using <sup>t</sup>BuOK, while the least activity was noted using Na<sub>2</sub>CO<sub>3</sub>. This trend is consistent with the order of stability and strengths of these bases and agrees with earlier findings in literature where stronger bases generate more active catalytic species.<sup>22</sup>

### 3.3.4.3 Variation of ketone substrates using complex **13**

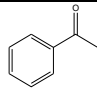
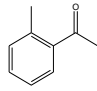
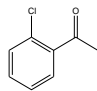
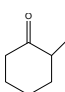
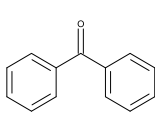
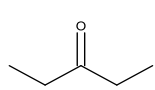
The ketone substrates were varied in order to gain more insight to the substrate scope that can be efficiently catalyzed by these catalysts. The transfer hydrogenation of 2-methylacetophenone, 2-chloroacetophenone, 3-pentanone, benzophenone and 2-methylcyclohexanone using catalyts **13** were investigated (Table 3.4 and Figure 3.7).



**Figure 3.7.** Effect of ketone substrate on the THK using complex **13**.

It was observed that changing the ketone substrate resulted in different catalytic activities. The introduction of electron-donating or withdrawing groups at the ortho position of acetophenone affected the percentage conversion of such substrates (Figure 3.7). For instance, conversions of 78 % ( $1.625 \times 10^{-3} \text{ h}^{-1}$ ) were obtained for 2-methylacetophenone and 88% ( $1.833 \times 10^{-3} \text{ h}^{-1}$ ) for 2-chloroacetophenone (Table 3.4, entries 2 vs 3). These findings are in contrast with those of Yu *et al.*<sup>23</sup> who reported that the electron-donating groups seem to accelerate the catalytic activity. Significantly, we reported diminished catalytic activities of 51 % ( $1.063 \times 10^{-3} \text{ h}^{-1}$ ) and 35 % ( $7.29 \times 10^{-3} \text{ h}^{-1}$ ) for 2-methylcyclohexanone and aliphatic 3-propanone, respectively. Aromatic ketone substrates exhibit higher reactivity compared to aliphatic analogues. This can be observed from acetophenone and its derivative substrates, confirming that the aromatic ring plays a role in increasing substrate reactivity.<sup>24</sup> The relatively lower reactivity of 72 % ( $1.500 \times 10^{-3} \text{ h}^{-1}$ ) observed for benzophenone compared to acetophenone could be largely assigned to ring strain occasioned by the two bulky phenyl rings in benzophenone.

**Table 3.4.** Effect of substrate scope on the transfer hydrogenation reactions by **13**

Entry	Substrate	%Conversion <sup>b</sup>	TOF x 10 <sup>-3</sup> (h <sup>-1</sup> )
1		84	1 750
2		78	1 625
3		88	1 833
4		51	1 063
5		72	1 500
6		35	729

<sup>a</sup>Conditions: ketone, 2 mmol; catalyst, 0.02 mmol (1 mol %); base, K<sup>+</sup>H<sup>-</sup> 0.4M of K<sup>+</sup>H<sup>-</sup> in 2-propanol (5 mL), temperature 82 °C. <sup>b</sup>Determined by <sup>1</sup>H NMR spectroscopy. TOF= (mmol of substrate)/(mmol of catalyst)\*(h of time)

### 3.4 Conclusions

Attempted syntheses of chiral compounds using CBS failed due to a possible coordination of the CBS catalyst with pyridine nitrogen atom which deactivated it. The reactions of racemic mixtures of 2-[1-(3,5-dimethylpyrazol-1-yl)ethyl]pyridine ligand (**L4**) with NiCl<sub>2</sub> or NiBr<sub>2</sub> salts produce five coordinate dinuclear complexes while 2-[1-(3,5-diphenylpyrazol-1-yl)ethyl]pyridine ligands (**L5**) produce four coordinate mononuclear complexes. In the study of THK we observed that all complexes form active catalysts for the transfer hydrogenations of ketones, with iron(II) complexes being more active than analogous nickel(II) complexes. The mononuclear complexes were the more active than their dinuclear analogues. The



optimum reaction conditions and the reactivity of various ketones were successfully established.

### 3.5 References

- 
1. R. Noyori. *Asymmetric catalysis in organic synthesis*, Wiley; New York, 1994. pg 56-82.
  2. M. Bullock, *Angew. Chem. Int. Ed.*, 2007, **46**, 7360-7363.
  3. J. Vaclavik, P. Sot, B. Vilhanova, J. Pechacek, M. Kuzma , P. Kacer, *Molecules*, 2013, **18**, 6804-6828
  4. D. Pandiarajan, R. Ramesh. *J. Organomet. Chem.*, 2013, **723**, 26-35.
  5. N. Arai, T. Ohkuma, *Reduction of Carbonyl Groups: Hydrogenation*, In: *Science of Synthesis: Stereoselective Synthesis*, G .A Molander, Thieme Stuttgart, Germany, 2010, Ed. **2**, pg 9-57.
  6. J. Vaclavik, P. Sot, B. Vilhanova, J. Pechacek, M. Kuzma, P. Kacer, *Molecules*, 2013, **18**, 6804-6828.
  7. S. Hashiguchi, A. Fujii, J. Takehara, T. Ikariya, R. Noyori, *J. Am. Chem. Soc.*, 1995, **117**, 7562–7563.
  8. J. G. Quallich, T. M. Woodall, *Tetrahedron Lett.*, 1993, **34**, 785–788.
  9. V. Stempaneko, M. Jesus, W. Correa, I. Guzman, C. Vazquez, L. Ortiz, M. Ortiz-Marcials, *Tetrahedron: Asymmetry*, 2007, **18**, 2738-2745.
  10. S. O. Ojwach, I. A. Guzei, L. L. Benade, S. F. Mapolie, J. Darkwa. *Organometallics*, 2009, **28**, 2127-2133.
  11. F. A. Cotton, G. Wilkinson, C. A. Mulrillo, M. Bochman, *Advanced Inorganic Chemistry*, John Wiley, New York, 1999, Ed. **6**, pg 835.
  12. J. Johnson, C. Ronald, F. Basolo, *Coordination chemistry: the chemistry of metal complexes*. Benjamin Inc. 1964, Ed **7**, pg 40-44.

- 
13. W. H. Sun, K. Wang, K. Wedeking, D. Zhang, S. Zhang, J. Cai, Y. Li., *Oganomettallics* 2007, **26**, 4781-4790.
  14. E. C Alyea, D. W. Meek, *J. Am. Chem. Soc.*, 1969, **91**, 5761-5768.
  15. A. Terzis, K. N. Raymond, T. G. Spiro, *Inorg Chem.*, 1970, **9**, 2415-2420.
  16. A. R. Karam, E. L. Catari, F. L. Linares, G. Agrifoglio, C. L. Albano, A. D. Barrios, T. E. Lehmann, S. V. Pekerar, L. A. Albornoz, R. Atencio, T. Gonzalez, H. B. Ortega, P. Joskowics, *Appl. Catal. A: Gen.*, 2005, **280**, 165-173.
  17. J. D. Hoeschele, J. E. Turner, W. E. England, *Sci. Total Environ.*, 1991, **109/110**, 477-492.
  18. H. J. A. Terzis, K. N. Raymond, T. G. Spiro, *Inorg Chem.*, 1970, **9**, 2415-2420.
  19. M. E. Carroll, B. E. Barton, D. L. Gray, *Inorg. Chem.*, 2011, **50**, 9554-9563.
  20. A. A. Mikhailine, M. I. Maishan, A. J. Lough, R. H. Morris, *J. Am. Chem Soc.*, 2012, **134**, 12266-12280.
  21. S. A. Svejda, M. Brookhart, *Organometallics*, 1999, **18**, 65-74.
  22. R. N. Prabhu, R. Ramesh., *J. Organomet. Chem.*, 2012, **718**, 43-51.
  23. S. L. Yu, Y. Y. Li, Z. R. Dong, J. X. Gao, *Chin. Chem. Lett.*, 2012, **23**, 395-398
  24. B. Ak, M. Aydemir, F. Durap, N. Meriç, A. Baysal., *Inorg. Chim. Acta*, 2015, **438**, 42-51.

## CHAPTER FOUR

### General concluding remarks and future prospects

#### 4.1 General conclusions

In summary, this dissertation reports a systematic examination of (pyrazolyl)pyridine nickel(II) and iron(II) complexes as catalysts for transfer hydrogenation of ketones. The four ligand systems; 2-(3,5-dimethylpyrazolyl)pyridine (**L1**), 2,6-bis(3,5-dimethylpyrazolyl)pyridine (**L2**) and 2,6-bis(3,5-dimethylpyrazolyl)pyridine (**L3**) were used to produce the respective nickel(II) and iron(II) complexes in good yields. The complexes of 2-[1-(3,5-dimethylpyrazolyl)ethyl]pyridine ligand **L4** and 2-[1-(3,5-diphenylpyrazolyl)ethyl]pyridine ligand **L5** were synthesized with anticipation to generate chiral complexes as potential catalyst in asymmetric transfer hydrogenation of ketones, but only the racemic mixtures of R and S configurations were obtained.

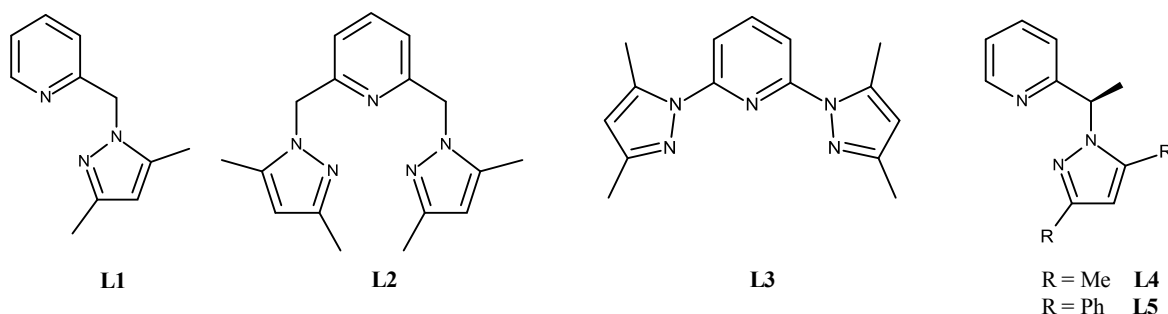


**Figure 4.1.** Four system ligands used in this research project

The complexes were characterized by combination of spectroscopic techniques such as mass spectroscopy, elemental analysis, magnetic moments and X-ray analyses. The molecular structures revealed the bonding characteristics of the two tridentate ligands **L2** and **L3**. The molecular structures of complexes **4** and **6** display two tridentately bound **L2** units in the metal coordination sphere to give six-coordinate cationic species, while complexes **7** and **8** display

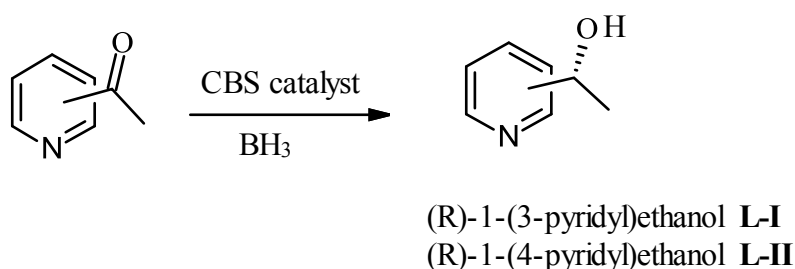
one tridentately bound **L3** units. The ligands **L4** and **L5** form dinuclear nickel(II) complex **10** and mononuclear nickel(II) complex **13** respectively.

All the complexes (**1-13**) were applied in the transfer hydrogenation of ketones reactions, and were found to form active catalysts for the transfer hydrogenation of acetophenone in 2-propanol at 82° C. The nature of the metal atom, ligand structure, base and substrate influenced the catalytic activities of the complexes towards the transfer hydrogenation ketones. Iron(II) complexes were generally more active than the nickel(II) complexes. The nickel(II) and iron(II) complexes derived from bidentate ligand **L1** displayed higher catalytic activity than the corresponding complexes derived from tridentate ligand **L2**. In the same way, the complexes supported by tridentate ligand **L3** complexes were more active than the complexes supported by tridentate ligand **L2**. It was also noted that the dinuclear nickel(II) complexes are less active compared to the mononuclear nickel(II) complexes. The behaviors of catalysts are also affected by the change of base, catalyst amount and type of substrate. Overall, the synthesized nickel(II) and iron(II) complexes offer promising prospect to the transfer hydrogenation of ketones reactions and to the development of more robust and affordable alternatives to the ruthenium catalysts.

#### **4.2 Future prospects**

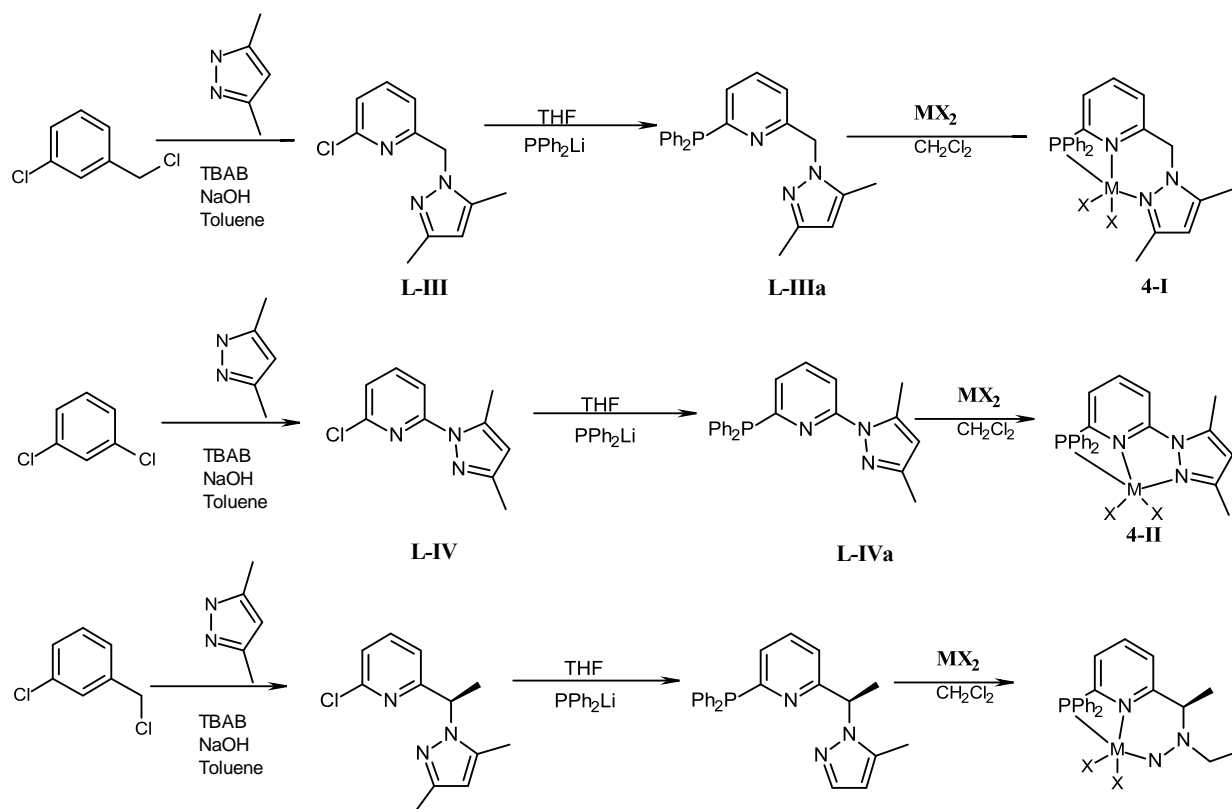
All the nickel(II) and iron(II) complexes of (pyrazolylmethyl)pyridine were found to form active catalysts in the transfer hydrogenation of ketones. However, the complexes of 2-(1-(pyrazolyl)ethyl)pyridine ligands (**L4** and **L5**) were not enantioselective to be applied in the asymmetric transfer hydrogenation. Therefore the asymmetric transfer hydrogenation of ketones needs further study. In future studies, the synthesis of pure enantioselective ligands should be carried out following a different approach. We have observed that the reduction of 2-acetylpyridine with CBS-BH<sub>3</sub> catalyst results in racemic alcohol products. To achieve good

enantioselectivity, we propose the reduction of 3-acetylpyridine or 4-acetylpyridine, as it has been reported with high to excellent enantioselectivities of **L-I** and **L-II** (Scheme 4.1).<sup>1</sup> Another alternative that has been reported in a related work is the protection of the pyridine nitrogen by the methyl or allylic group in order to increase the enantioselectivity of the product.<sup>2</sup> The successful chiral ligand syntheses will lead to synthesis and application of chiral nickel(II) and iron(II) complexes in the asymmetric catalytic reactions.



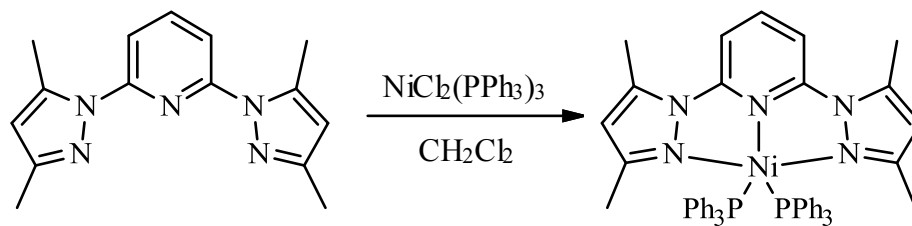
**Scheme 4.1.** Proposed route for synthesis of (R)-1-(pyridyl)ethanol

Although the nickel(II) and iron(II) complexes of (pyrazolylmethyl)pyridine were found to form active catalysts in the transfer hydrogenation of ketones, their activities were found to be relatively lower than the existing nickel(II) and iron(II) catalysts used in transfer hydrogenation of ketones. This observation is essentially attributed to their electronic and to some extent steric properties. The most active nickel(II) and iron(II) transfer hydrogenation catalysts reported bear phosphine ligands which are known to be good  $\pi$ -acceptors causing the metal centre to be more electrophilic. We therefore recommend modification of the ligands to bear phosphine donor moieties and/or including ancillary phosphine ligands. Scheme 4.2 shows the proposed synthetic route to be considered for future work.



**Scheme 4.2.** Synthetic routes of ligands bearing phosphine ligands, and their corresponding metal complexes.

The new ligands bearing  $\text{PPh}_2$  can be synthesized from the reaction of ligand, **L-III**, **L-IV**, **L-V** with lithium diphenylphosphine ( $\text{PPh}_2$ ) to give ligands, **L-IIIa**, **L-IVa**, **L-Va** bearing phosphine ligand and their respective metal complexes. The complexes can also be reacted with triphenylphosphine ( $\text{PPh}_3$ ) for the introduction of ancillary phosphine ligands (Scheme 4.3).



**Scheme 4.3.** Examples of an introduction of ancillary phosphine ligands in the metal complexes.

### 4.3 References

- 
1. V. Stempaneko, M. Jesus, W. Correa, I. Guzman, C. Vazquez, L. Ortiz, M. Ortiz-Marcials, *Tetrahedron: Asymmetry*, 2007, **18**, 2738-2745.
  2. E. J. Corey, C. J. Helal, *Tetrahedron Lett.*, 1996, **37**, 5675-5678.